1. Report No. FHWA/TX-08/0-5516-2	2. Government Accession No.	3. Recipient's Catalog No.
4. Title and Subtitle REPORT SYNTHESIS OF WAVE LOAD DESIGN METHODS FOR COASTAL BRIDGES		5. Report Date October 2006 Published: February 2008
		6. Performing Organization Code
7. Author(s) Francisco Aguíñiga, Kevin Matakis, Hector Estrada, Joseph Sai, Pat Leelani, and Jeff Shelden		8. Performing Organization Report No. Report 0-5516-2
9. Performing Organization Name and Address Texas A&M University-Kingsville 700 University Blvd., MSC 194 Kingsville, Texas 78363		10. Work Unit No. (TRAIS)
		11. Contract or Grant No. Project 0-5516
12. Sponsoring Agency Name and Address Texas Department of Transportation Research and Technology Implementation Office P. O. Box 5080 Austin Texas 78763-5080		13. Type of Report and Period Covered Technical Report: September 2005 – August 2006
		14. Sponsoring Agency Code

15. Supplementary Notes
Project performed in cooperation with the Texas Department of Transportation and the Federal Highway Administration.
Project Title: Synthesis of Wave Load Design Methods for Coastal Bridges
URL: http://users.tamuk.edu/kfgfa00/Wave%20Loads.HTM

16. Abstract

Several coastal bridges have been destroyed by historic and recent hurricanes. Currently no guidelines exist for the design of bridge superstructures when subjected to the action of waves. This document presents an introduction to weather and hurricanes, fundamental concepts of water waves, and a compilation of available sources of information that contain information related to forces produced by waves acting on engineering structures such as sea walls, suspended walls, and bridge decks. A section on the parameters most relevant to the design of bridge superstructures against hurricane waves is included in this document. This report provides a synthesis of data found in several historical databases and database maintained regularly by government organizations and research laboratories. A methodology to update the database is also presented. A plan of action to develop design methodology is also included and followed by a chapter on benefits of expanding this research beyond the synthesis stage. The document ends with a set of conclusions and recommendations.

17. Key Words Bridge, Wave, Period, Height, Path, Sea, Level, Significant, Wind, Speed, Buoy, Hurricane, Design, Force, Buoyancy, Impact, Hydrostatic	18. Distribution Statement No restrictions. This document is available to the public through NTIS: National Technical Information Service 5285 Port Royal Road Springfield, Virginia 22161		
19. Security Classif.(of this report) Unclassified	20. Security Classif.(of this page) Unclassified	21. No. of Pages 178	22. Price

REPORT SYNTHESIS OF WAVE LOAD DESIGN METHODS FOR COASTAL BRIDGES

by

Francisco Aguíñiga
Assistant Professor
Texas A&M University-Kingsville

Kevin Matakis
Research Assistant
Texas A&M University-Kingsville

Hector Estrada
Professor
University of the Pacific

Joseph Sai
Professor
Texas A&M University-Kingsville

Pat Leelani
Professor
Texas A&M University-Kingsville

and

Jeff Shelden
Consulting Engineer
Moffatt and Nichol Engineers

DISCLAIMER

The contents of this report reflect the views of the authors, who are responsible for the facts and the accuracy of the data presented herein. The contents do not necessarily reflect the official view or policies of the Texas Department of Transportation or the Federal Highway Administration. This report does not constitute a standard, specification, or regulation. This report is not intended for construction, bidding, or permit purposes. The researcher in charge of the project was Francisco Aguíñiga. This research report was reviewed by Pat Leelani, who holds Texas P.E. license # 49389. Use of the material presented in this report is the sole responsibility of the user.

ACKNOWLEDGMENTS

TABLE OF CONTENTS

TABLE OF CONTENTS (CONT.)

Page

TABLE OF CONTENTS (CONT.)

LIST OF FIGURES

LIST OF FIGURES (CONT.)

LIST OF TABLES

TABLE   Page

I. INTRODUCTION

Over the years the population growth near seashores has advanced continuously due to the advantages of climate and recreational activities. As a result the property and population at risk at the seacoast are conspicuously higher than elsewhere. Statistics show that the population doubled in 20 years by the late 1970s in the areas of Houston, Miami, and the middle Atlantic states (Simpson and Riehl, 1981). In recent decades, oil platforms have experienced damage or failure due to waves produced by hurricanes (Bea, 1999). For this reason, the design of offshore platforms for the oil industry has devoted considerable effort to study the effects of wave loads on offshore platform decks. Highway bridges, on the other hand, typically had not had major problems surviving hurricane waves. This happened because most bridges were built away from the shore. Nevertheless, population growth has pushed the limits on available land for infrastructure, and now it is very common to find bridges spanning sea inlets. The bridges on U.S. HW 90 across Biloxi Bay and St. Louis Bay were heavily damaged by hurricane Camille in 1969 (Denson, 1980). In 2004, hurricane Ivan overturned several spans of Escambia Bay Bridge in Florida. Shortly after this research began, hurricane Katrina severely damaged the bridge on U.S. HW 90 across St. Louis Bay, MS, the bridge on U.S. HW 90 across Biloxi Bay, MS, and the bridge on I-10 across Lake Pontchartrain in New Orleans, LA. Hurricane Katrina by itself caused the largest natural disaster in U.S. history, resulting in 1800 lives lost and billions of dollars in property damage. A preliminary review of the existing design codes and guidelines for the design of bridge decks subjected to wave loads revealed that there is limited information available, and some of it is difficult to find or to interpret. This indicates the need to carry out an extensive literature search that summarizes the information available and present sources of bridge design parameters such as wave heights.

This research report will begin by providing the structural engineer without knowledge of ocean engineering with a background on weather and hurricanes. Then, basic concepts of water waves are introduced. After that, a description of literature related to available methods for the design of structures subjected to sea waves is presented. Then, a description of the relevant design parameters is given, followed by databases containing parameters that can be used to estimate bridge wave loads. A description of the recommended process to update the database is given next. This report then describes the recommended plan of action to develop non-existent design methodologies, and finishes with an exploration of the financial and safety benefits incurred by expanding this research beyond the synthesis stage.

II. WEATHER AND HURRICANES

Hurricane is the name given to tropical revolving storms with wind velocities greater than 74 mph. They are called typhoons in the western Pacific and tropical cyclones in the other oceans. A full-grown hurricane can have a diameter of 600 miles and on average will be a two-day event. The duration of the most severe weather seldom exceeds 6 hours. Tropical cyclones that cross from Africa to America have a staggering frequency of occurrence of one event every two weeks. This section describes the formation of hurricanes and the forces they produce.

FORMATION OF HURRICANES

This section contains the definition of hurricane and the factors affecting its formation, such as climatology, storm clouds, and the Coriolis effect.

What is a hurricane?

A hurricane is formally defined as a cyclonic storm (with wind spiraling counter-clockwise in the Northern Hemisphere and clockwise in the Southern Hemisphere) of tropical origin, which has a maximum wind speed in excess of 74 miles per hour (Simpson and Riehl, 1981). Prior to hurricane status, wind is classified by the Beaufort Wind Scale. Not mentioned in the Beaufort Scale is that a storm less than or equal to Beaufort force 7 is called a Tropical Depression, and storms between force 7 and force 12 are called Tropical Storms. The Beaufort scale is shown in Table 1.

Table 1. Beaufort scale categorizing wind speed and qualitative state description (Met Office, 2006 and Kamphuis, 2000).

Beaufort force	Wind speed (mph)	Probable wave height (ft)	T (sec)	Wind description	State of sea	Effects on land
0	<1	0	0	Calm	Mirror-like	Smoke rises vertically
1	1-3	0.3	2	Light	Air ripples look like scales; no crests of foam	Smoke drift shows direction of wind
2	4-7	0.7	3	Light breeze	Small but pronounced wavelets; crests do not break	Wind vanes move; Leaves rustle; Can feel wind on the face
3	8-12	2.0	4	Gentle breeze	Large wavelets; crests break; glassy foam; a few whitecaps	leaves and small twigs move constantly; small light flags are extended
4	13-18	3.3	5	Moderate breeze	Longer waves; many whitecaps	Winds lift dust and loose paper; small branches move
5	19-24	6.6	6	Fresh breeze	Moderate long waves; many whitecaps; some spray	Small trees with leaves begin to move
6	25-31	9.8	8	Strong breeze	Some large waves' crests of white foam; spray	Large braches move; telegraph wires whistle; hard to hold umbrellas
7	32-38	13	10	Near gale	White foam from breaking waves blows in streaks with the wind	Whole trees move; resistance felt walking into wind
8	39-46	18	13	Gale	Waves high and moderately long; crests break into spin drift blowing foam in well marked streaks	Twigs and small braches break off trees; difficult to walk
9	47-54	23	16	Strong gale	High waves with wave crests that tumble; dense streaks of foam in wind; poor visibility from spray	Slight structural damage
10	55-63	30	18	Storm	Very high waves with long, curling crests; sea surface appears white from blowing foam; heavy tumbling of sea; poor visibility	Trees broken or uprooted; considerable structural damage
11	64-73	38	20	Violent storm	Waves high enough to hide small and medium sized ships; sea covered with patches of foam; edges of wave crests blown into froth; poor visibility	Seldom experienced inland; considerable structural damage
12	>74	45	22	Hurricane	Sea white with spray; foam and spray render visibility almost non-existent; widespread damage	Very rarely experienced on land

Hurricanes are divided into five categories based on wind speed, central pressure, surge, and potential damage, according to the Saffir/Simpson scale. This is summarized in Table 2.

Table 2. Saffir/Simpson damage potential scale ranges (Simpson and Riehl, 1981).

Scale number (category)	Central pressure		Winds (mph)	Surge (ft)	Damage
	Millibars	Inches			
1	>= 980	>= 28.9	74-95	4-5	Minimal
2	965-979	28.5-28.9	96-110	6-8	Moderate
3	945-964	27.9-28.5	110-130	9-12	Extensive
4	920-944	27.2-27.9	131-155	13-18	Extreme
5	< 920	<27.2	>155	>18	Catastrophic

Climatology

Oceans cover about 70% of the Earth and consequently they play a very large part in moderating the climate of the world. The Earth absorbs more solar radiation near the equator. This is due to a more direct angle of incidence between the Earth and the Sun and less refraction by the atmosphere. This increase in absorbed energy near the equator heats the surface of the ocean and is transported from low to high latitudes by the ocean currents. The air is then warmed as it passes over the surface. As the air is warmed it becomes less dense than the air above it, causing it to rise. The rising air is replaced convectively by cooler, denser air causing a low surface atmospheric pressure. The tropical convergence zone or equatorial trough is an area of low atmospheric pressure ranging from the equator to 38° latitude. This area of warm water and low pressure provides the ideal beginning for tropical storms.

Storm clouds

Warm water and low-pressure conditions are only the beginning of the life cycle of a tropical storm. The warm water heats the air above it increasing the capacity of the air to hold water vapor. This warm and saturated air then begins to rise, cooling as it does so. Once cooled the water vapor molecules begin to condense forming storm clouds. In the case of a tropical storm, these cloud masses can be several miles in diameter. The warm air rises and is cooled while the denser, cooler air falls near the outer edges of the storm system, creating a pressure difference between the rising and descending air. A pictorial representation is given in Figure 1.

5
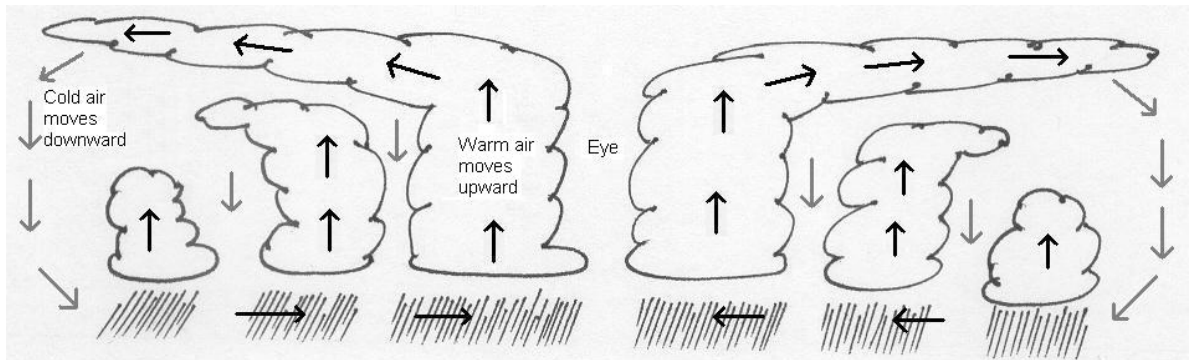
Figure 1. Illustration of the rise of warm air and fall of cold air.

This distribution of high and low pressures releases energy into the system. This kinetic energy generates wind, causing the air to circulate within the storm from areas of high pressure to areas of low pressure. This motion is in accordance with Buys Ballot's Law, stating that air will move from areas of high pressure to areas of low pressure.

Trade winds

Trade winds blow along both sides of the equator in a westerly direction. This is due to lower atmosphere air moving in toward the equator due to its low pressure. In the trade wind areas air "tends to move toward low pressure at a small angle of just the right size so that the pressure force precisely cancels the frictional force (surface wind shear) opposing the motion of the storm" (Simpson and Riehl, 1981). The reason the winds do not move directly north to south is due to the rotation of the Earth, known as the Coriolis effect.

6

HURRICANE WINDS

Hurricanes are classified by their wind speed, but the most severe impact derives from the waves and storm surge generated by the stresses imposed by winds on the sea surface (Simpson and Riehl, 1981).

As the hurricane makes its way over the ocean it does not have a symmetric band of winds around the low-pressure system (eye). This is illustrated in Figure 2. On the right side of the eye, the speed of the hurricane movement adds to the wind speed. On the left, the wind blows in the opposite direction in which the hurricane travels reducing the wind speed (Allaby, 1997).
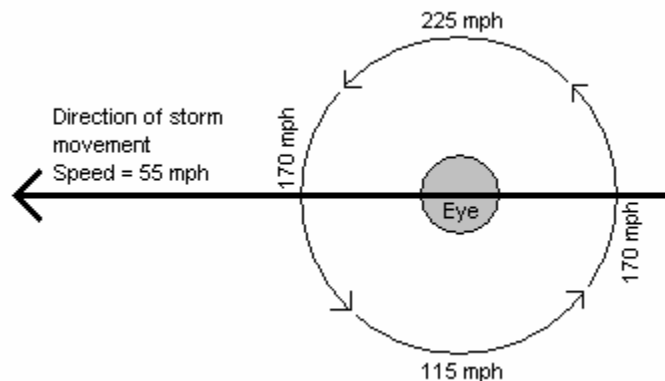
Figure 2. Depiction of difference in wind speeds throughout a hurricane.

The maximum wind speeds are usually observed as the tangential components of the rotating winds. These can be obtained using the following formula (Simpson and Riehl, 1981):

$$u = V \cos \beta \qquad \text{Equation 1}$$

where u is the wind speed, V is the total wind speed, and β is the crossing angle between streamlines and isobars. Although if surface friction is neglected and angular momentum is added to the system, that angular momentum, Ω, is

$$\Omega = ur + \frac{fr^2}{2} \qquad \text{Equation 2}$$

where f is the Coriolis parameter and r is the distance from the center of the cyclone. Equation 2 solved for u yields

$$u = \frac{\Omega}{r} - \frac{fr}{2} \qquad \text{Equation 3}$$

Air spiraling around the hurricane center transports angular momentum from the outside toward the center. At the same time the mean value of u at any radius, r, increases according to Equation 3 (Simpson and Riehl, 1981).

Within a hurricane the wind speed varies with altitude. The strongest winds have almost the same speeds up to a height of 2.5 to 3 miles as indicated in Figure 3.

According to Simpson and Riehl hurricane force winds decrease with height due to frictional stresses, and the variation of a representative mean wind speed with height in the surface (friction) layer is given by

$$u' = \frac{u''}{k}\left[\ln\frac{z}{zo} - \psi\right] \qquad \text{Equation 4}$$

where u' is the mean wind velocity at a height, z; u'' is the frictional velocity, a function of surface stress; k is a scaling constant whose value is generally agreed to be approximately 0.35; zo is a measure of spacing of surface irregularities, and Ψ is a function of the static stability of the atmosphere (Simpson and Riehl, 1981). Although for the friction layer engineers commonly use Hellman's formula:

$$V_z = V_{10}\left(\frac{z}{10}\right)^x \qquad \text{Equation 5}$$

where V_z is the wind speed at any given altitude, z; V_{10} the wind speed at standard anemometer height (33 ft); and z, the height (*ft*) at which V_z is observed (Simpson and Riehl, 1981). A typical model developed to estimate wind speed at different heights in tropical cyclones is shown in Figure 4. Surface wind loads greatly intensify the waves that impact shore.
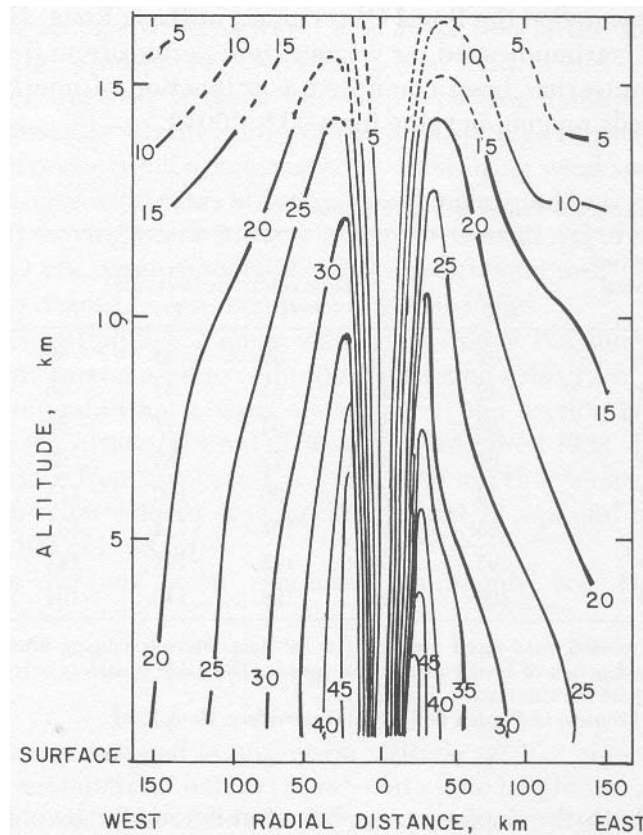
Figure 3. Cross section of wind speeds (meters per second) around the eye of hurricane Hilda, source: (Simpson and Riehl, 1981).

Wind gusts are another factor that may contribute to hurricane damage. A wind gust represents deviations from the mean wind caused by turbulent eddies. These eddies are a function of the terrain roughness, appear locally as rapid acceleration of wind speeds to peak values that may exceed the sustained wind speed, in smooth terrain, by an average of about 30%. At a coastline gusts may occasionally exceed sustained wind speeds by 50%. Figure 5 shows a typical example of hurricane gustiness.
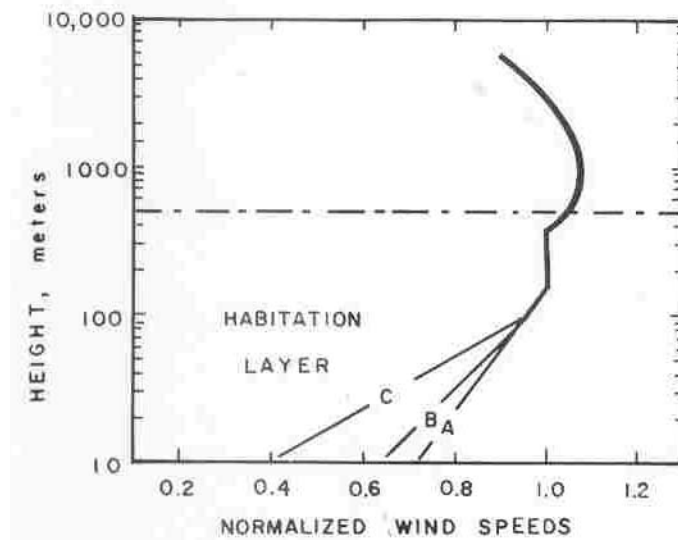
Figure 4. Model of wind-speed variation with height; A is over water and C over land, source: (Simpson and Riehl, 1981).
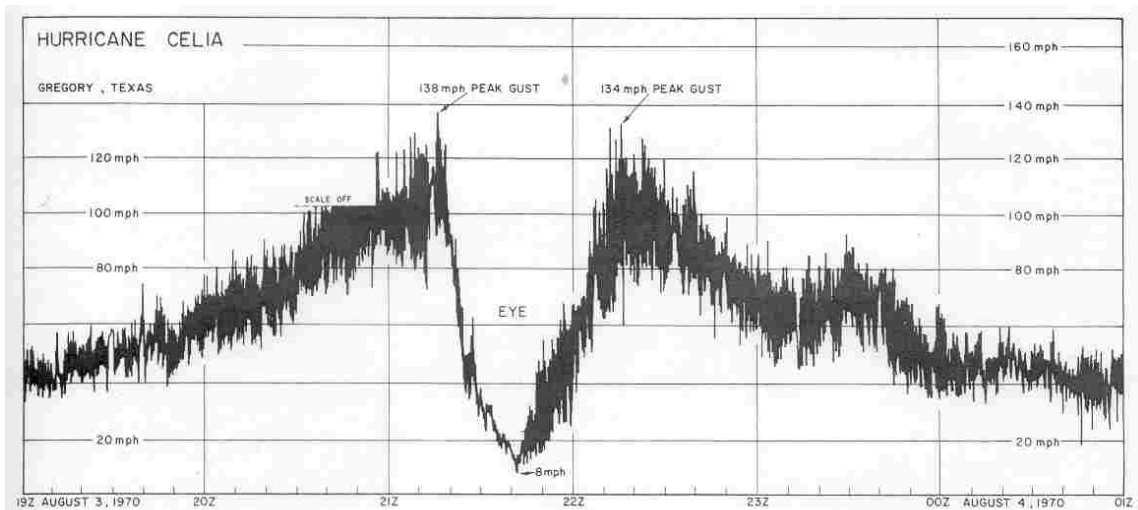
Figure 5. Anemometer (wind speed) record during the passage of hurricane Celia at Gregory Texas on August 3, 1970. The eye passed directly over the station, source: (Simpson and Riehl, 1981).

A description of winds in coastal and marine areas and a procedure for estimation of winds for wave prediction is given in Chapter 2 of the Coastal Engineering Manual (CEM, 2003).

III. CONCEPTS OF WATER WAVES

This section describes the basic concepts used to describe water waves including linear and non-linear wave theories and wave deformations. This section ends with an introduction to wave statistics, where the significant wave is defined, and a description of short- and long-term statistics.

BASIC CONCEPTS AND DESIGN WAVE PREDICTION

Surface water waves can cause large dynamic forces on structures. Therefore, their study is vital to make reasonable estimates of wave forces induced on structures. Although sea waves generated by storms can reach heights greater than 100 ft (Faltinsen, 1990), severe conditions rarely persist long enough in space and time to generate an organized field of significant waves with heights of 65 ft (Simson and Riehl, 1981).

Before we can discuss waves there are some terms that need to be defined.
- *Wave crest*: the highest point of the wave above the average water level.
- *Wave trough*: the valley between wave crests below average water level.
- *Wave height*: the vertical distance between a wave crest and the adjacent trough.
- *Wavelength*: the horizontal distance between two successive crests (or troughs).
- *Wave period*: the time it takes for a wave to move a distance of one wavelength.
- *Wave frequency*: the number of wavelengths that pass a fixed point per second.
- *Deep-water waves*: waves moving through water that is deeper than half their wavelength.
- *Shallow-water waves*: waves moving through water that is less deep than $1/20^{th}$ of their wavelength.
- *Swell*: mature waves from a storm that have similar wavelengths and speeds.
- *Wave train*: groups of mature waves with the same origin and wavelength.

- *Fetch*: the uninterrupted distance over which wind blows without significant change in direction.

The wind waves generated are affected by three factors: wind speed, wind duration, and fetch. Below is a table of common wind wave conditions.

Table 3. Conditions necessary for a fully developed sea (Garrison, 2005).

Wind			Wave		
Speed in one direction (mph)	Fetch (miles)	Duration (h)	Average height (ft)	Average wavelength (ft)	Average period (s)
12	12	2	0.9	28	3
23	86	10	4.9	111	5.7
35	322	23	13.6	251	8.6
46	816	42	27.9	446	11.4
58	1633	69	48.7	696	14.3

Linear wave theory

The simplest theory developed to explain the mechanics of waves is called linear theory. The main variables that describe a wave used in linear theory are shown in Figure 6. Definitions of the variables used in linear wave theory are as follows:

H = Wave height (distance between crest and trough), *ft*

T = Wave period (time between two successive wave crests), *sec*

L = Wave length (distance between two wave crests measured at the same time), *ft*

d = Still water depth (distance from the sea bottom to the free surface if no waves are present), *ft*

c = Wave celerity (speed at which a wave crest moves in the x-direction), *ft/sec*

η = Free surface profile (vertical distance measured from the still water level), *ft*

a_c = Height of the crest, *ft*

a_t = Depth of the trough, *ft*

ω = $2\pi/T$ = wave circular frequency, *rad/sec*

k $= 2\pi/L =$ wave number, ft^{-1}

g $=$ Acceleration of gravity, ft/sec^2

s $= d + \eta =$ Distance from sea bottom to water surface, ft
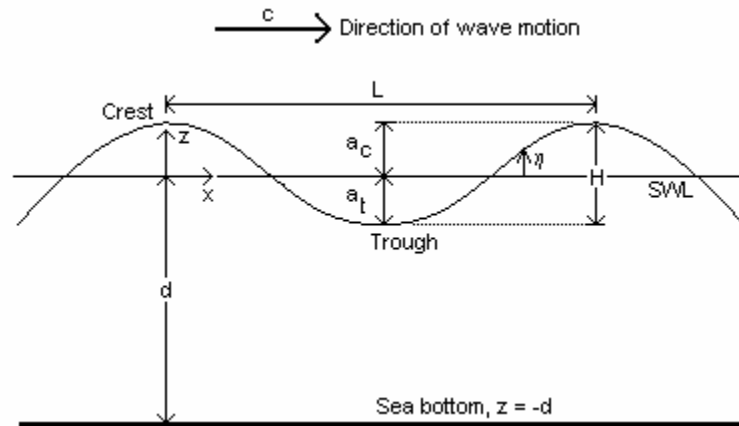
Figure 6. Surface wave parameters.

Linear wave theory implies that the following set of simplifying assumptions is met, which are adequate for waves in intermediate to deep water depths over a silt or sand bottom:

- incompressible fluid;
- irrotational flow (no dissipation);
- horizontal, impermeable, and rigid bottom;
- no surface stress (pressure, wind, or surface tension);
- no currents; and
- wave height is small with respect to the wavelength and water depth ($H \ll L, d$).

To comply with the assumptions of irrotational motion and incompressible fluid for two-dimensional (2-D) fluid motion, the scalar velocity potential ϕ pertaining to the fluid region should satisfy the continuity equation:

$$\nabla^2 \phi = \frac{\partial^2 \phi}{\partial x^2} + \frac{\partial^2 \phi}{\partial z^2} = 0 \qquad\qquad \text{Equation 6}$$

And will be subject to the following boundary conditions

$$\frac{\partial \phi}{\partial z} = 0 \qquad \text{at } z = \text{-d} \qquad\qquad \text{Equation 7}$$

$$\frac{\partial \eta}{\partial t} + \frac{\partial \phi}{\partial x}\frac{\partial \eta}{\partial x} - \frac{\partial \phi}{\partial z} = 0 \qquad \text{at } z = \eta \qquad\qquad \text{Equation 8}$$

$$\frac{\partial \phi}{\partial t} + \frac{1}{2}\left[\left(\frac{\partial \phi}{\partial x}\right)^2 + \left(\frac{\partial \phi}{\partial z}\right)^2\right] + g\eta = f(t) \qquad \text{at } z = \eta \qquad\qquad \text{Equation 9}$$

$$\phi(x,z,t) = \phi(x - ct, z) \qquad\qquad \text{Equation 10}$$

where η(x, t) is the water surface elevation measured above the still water level z = 0 (Sarpkaya and Isaacson, 1981).

The solution of Equation 10 is presented in Table 4, where parameters such as wave celerity, particle displacements, velocities, and accelerations can be determined, knowing the wave frequency, f, wave number, k, and the coordinates of the point of interest, x and z. A detailed derivation of wave equations can be found in the book "Water Wave Mechanics for Engineers and Scientists" by Dean and Dalrymple (Dean and Darlrymple, 1991).

Dispersion Equation

The dispersion equation is used to define the relationship among the wave number, wave frequency, and water depth. This relationship is derived by applying the kinematics of the free surface boundary conditions. The dispersion equation can be written in the following two forms:

$$\omega^2 = gk \tanh(kd) \qquad \text{Equation 11a} \qquad\qquad L = \frac{gT^2}{2\pi}\tanh\left(\frac{2\pi d}{L}\right) \qquad \text{Equation 11b}$$

When *d/L* is large, then Equation 11b becomes:

$$L_o = \frac{gT^2}{2\pi} \qquad\qquad \text{Equation 12}$$

In the previous equation $L_o = 1.56\ T^2$ for SI units (L in m) and $L_o = 5.12\ T^2$ for English units (L in ft). Deep water is a condition when d/L is large and is typically taken as $d/L > \frac{1}{2}$. L_o is typically used to denote deep-water wavelength. A value of $d/L < 1/20$ is typically used to represent shallow water conditions. For shallow water, Equation 11b can be simplified to $L = (gd)^{1/2}\ T$. Water depths between these limits are considered intermediate, and Equation 11 cannot be simplified.

An approximate solution of the dispersion equation can be done numerically, by trial-and-error solutions and can also be found in the form of tables of graphs such as given in the Coastal Engineering Manual (CEM, 2003). The energy of linear waves, E, is called the wave energy density and is the energy per unit area of horizontal surface. Sarpkaya and Isaacson provide a complete set of equations for shallow- and deep-water approximations for linear wave theory (Sarpkaya and Isaacson, 1981).

Sarpkaya and Isaacson suggest the following procedure to be used for design using linear wave theory. First, estimate the wave height, H, wave period, T, and sea depth, d, then evaluate d/gT^2. After that obtain the value of kd from a table based on Equation 13 (or from Figure 7). Then the formulae from Table 4 can be used directly to evaluate the desired parameters such as water particle velocity.

$$kd \cdot \tanh(kd) = 4\pi^2 \frac{d}{gT^2} \qquad\qquad \text{Equation 13}$$

An approximation of the shallow water celerity is obtained by (Sarpkaya and Isaacson, 1981):

$$c = \sqrt{gd} \qquad\qquad \text{Equation 14}$$

Table 4. Results of linear wave theory equation (Sarpkaya and Isaacson, 1981).

Velocity potential	$\phi = \dfrac{\pi H}{kT}\dfrac{\cosh(ks)}{\sinh(kd)}\sin\theta$
Dispersion relation	$c^2 = \dfrac{\omega^2}{k^2} = \dfrac{g}{k}\tanh(kd)$
Surface elevation	$\eta = \dfrac{H}{2}\cos\theta$
Horizontal particle displacement	$\xi = -\dfrac{H}{2}\dfrac{\cosh(ks)}{\sinh(kd)}\sin\theta$
Vertical particle displacement	$\varsigma = \dfrac{H}{2}\dfrac{\sinh(ks)}{\sinh(kd)}\cos\theta$
Horizontal particle velocity	$u = \dfrac{\pi H}{T}\dfrac{\cosh(ks)}{\sinh(kd)}\cos\theta$
Vertical particle velocity	$w = \dfrac{\pi H}{T}\dfrac{\sinh(ks)}{\sinh(kd)}\sin\theta$
Horizontal particle acceleration	$\dfrac{\partial u}{\partial t} = \dfrac{2\pi^2 H}{T^2}\dfrac{\cosh(ks)}{\sinh(kd)}\sin\theta$
Vertical particle acceleration	$\dfrac{\partial w}{\partial t} = \dfrac{2\pi^2 H}{T^2}\dfrac{\sinh(ks)}{\sinh(kd)}\cos\theta$
Pressure	$p = -\rho gz + \dfrac{1}{2}\rho gH\dfrac{\cosh(ks)}{\cosh(kd)}\cos\theta$
Group velocity	$c_G = \dfrac{1}{2}\left[1 + \dfrac{2kd}{\sinh(2kd)}\right]c$
Average energy density	$E = \dfrac{1}{8\rho gH^2}$
Energy flux	$P = Ec_G$
Radiation stress	$S_{xx} = \left[\dfrac{1}{2} + \dfrac{kd}{\sinh(2kd)}\right]E$ $S_{xy} = S_{yx} = 0$ $S_{yy} = \left[\dfrac{kd}{\sinh(2kd)}\right]E$

For deep water the wave celerity can be approximated by

$$c = \dfrac{gT}{2\pi} \qquad\qquad \text{Equation 15}$$

16
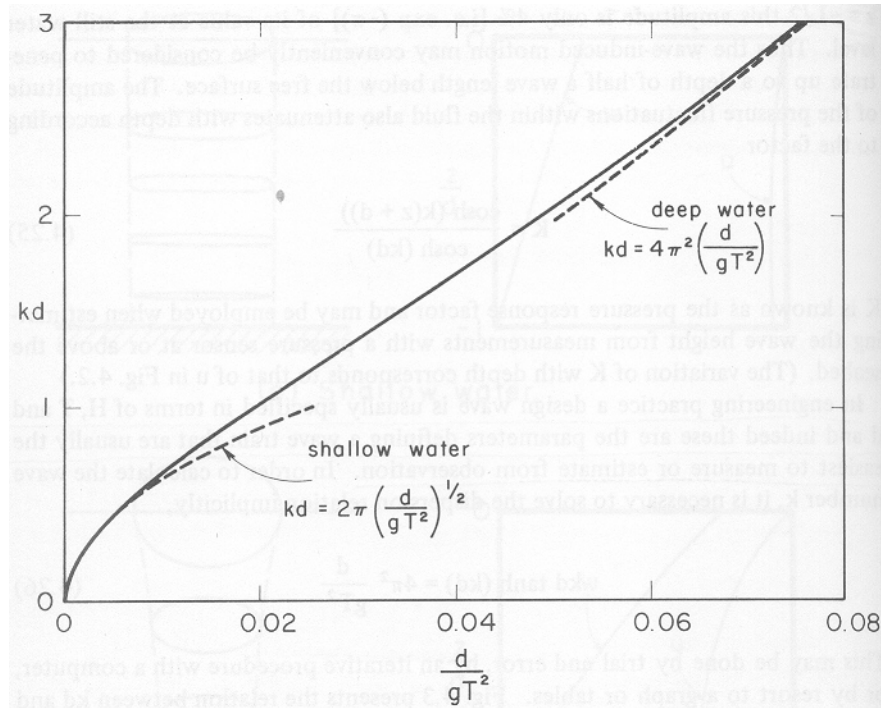
Figure 7. Variation of *kd* with *d*/*gT*² for small amplitude waves, source: (Sarpkaya and Isaacson, 1981).

Shallow water waves are controlled by gravity and wavelength. As deep-water waves approach the shore, they are transformed into shallow water waves when the slope of the ocean floor confines them. They bunch up, and their speed decreases. These groups of waves are called wave trains.

These wave trains travel at a constant velocity known as the group velocity. The speed of individual waves within the group slows when deep-water waves move into shallow water, until wave speed equals group velocity (Garrison, 2005).

As wind waves approach the shore they form wave trains, and their wavelength decreases due to the interference of the ocean floor. Listed below is an outline of the events leading to wave break (Garrison, 2005):

17

1. The wave train moves toward shore. When the depth of the water is less than half the wavelength, the wave begins to be affected by the bottom.
2. The circular motion of water molecules in the wave is interrupted. Circles near the bottom flatten to ellipses. The wave's energy must now be packed into less water depth, so the wave crests become peaked rather than rounded.
3. Interaction with the bottom slows the wave. The waves behind it continue toward shore at the original rate. Wavelength therefore decreases, but period remains unchanged.
4. The wave becomes too high for its wavelength, approaching the critical 1/7 (wave height to wavelength) wave steepness ratio for deep water (Mitchell, 1893).
5. As the water becomes even shallower, the part of the wave below average sea level slows because of the restricting effect of the ocean floor on wave motion. Waves of any size break when the speeds of local water particles at the wave crest exceed the celerity of the wave. The critical ratio for shallow water is $d/H = 1.28$ (Munk, 1949).

Water Particle Velocities

Water particles show a circular motion with the diameter of the circular orbit decreasing exponentially from the free surface to the sea bottom in deep-sea water conditions. In shallow water conditions the particle motions follow an elliptic trajectory with a constant size with depth for the major axis of the ellipse and a deceasing size with depth for the minor axis as indicated in Figure 8. The major and minor axes of the elliptical motion of particles decrease in size with depth for intermediate water depth.
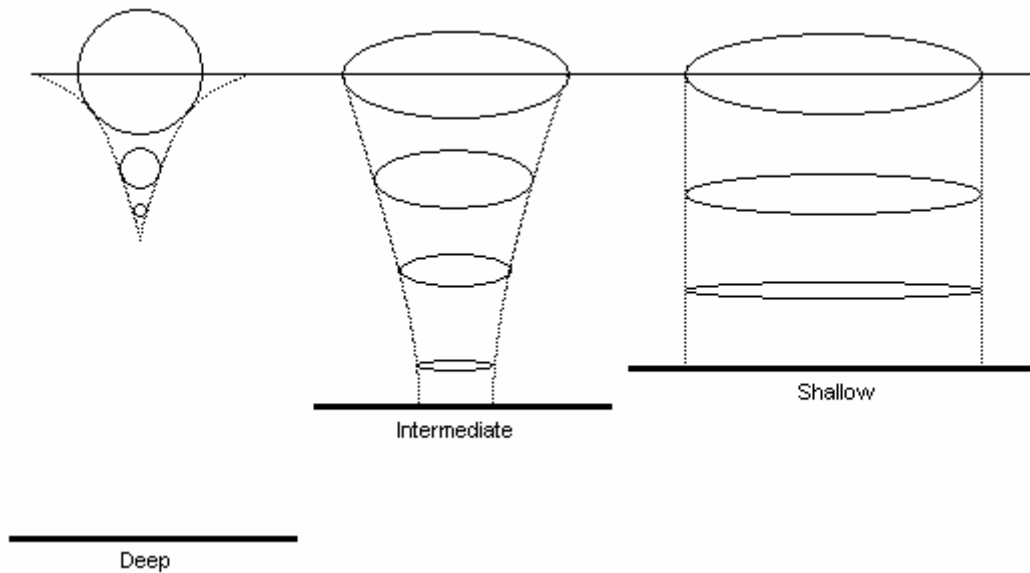
Figure 8. Water particle orbits of a wave in deep, intermediate, and shallow water.

Nonlinear waves

Linear waves rarely develop on the ocean surface, since wind blowing from different directions, refraction, and other factors produce nonlinearities on the wave profile. When this happens, the wave profile can no longer be described by a simple harmonic function, and some of the hypotheses of linear wave theory are violated. Thus, theories for nonlinear waves were developed to more accurately model actual waves.

Nonlinear waves have higher and sharper crests as well as shallower and longer troughs than linear waves. A typical nonlinear wave is compared to a linear wave in Figure 9. Linear waves may not be an accurate model when: (a) the wave kinematics needs to be determined near the surface, since linear wave theory is least accurate at the surface, and (b) when design waves need to be determined, since for extreme wave conditions H/L is not small. Stokes wave theory and the cnoidal theory are the most common analytical wave theories of nonlinear waves (Tedesco et al., 1999). The Specialist Committee on Environmental Modeling of the International Towing Tank

19

Conference (ITTC) recommends that due to nonlinear effects extreme crests in deep water should be expected to be higher than Rayleigh estimates (ITTC, 1999).
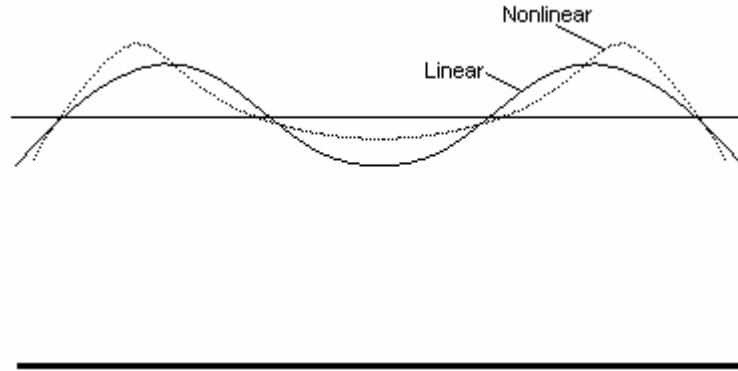
Figure 9. Illustration of linear and nonlinear waves.

Stokes Wave Theory

Stokes theory provides a solution to the velocity potential function without the limitation that *H/L* << 1, with the following expression:

$$\phi(x,z,t) = \frac{c}{k}\sum_{n=1}^{N}\varepsilon^{n}\lambda_{n}\cosh[nk(d+z)]\sin[n(kx-\omega t)] \qquad \text{Equation 16}$$

Where *N* is the order of the solution, $\varepsilon = H/L$, and λ_n denotes a constant that is a function of *kd*. For small ε the equation simplifies to the linear wave theory. If ε is not small and the solution is truncated at ε^2, for *N* = 2, we obtain the Stokes 2nd order solution.

Cnoidal Wave Theory

This theory models accurately steep waves in shallow water. In this theory the parameter $U_r = HL^2/d^3$, called Ursell number, is used. In this case, if $U_r < 25$ Stokes wave theory is a better model, while if $U_r > 25$ cnoidal theory is applicable. A solution for cnoidal waves is given by Leenknecht et al. (Leenknecht et al., 1992).

As indicated by Sarpkaya, selecting the appropriate wave theory for a given application depends on the characteristics of interest and there can be no unique answer. However, most analysis will begin once the main design parameters H, T, and d have been defined. Figure 10 shows the regions of suitability for various wave theories.
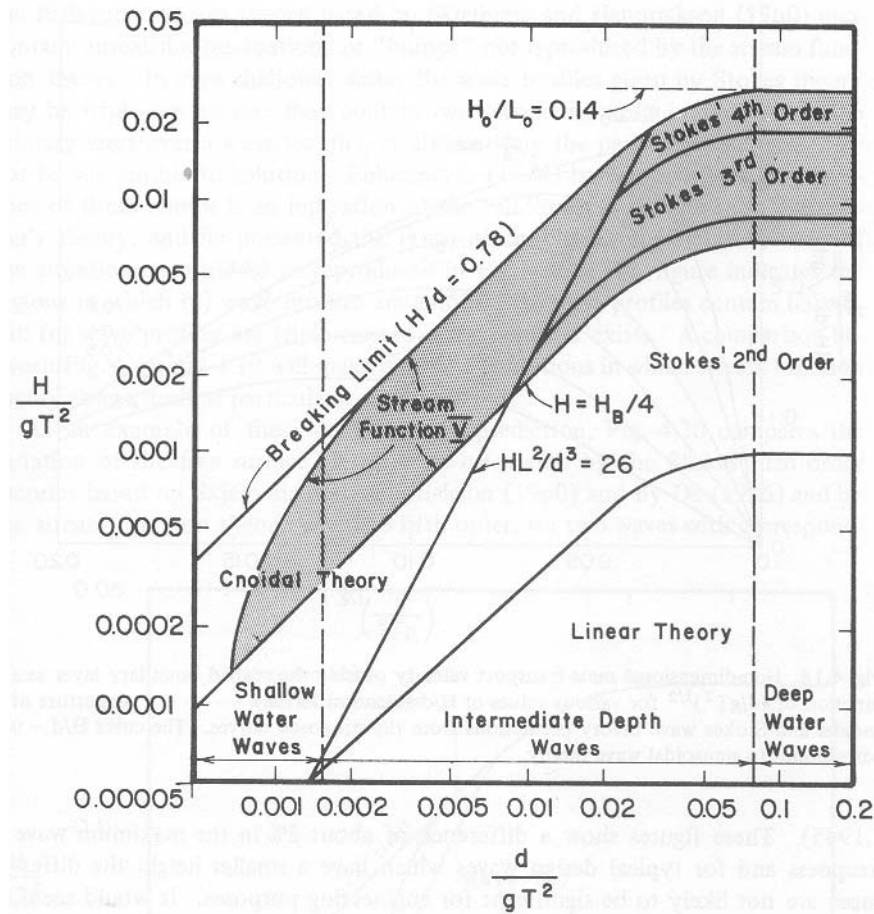
Figure 10. Ranges of applicability for different wave theories as suggested by Le Méhauté, source: (Sarpkaya and Isaacson, 1981).

Stream Function Theory

Based on a stream function representation of the flow, Dean presented a numerical method to predict two-dimensional wave properties (Dean, 1965). Dean solved the problem to obtain numerically a stream function that represents a wave with a

given profile. The solution presented here pertains to the special case of constant free surface pressure distribution without an underlying current.

Following Sarpkaya and Isaacson's derivation, if a coordinate system (x, z) is chosen to move with the waves, then the problem becomes one of steady flow (Sarpkaya and Isaacson, 1981). The new coordinate system would be (x', z), however the primes will be omitted for simplicity. A stream function ψ exists for this scenario because the flow is two-dimensional, and fulfillment of Laplace's equation is required for the flow to be irrotational:

$$\frac{\partial^2 \psi}{\partial x^2} + \frac{\partial^2 \psi}{\partial y^2} = 0 \qquad \text{Equation 17}$$

This equation needs to comply with the following boundary conditions at sea-bed and at the surface

$$\frac{\partial \psi}{\partial x} = 0 \qquad \text{at z = - d (sea bed)} \qquad \text{Equation 18}$$

$$w = u\frac{\partial \eta}{\partial x} \qquad \text{at z = } \eta \text{ (sea surface)} \qquad \text{Equation 19}$$

$$\frac{1}{2g}\left(u^2 + w^2\right) + \eta = Q \qquad \text{at z = } \eta \text{ (sea surface)} \qquad \text{Equation 20}$$

where Q is Bernoulli's constant. Complying with surface and sea-bed boundary conditions, the stream function $\psi = \psi(x, z)$ can be assumed as

$$\psi(x,z) = cz + \sum_{n=1}^{N} X_n \sinh(nk(z+d))\cos(nkx) \qquad \text{Equation 21}$$

This function fits a symmetrical wave profile. This function satisfies Laplace's equation and the boundary conditions. The value of the stream function at the surface ψ (x, η) is a constant, ψ_η, given by

$$\psi_\eta = c\eta + \sum_{n=1}^{N} X_n \sinh(nk(\eta+d))\cos(nkx) \qquad \text{Equation 22}$$

The coefficients X_n, the wave number k, and the value of the stream function at the surface are determined by the dynamic free surface boundary condition (Equation 20). The solution can be obtained by guessing values using linear wave theory, for example. Then the approach followed by Dean was to minimize the error between the solution obtained and the dynamic free surface boundary condition. This can be done using least squares. When the improved values of the surface streamline have been determined, the stream function can be computed as:

$$\psi_\eta^{(j+1)} = \frac{1}{L}\left[\sum_{n=1}^{N} X_n^{(j+1)} \sinh\left(nk\left(\eta^{(j+1)}+d\right)\right)\cos(nkx)\right]dx \qquad \text{Equation 23}$$

where $(j+1)$ is the iteration number, and L is the wave length. The values of the components of velocity u, w at the free surface can be obtained. Dean has provided Tables for the application of the stream function theory (Dean, 1974). The tables list values for particle velocities and accelerations, the pressure at specific locations and times, and integrals to obtain the energy and momentum of the wave train.

Other Wave Theories

Sarpkaya and Isaacson discuss other wave theories such as: trochoidal wave theory, linearized long wave theory, solitary wave theory, and hyperbolic wave theory (Sarpkaya and Isaacson, 1981). The Coastal Engineering Manual describes other wave theories such as: Korteweg and de Vries, Boussinesq, and Fenton's theory (CEM, 2003).

Wave transformations

When waves propagate toward shore they experience transformations such as: shoaling, refraction, diffraction, dissipation, reflection, and breaking. A simple approximation to account for those effects is given in the Coastal Engineering Manual (CEM, 2002), assuming each transformation is independent of others as:

$$H = K_S K_R K_D K_F H_O \qquad \text{Equation 24}$$

where,

H = Local wave height, ft

H_O = Deep water wave height, ft

K_S = Shoaling coefficient

K_R = Refraction coefficient

K_D = diffraction coefficient

K_F = dissipation coefficient

Shoaling

When waves propagate into shallow waters the wave length decreases, the wave celerity diminishes, and the wave height rises. K_S is given by the following expression:

$$K_S = \left(\frac{c_o}{c}\right)^{1/2}$$
<div align="right">Equation 25</div>

which is the square root of deep-water group celerity, c_o, divided by local wave celerity, c. For linear wave theory this is equivalent to (Sarpkaya and Isaacson, 1981):

$$K_S = \left[\tanh(kd)\right]^{-1/2} = \frac{1}{2\pi}\left(\frac{gT^2}{d}\right)^{1/2}$$
<div align="right">Equation 26</div>

Refraction

A wave that approaches a bottom slope obliquely travels with different speeds. The portion of the wave in deep water will travel faster than that in shallow water. Thus, the axis of the wave crest is shifted to align closer with the bottom contours. Refraction also affects the angle with which waves will reach a structure. A common visualization technique is to draw wave rays, which are drawn perpendicular to the local crest alignment, thus pointing in the direction in which waves travel. Examples of the effect of bottom contours in wave ray direction are shown in Figure 11. It can be seen in Figure 11 that wave rays are concentrated on headlands and diverge in the bays. Wave height increases when the distance between wave rays diminishes. An expression given by Snell's law, developed for straight bottom contours parallel to shore, can be used to obtain the refraction coefficient:

$$K_R = \left(\frac{1 - \sin^2\theta_o}{1 - \sin^2\theta}\right)^{1/4} = \left[\frac{1 - \sin^2\theta_o}{1 - (c/c_o)^2 \sin^2\theta_o}\right]^{1/4} \qquad \text{Equation 27}$$

where,

θ_o = Deep water wave angle, deg

c_o = Deep water celerity, ft/sec

θ = Local wave angle, deg

c = Local celerity, ft/sec
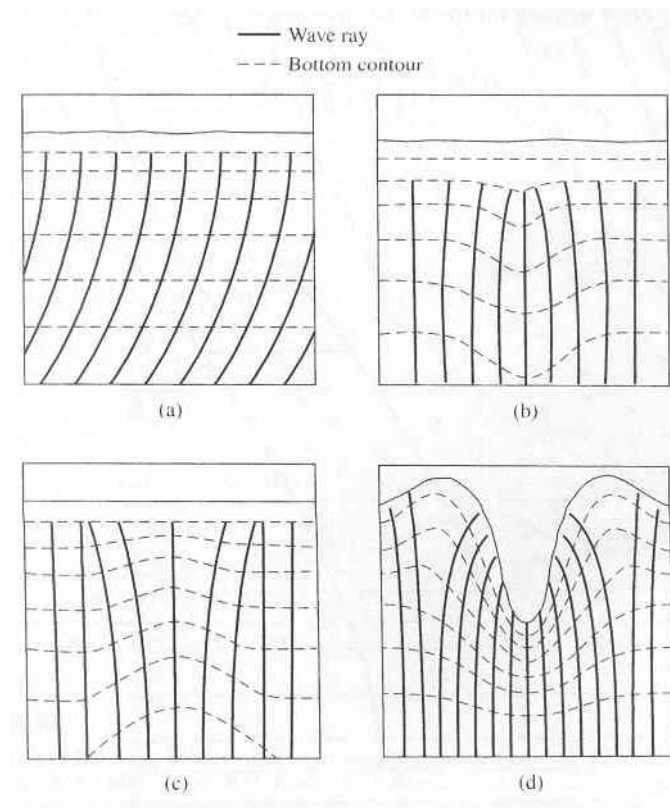
Figure 11. Effect of different bottom and shoreline contours on wave ray direction, source: (Tedesco et al., 1999).

For bathymetries differing significantly from straight and parallel contours, other techniques are available to estimate K_R. One such technique is described in the Coastal Engineering Manual (CEM, 2006).

Diffraction

Diffraction is defined as the transfer of wave energy to the sides of a wave crest due to height gradients along the crest. Crest height gradients can be developed when waves traverse a fixed structure. Analytical solutions developed for flat sea bottoms are given by the Coastal Engineering Manual (CEM, 2003) and Goda (Goda, 1985) for different structures and wave angles. Figure 12 shows the diffraction of waves on a bay.
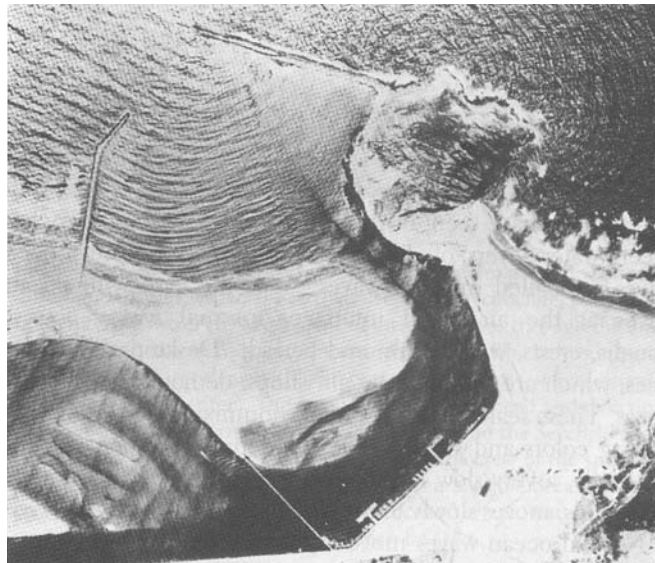
Figure 12. Diffraction of waves by a breaker at Morro Bay, California, source: (Garrison, 2005).

Dissipation

Waves lose energy through viscous dissipation or through interaction with the seabed when they travel. However, wave dissipation tends to reduce the wave height. Thus, wave height estimations that do not account for dissipation should be conservatively higher.

Breaking

Breaking waves are difficult to model analytically and are controlled by the slope of the beach. Breaking waves can be grouped in three types: spilling, plunging, and surging as shown in Figure 13. Spilling breakers develop on low slope beaches. Plunging

breakers occur on beaches with moderate slope. Surging breakers occur on steep beaches.
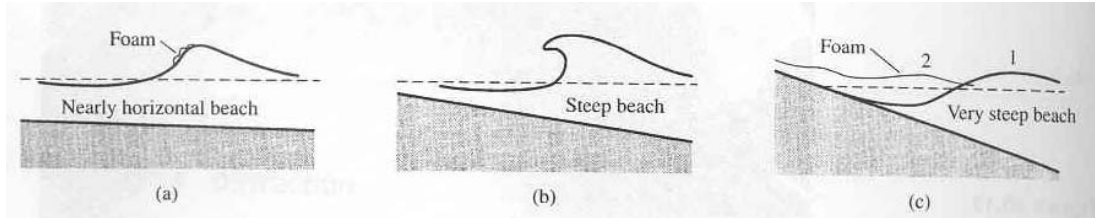
Figure 13. Types of breaking waves (a) spilling, (b) plunging, (c) surging, source: (Tedesco et al., 1999).

Weggel's expression can be used to estimate the height of a breaking wave (Weggel, 1972):

$$\frac{H_b}{d_b} = b(m) - a(m)\frac{H_b}{gT^2} \qquad\qquad \text{Equation 28}$$

where,

$$a(m) = 43.75\left(1 - e^{-19m}\right)$$

$$b(m) = \frac{1}{0.64\left(1 + e^{-19.5m}\right)}$$

H_b = Height of breaking wave

d_b = Depth of the water where the wave breaks

T = Wave period

m = Beach slope (tangent of the angle the beach makes with the horizontal)

Sources of wave information

The main sources of wave information are measured data and hindcasts.

27

Wave measurements

A number of techniques exist to measure the wave profile. Some measure the location of the free surface as a function of time, in other cases the surface is detected by sonic or ultrasonic systems. Some sources where data can be obtained include:

- The Littoral Environment Observation (LEO) maintained by the Corps of Engineers.
- The National Oceanic and Atmospheric Administration (NOAA) maintains several oceanographic buoys. The recorded information includes wind speed and direction, peak gust data, pressure at sea level, air temperature, sea surface temperature, significant wave height, and dominant wave period.
- Wave observations have also been made aboard ships over many years. The observations include average wave height, period, and direction.
- The Division of Nearshore Research through the Texas Coastal Ocean Observation Network collects sea data continually. Data is collected at 32 stations along the Texas coast. Some of the data available includes water level, wave period and height, temperature, wind speed and direction, barometric pressure and cumulative rainfall, water velocity and tides. Additional sources of wave and wind data are listed in Table 5.

Most engineering designs are made using data not measured at the structure's location. This happens because years of data are necessary to make extreme value estimates for the design. Thus, oftentimes the data obtained from previous long-term wave measurements made at a different location are used for the design.

Table 5. Sources of wave and wind information (Tedesco et al, 1999).

Alaska Coastal Data Collection Program
Plan Formulation Section
U.S. Army Engineer District, Alaska
Pouch 898
Anchorage, AK 99506-0898
Telephone (907) 753-2620
California Coastal Data Information Program
Scripps Institute of Oceanography
Mail Code A022
University of California, San Diego
LaJolla, CA 92093
Telephone (619) 534-3033
Coastal Engineering Information and Analysis Center
USAEWES
3909 Halls Ferry Road
Vicksburg, MS 39180-6199
Coastal Data Network
Coastal and Oceanographic Engineering Department
336 Weil Hall
University of Florida
Gainesville, FL 32611
Telephone (352) 392-1051
National Oceanographic Data Center
User Service (Code OC21)
1825 Connecticut Ave., NW
Washington, DC 20235
Telephone (202) 673-5549
National Climate Data Center
Federal Building
Asheville, NC 28801
Telephone (704) 259-0682

Hindcasts

When measured wave data is not available close to a design site, historical storm events can be used. Wave hindcasting is the generation of waves at a given site using a model fed with this historical event database. For example, hurricane waves that could not be measured at the site of interest can be estimated by introducing the geometric configuration of the coast, bathymetry, wave data recorded at buoys near the site, etc., into a hindcasting model (software), and thus estimating the wave parameters at the site of interest. We could say that hindcasting is equivalent to extrapolating data recorded from a past event at a given site, to another site. Based on 20 years of weather records

the Corps of Engineers has performed hindcasts for all the coasts of the United States. The results are available at the U.S. Army Waterways Experiment Station (WES), Coastal Engineering Research Center.

When WES hindcasts or wave measurements are not available, a hindcasting method described in the Coastal Engineering Manual can be used (CEM, 2003).

Hindcasting is also commonly done by private firms such as Oceanweather, Inc. (Oceanweather, 2006).

IV. DESIGN METHODS

This chapter describes the methods currently available in the literature for the design of bridges to sustain wave forces. The information is focused on bridge superstructures. Information on design guidelines or government documents related to bridge superstructure design is presented first. A section that contains information about wave loads on bridge superstructures or similar elements that includes summaries of journal articles, books chapters, and research reports is also included in this section. This chapter ends with sections on guidelines and information about the design of bridge substructures and bridge revetments.

DESIGN GUIDELINES FOR WAVE FORCES ON BRIDGE SUPERSTRUCTURE

Current bridge design codes appear to provide limited guidance for the design of bridge superstructures subjected to storm wave and surge forces. Many books and design aids are currently available for bridge designers (AASHTO, 2004; CALTRANS, 2005a,b,c; Chen and Duan, 1999; Taly, 1998; TxDOT, 1997; TxDOT, 2001; Xhantakos, 1995; ASCE/SEI 24-05, 2006; ASCE/SEI 7-05, 2006; FEMA, 2000; CEM, 2006). The design of bridge superstructures spanning a body of water typically does not account for water flow forces. A description of current design aids and specifications as they impact the design of bridge superstructures subjected to water flow forces is given next.

A number of references indicate that during a bridge design it seems that they all imply that the bridge type is selected to safely accommodate any flow underneath the superstructure (AASHTO, 2004; CALTRANS, 2005b; Chen and Duan, 1999; Taly 1998; TxDOT, 1997; Xhantakos, 1995).

California Department of Transportation – Bridge Design - 2005

The maximum water level expected to occur during the design life of the bridge is estimated, and the height of the superstructure above the maximum water level is selected (CALTRANS, 2005b). This height is typically greater than 6 ft (CALTRANS 2005a). That is, bridge superstructures are typically not designed to sustain flow forces derived from a storm surge. In this regard, the Bridge Design Specifications of the California Department of Transportation indicate that: "In cases where the corresponding top of water elevation is above the low beam elevation, stream flow loading on the superstructure shall be investigated" (CALTRANS, 2005c). However, the specifications indicate that "The stream flow pressure acting on the superstructure may be taken as P_{max} with a uniform distribution," (CALTRANS, 2005c). The pressure P_{max} is equal to twice the pressure P_{avg}, where P_{avg} is computed with the following expression:

$$P_{avg} = K\left(V_{avg}\right)^2 \qquad \text{Equation 29}$$

where,

P_{avg} = average stream pressure, in pounds per square foot

V_{avg} = average velocity of water in feet per second; computed by dividing the flow rate by the flow area

K = a constant, being 1.4 for all piers subjected to drift buildup and square-ended piers, 0.7 for circular piers, and 0.5 for angle-ended piers where the angle is 30 degrees or less

Taly and Xanthakos do not mention water flow forces for the design of bridge superstructures (Taly, 1998; Xanthakos, 1995).

Section 1.10 of the Bridge Design Practice Manual of the California Department of Transportation recommends the use of box girders or slabs for bridge superstructures

where less than 6 feet of clearance are provided over a stream carrying drift (CALTRANS, 2005a).

AASHTO – LRFD Bridge Design Specifications – 2004

The American Association of State Highway and Transportation Officials (AASHTO) LRFD Bridge Design Specifications contains no recommendations for superstructure design against water flow forces (AASHTO, 2004). Section 3.7.4 of the AASHTO Bridge Design Specifications recommends the use of the Shore Protection Manual to account for wave loads in the design of bridge structures, although it does not specifically address superstructures. The commentary of Section 2.6.4.3 of the AASHTO Bridge Design Specifications indicates that trial combinations for the size of a bridge should take into account the clearances between the floodwater elevations and low sections of the superstructure to allow passage of ice and debris. Section 2.3.1.2 of the AASHTO Bridge Design Specifications also indicates that: "It is generally safer and more cost effective to avoid hydraulic problems through the selection of favorable crossing locations than to attempt to minimize the problems at a later time in the project development process through design measures."

TxDOT – Hydraulic Design Manual – 1997

Section 8.11.6 Minimizing Hydraulic Forces and Debris Impact on the Superstructure of the Hydraulic Design Manual published by the Texas Department of Transportation states that (TxDOT, 1997): "The most obvious design objective is to avoid the imposition of hydraulic forces on a bridge superstructure by placing the bridge at an elevation above which the probability of submergence is small." The manual also indicates that: "Where there is even a small probability of total or partial submergence, the designer should ensure that there is minimum potential for the bridge deck to float away. If the dead load of the structure' (superstructure) 'is not sufficient to resist

33

buoyant, drag, and debris impact forces, it will be necessary to anchor the superstructure to the substructure. Air holes should also be provided through each span and between each girder to reduce the uplift pressure."

In a previous section it is mentioned that the Bridge Design Practice Manual of CALTRANS recommends the use of box girders or slabs for bridge superstructures (CALTRANS, 2005a). However, section 8.11.6 of the Hydraulic Design Manual of TxDOT makes the opposite recommendation: "Box girders which would displace great volumes of water and have a relatively small weight compared to the weight of the water displaced are not a good design alternative unless the probability of submergence is small."

Bridges located in a coastal area where hurricanes are recurring events need to be designed for such events. As mentioned in the bridge superstructure section, the best approach is to avoid having the superstructure coming in contact with the flow of water for the extreme flood event. However, as mentioned in section 8.11.6 of the Hydraulic Design Manual of TxDOT, that is not always physically feasible. During a hurricane, the bridge superstructure may be subjected not only to water flow forces, but to vessel or debris collision as well.

U.S. Army Corps of Engineers – Coastal Engineering Manual – 2006

The Coastal Engineering Manual (CEM) is one of the most widely used sources for the design of coastal structures in the U.S. The manual is a good source of information to obtain data on wave theories and design methods for different coastal structures. The part of the manual most closely related to wave forces on a bridge deck is found under Part VI Introduction to Coastal Project Element Design, Chapter 5, Fundamentals of Design, Section VI-5-4 Vertical-Front Structure Loading and Response. This section of the manual indicates that the pressures generated by waves on

the structures are difficult to obtain with certainty and are a function of the wave conditions and structure geometry. The manual recommends the formulae presented in that section to be used only for preliminary design, accounting for the limitations of each parameter and all uncertainties. They also recommend the final design of an important structure to include laboratory tests. The manual identifies three different wave types affecting vertical walls: non-breaking waves, breaking waves with almost vertical fronts, and breaking waves with large air pockets. It is mentioned that there are no reliable formulae for prediction of impulsive pressures produced by breaking waves due to the extremely stochastic nature of wave impacts. The impulsive loads produced by breaking waves can be quite large, and the extreme load risk increases with the number of breaking waves. Frequent wave breaking is not expected on vertical structures with an angle of wave incidence larger than 20º from the normal incidence. The slope of the seabed also influences the effect of breaking waves. Mild slopes of approximately 1:50 or less over a distance of several wave lengths are not likely to make waves break on the structure.

The CEM indicates that the total hydrodynamic pressure distribution on a vertical wall has two components: the hydrostatic pressure produced by the instantaneous water depth at the wall, and a dynamic component due to the water particle accelerations. The pressure equations used by the manual on vertical walls are mainly based on the equations derived by Goda and modified by others to design for a variety of conditions (Goda, 1974). The equations given in the CEM are shown in Figures 14, 15, and 16. A summary of a book written by Goda is given under the section of relevant literature about wave forces on bridge superstructures.
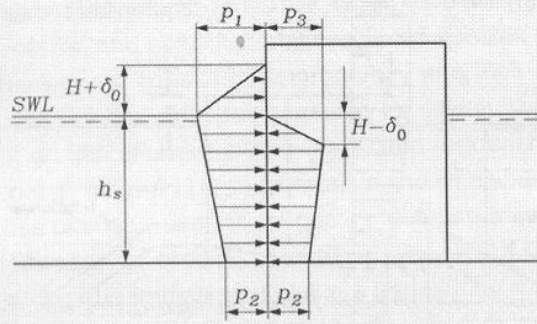
$$p_1 = (p_2 + \rho_w g h_s)\frac{H + \delta_o}{h_s + H + \delta_o}$$

$$p_2 = \frac{\rho_w g H}{\cosh(2\pi h_s/L)}$$

$$p_3 = \rho_w g(H - \delta_o)$$

$$\delta_o = \frac{\pi H^2}{L}\coth\frac{2\pi h_s}{L}$$

where H =   Wave height. In case of irregular waves, H should be taken
as a characteristic wave height. In Japan $H_{1/3}$ is used, while
in other countries $H_{1/10}$ might be used.

p_1 = Wave pressure at the still water level, corresponding to wave crest

p_2 = Wave pressure at the base of the vertical wall

p_3 = Wave pressure at the still water level, corresponding to wave trough

δ_o = Vertical shift in the wave crest and wave trough at the wall

ρ_w = Water density

h_s = Water depth at the foot of the structure

L = Local wave length.

Remarks. The Sainflou formula for conditions under wave crest and wave trough were derived
theoretically for the case of regular waves and a vertical wall. The formula cannot be applied in
cases where wave breaking and/or overtopping takes place.

**Figure 14. The Sainflou formula for head-on, fully reflected, standing regular waves, modified from:
(CEM, 2006).**

36

$$\eta^* = 0.75(1 + cos\beta)\,\lambda_1 H_{design}$$
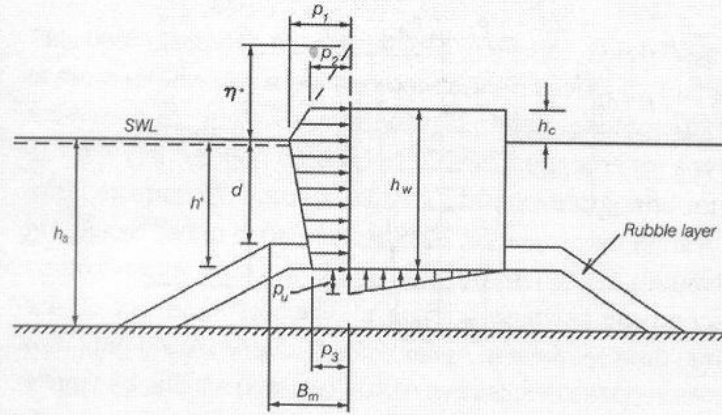
$$p_1 = 0.5(1 + cos\beta)(\lambda_1\alpha_1 + \lambda_2\alpha_* cos^2\beta)\,\rho_w\,g\,H_{design}$$

$$p_2 = \begin{cases} \left(1 - \frac{h_c}{\eta^*}\right)p_1 & \text{for } \eta^* > h_c \\ 0 & \text{for } \eta^* \le h_c \end{cases}$$

$$p_3 = \alpha_3\,p_1$$

$$p_u = 0.5(1 + cos\beta)\lambda_3\alpha_1\alpha_3\rho_w g\,H_{design}$$

where

β	$=$	Angle of incidence of waves (angle between wave crest and front of structure)
H_{design}		Design wave height defined as the highest wave in the design sea state at a location just in front of the breakwater. If seaward of a surf zone Goda (1985) recommends for practical design a value of $1.8\ H_s$ to be used corresponding to the 0.15% exceedence value for Rayleigh distributed wave heights. This corresponds to $H_{1/250}$ (mean of the heights of the waves included in 1/250 of the total number of waves, counted in descending order of height from the highest wave). Goda's recommendation includes a safety factor in terms of positive bias as discussed in Table VI-5-55. If within the surf zone, H_{design} is taken as the highest of the random breaking waves at a distance $5H_s$ seaward of the structure.

$$\alpha_* = \alpha_2$$

$$\alpha_1 = 0.6 + 0.5\left[\frac{4\pi h_s/L}{sinh\,(4\pi h_s/L)}\right]^2$$

$$\alpha_2 = \text{the smallest of } \frac{h_b - d}{3\,h_b}\left(\frac{H_{design}}{d}\right)^2 \text{ and } \frac{2d}{H_{design}}$$

$$\alpha_3 = 1 - \frac{h_w - h_c}{h_s}\left[1 - \frac{1}{cosh\,(2\pi h_s/L)}\right]$$

L	$=$	Wavelength at water depth h_b corresponding to that of the significant wave $T_s \simeq 1.1T_m$, where T_m is the average period.
h_b	$=$	Water depth at a distance of $5H_s$ seaward of the breakwater front wall.

λ_1, λ_2 and λ_3 are modification factors depending on the structure type. For conventional vertical wall structures, $\lambda_1 = \lambda_2 = \lambda_3 = 1$. Values for other structure types are given in related tables.

Figure 15. Goda formula for irregular waves, modified from: (CEM, 2006).

37

The modification of Goda's formula concerns the formula for the pressure p_1 at the still water level (SWL). The coefficient α_* is modified as

$$\alpha_* = \text{largest of } \alpha_2 \text{ and } \alpha_I$$

$$\alpha_2 = \text{the smallest of } \frac{h_b - d}{3\,h_b}\left(\frac{H_{design}}{d}\right)^2 \text{ and } \frac{2d}{H_{design}}$$

$$\alpha_I = \alpha_{I0} \cdot \alpha_{I1}$$

$$\alpha_{I0} = \begin{cases} H_{design}/d & \text{for } H_{design}/d \leq 2 \\ 2.0 & \text{for } H_{design}/d > 2 \end{cases}$$

$$\alpha_{I1} = \begin{cases} \dfrac{\cos \delta_2}{\cosh \delta_1} & \delta_2 \leq 0 \\[2mm] \dfrac{1}{\cosh \delta_1 \cdot (\cosh \delta_2)^{\frac{1}{2}}} & \delta_2 > 0 \end{cases}$$

$$\delta_1 = \begin{cases} 20 \cdot \delta_{11} & \text{for } \delta_{11} \leq 0 \\ 15 \cdot \delta_{11} & \text{for } \delta_{11} > 0 \end{cases}$$

$$\delta_{11} = 0.93\left(\frac{B_m}{L} - 0.12\right) + 0.36\left(\frac{h_s - d}{h_s} - 0.6\right)$$

$$\delta_2 = \begin{cases} 4.9 \cdot \delta_{22} & \text{for } \delta_{2\,2} \leq 0 \\ 3 \cdot \delta_{22} & \text{for } \delta_{22} > 0 \end{cases}$$

$$\delta_{22} = -0.36\left(\frac{B_m}{L} - 0.12\right) + 0.93\left(\frac{h_s - d}{h_s} - 0.6\right)$$

where H_{design}, L, d, h_s, h_b, B_m are given in the figure and text of Table VI-5-53.

Range of tested parameters: Regular waves
bottom slope 0.01 $h_s = 42\,\text{cm}$ and $54\,\text{cm}$
$d = 7 - 39\,\text{cm}$ $B_m = 2.5 - 200\,\text{cm}$
$H = 17.2 - 37.8\,\text{cm}$ $T\text{ - }1.8 - 3\,\text{sec.}$

Figure 16. Goda formula modified to include impulsive forces from head-on breaking waves, source: (CEM, 2006).

The older breaking wave force method proposed by Minikin (Minikin, 1950) used in the Shore Protection Manual (SPM, 1984) is not included in the Coastal Engineering Manual. It is considered that the Minikin method can result in estimates of wave forces, as high as 15 to 18 times those calculated for non-breaking waves. As such, the Minikin method is deemed overconservative.

ASCE/SEI 24-05 - Flood Resistant Design and Construction - 2006

This ASCE standard (ASCE/SEI 24-05, 2006) does not contain wave design forces per se. However, it addresses the subject of wave loads on structures. The standard uses the following relevant definitions among others:

Base Flood Elevation (BFE) – elevation of flooding, including wave height, having a 1% chance of being equalled or exceeded in any given year.

Base Flood – flood having a 1% chance of being equalled or exceeded in any given year.

Design Flood – greater of the following two flood events: (1) the *base flood*, affecting those areas identified as *special flood hazard areas* on the community's Flood Insurance Rate Map (FIRM); or (2) the flood corresponding to the area designated as flood hazard area on a community's *flood hazard map* or otherwise legally designated.

Design Flood Elevation (DFE) – elevation of the *design flood*, including wave height, relative to the datum specified on the community's *flood hazard map*.

High Velocity Wave Action – condition where wave heights are greater than or equal to 3.0 ft in height or where wave runup elevations reach 3.0 ft or more above grade.

The standards classify structures in different categories. Essential facilities such as causeways would fit in category IV, which is the highest rank.

The standards mentioned in section 4.8, that decks, concrete pads, and patios shall not transfer flood loads to the main structure. It indicates that they should be designed to break away cleanly during design flood conditions. The standards also indicate in Table 5-1 that the minimum elevation relative to the base flood elevation for a type IV structure shall be the greater of the base flood elevation plus 2 ft or the design flood elevation. Regarding wind generated waves the standard recommends to use the Shore Protection Manual – now called Coastal Engineering Manual (CEM, 2006) and a

document published by the National Academy of Sciences (National Academy of Sciences, 1977) if waves greater than 3 ft can develop at the site.

ASCE/SEI 7-05 – Minimum Design Loads for Buildings and Other Structures – 2006

This standard addresses loads on structures due to flooding in chapter 5 (ASCE/SEI 7-05, 2006). This standard has the design requirement that structural systems or buildings be designed, constructed, connected, and anchored to resist flotation, permanent lateral displacement due to flood loads, and collapse.

Wave loads are to be determined by: the methods given in the standard, advanced numerical modelling procedures, or laboratory test procedures.

Buildings shall be designed for the following loads: waves breaking on any portion of the building or structure, uplift forces caused by shoaling underneath a structure, wave runup striking any portion of the building, and wave-induced scour.

Non-breaking waves

In this case the structure shall be designed for hydrostatic and hydrodynamic loads. A detailed analysis should be carried out to determine the dynamic effects of moving water. When water velocities do not exceed 10 ft/sec it is permitted to account for the dynamic effects by using an equivalent hydrostatic load. Thus, the design flood elevation (DFE) should be increased by a depth d_h on the headwater side equal to:

$$d_h = \frac{aV^2}{2g}$$
Equation 30

where,

V = average velocity of water, *ft/s*

g = acceleration of gravity, 32.2 *ft/s²*

a   = coefficient of drag or shape factor (not less than 1.25)

Breaking wave loads on rigid vertical pilings and columns

       Breaking wave height shall be computed as:

$$H_b = 0.78 d_s \qquad\qquad \text{Equation 31}$$

where,

H_b = Breaking wave height, *ft*

d_s = Local still water depth, *ft*

       Unless more advanced studies are used, local still water depth can be computed using:

$$d_s = 0.65(BFE - G) \qquad\qquad \text{Equation 32}$$

where,

BFE   = Base flood elevation, *ft*

G   = Ground elevation, *ft*

       The net force produced by a breaking wave shall be assumed to act at the still water elevation and shall be computed by:

$$F_D = 0.5 \gamma_w C_D D H_b^2 \qquad\qquad \text{Equation 33}$$

where,

F_D = Net wave force, lb

γ_w = Unit weight of water, 62.4 *lb/ft³* for fresh water and 64 *lb/ft³* for salt water

C_D = Drag coefficient for breaking waves = 1.75 for circular piles or columns, and = 2.25 for square piles or columns

D   = Pile or column diameter, 1.4 times width of square pile or column, *ft*

Breaking wave loads on vertical walls

       The maximum pressures and net forces produced by a normally incident wave (depth limited in size, with $H_b = 0.78 d_s$) breaking on a rigid vertical wall shall be calculated by:

$$P_{max} = C_p \gamma_w d_s + 1.2 \gamma_w d_s \qquad \text{Equation 34}$$

and

$$F_t = 1.1 C_p \gamma_w d_s^2 + 2.4 \gamma_w d_s^2 \qquad \text{Equation 35}$$

where,

P_{max} = Maximum combined dynamic ($C_p \gamma_w d_s$) and static ($1.2 \gamma_w d_s$) wave pressures, also known as shock pressures, lb/ft^2

F_t = Net breaking wave force per unit length of structure, also known as shock, impulse, or wave impact force, developed near the still water elevation, lb/ft

C_p = Dynamic pressure coefficient (varies from 1.6 for temporary facilities to 3.5 for essential facilities)

d_s = Still water depth at base of building or structure where the wave breaks, ft

This procedure assumes the vertical wall reflects the wave to a height of $1.2 d_s$ as shown in Figure 17, and that the space behind the vertical wall is dry.

When there is water behind the wall the maximum combined pressure is given by Equation 34 and the net force shall be computed by:

$$F_t = 1.1 C_p \gamma_w d_s^2 + 1.9 \gamma_w d_s^2 \qquad \text{Equation 36}$$

where all the terms are as described before. This loading case is depicted in Figure 18.

The ASCE/SEI 7-05 document also contains some recommendations for breaking wave loads on non-vertical walls. The standards indicate the horizontal component of the breaking wave force is given by:

$$F_{nv} = F_t \sin^2 \alpha \qquad \text{Equation 37}$$

where,

F_{nv} = Horizontal component of breaking wave force, lb/ft

F_t = Net breaking wave force acting on a vertical surface, lb/ft

α = Vertical angle between non-vertical surface and the horizontal

The document also presents an expression to compute the load produced by an obliquely incident breaking wave:

$$F_{oi} = F_t \sin^2 \alpha \qquad \text{Equation 38}$$

where,

F_{oi} = Horizontal component of obliquely incident breaking wave force, *lb/ft*

F_t = Net breaking wave force (from normally incident waves) acting on a vertical surface, *lb/ft*

α = Horizontal angle between the direction of wave approach and the vertical surface
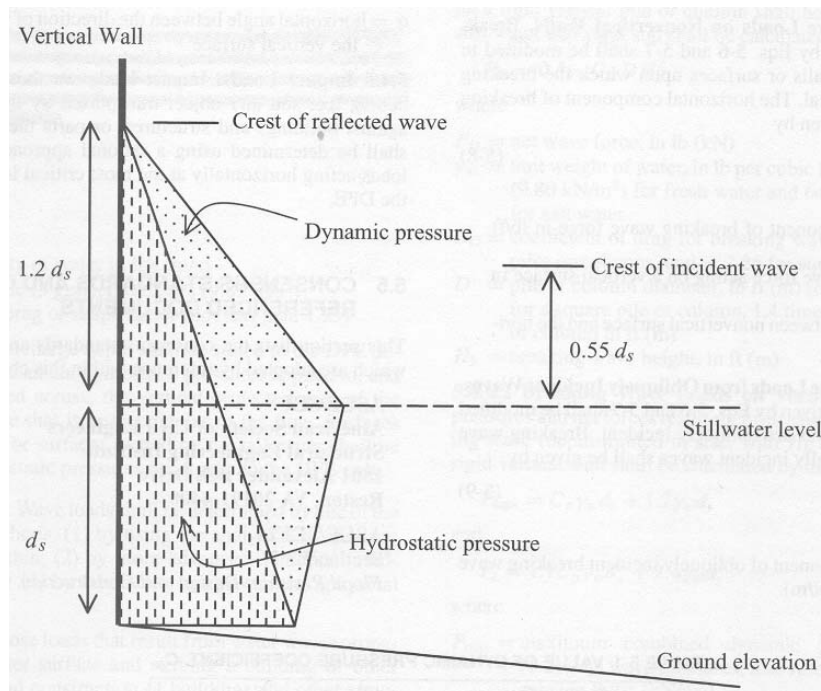
Figure 17. Wave pressures of normally incident wave breaking on a vertical wall, source: (ASCE/SEI 7-05).
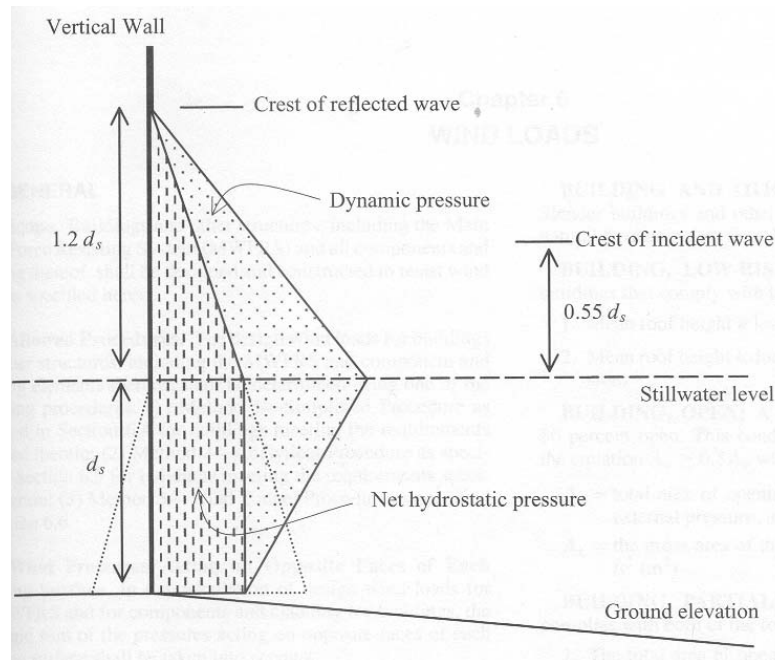
Figure 18. Normally incident breaking wave pressures acting on a vertical wall, source: (ASCE/SEI 7-05).

FEMA – Coastal Construction Manual – 2000

The Coastal Construction Manual of the Federal Emergency Management Agency provides a set of guidelines primarily intended for building these types of constructions located on coastal areas (FEMA, 2000). Chapter 11 of the Coastal Construction Manual describes flood and wave loads.

Design flood

For communities that adhere to the National Flood Insurance Program (NFIP), the design flood is equal to the base flood, the flood that has a 1% probability of being equaled or exceeded in any given year. The design flood should always be greater than or equal to the base flood.

Design flood elevation

The Design Flood Elevation can be higher than the Base Flood Elevation if the local officials choose a freeboard. The DFE should be equal or higher than the BFE. Figure 19 shows a schematic of the design flood elevations and other flood parameters.
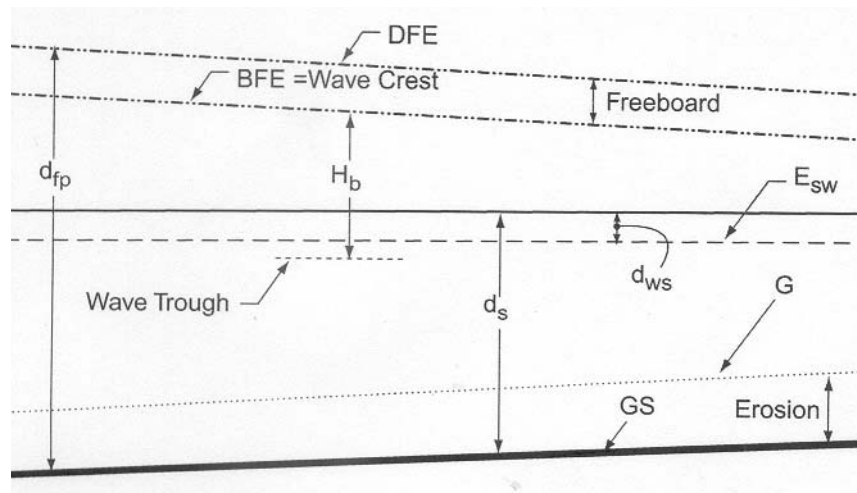
Figure 19. Parameters that determine flood depth, source: (FEMA, 2000).

The labels in Figure 19 represent the following parameters: *DFE* = Design Flood Elevation in feet above datum, d_{fp} = design flood protection in feet, *BFE* = Base Flood Elevation in feet above datum, *freeboard* = vertical distance in feet between *BFE* and *DFE*, H_b = breaking wave height = 0.78 d_s (note that 70% of wave height lies above E_{sw}), E_{sw} = design still water flood elevation in feet above datum, d_{ws} = wave setup in feet, d_s = design still water flood depth in feet, G = ground elevation, existing or pre-flood, in feet above datum, *Erosion* = loss of soil during design flood event in feet (not including effects of localized scour), *GS* = lowest eroded ground elevation adjacent to building in feet above datum (including the effects of localized scour).

Design flood depth

The design flood depth is given by the following equation:

$$d_s = E_{sw} + d_{ws} - GS$$
<div align="right">Equation 39</div>

where all the terms are as defined before.

Wave setup

FEMA recommends checking for wave setup, d_{ws}, in the *Hydrologic Analyses* section of the Flood Insurance Study (FIS) report, which is produced in conjunction with the FIRM for a community. FEMA also recommends checking the *Stillwater Elevation* table of the FIS for footnotes related to wave setup, because wave setup may not be included in the 100-year still water elevation.

Design wave height

The design wave height, H_b, shall be calculated as the height of depth-limited breaking waves, which are equivalent to 0.78 d_s. In this case 70% of the wave height lies above the still water flood level.

Design flood velocity

FEMA states that the estimation of design flood velocity in coastal flood hazard areas is highly uncertain. FEMA recommends flood velocities to be estimated conservatively, that is, assuming floodwaters can approach the structure from the most critical direction with a high velocity. FEMA provides the flowing equations to estimate flood velocity:

Lower bound	$V = d_s/t$	Equation 40
Upper bound	$V = \sqrt{gd_s}$	Equation 41
Extreme (tsunami)	$V = 2\sqrt{gd_s}$	Equation 42

where,

V = design flood velocity, *ft/sec*

d_s = design still water flood depth, *ft*

t = 1 *sec*

g = gravitational constant (32.2 *ft/sec²*)

FEMA recommends the design flood velocity in coastal areas to be taken between the upper and lower bounds. It is recommended that the lower bound be used for constructions located near the flood source or other buildings that may confine flood waters and increase flood velocities. It is advised to use the lower bound velocity where the structure is located in a site with a gentle slope and is unaffected by other structures. An equation is also given to estimate flood velocity for extreme events such as a tsunami.

Hydrostatic loads

FEMA also describes hydrostatic loads and the hydrostatic force per unit width is taken as:

$$f_{sta} = \frac{1}{2}\gamma d_s^2 \qquad \text{Equation 43}$$

where,

f_{sta} = hydrostatic force per unit width (*lb/ft*) resulting from loading against a vertical element with no water on the other side

γ = specific weight of water (62.4 *lb/ft³* for fresh water and 64.0 *lb/ft³* for salt water)

d_s = design still water flood depth in feet

Buoyancy force

$$F_{buoy} = \gamma Vol \qquad \text{Equation 44}$$

where γ is as described before and,

F_{buoy} = vertical hydrostatic force in *lb* resulting from the displacement of a given volume of flood water

47

Vol   = volume of flood water displaced by a submerged object in ft^3

Wave loads

      Wave load calculation requires knowledge of wave heights, which are assumed to be depth limited at the site of interest in the FEMA manual. FEMA uses its Wave Height Analysis for Flood Insurance Studies (WHAFIS) to estimate wave heights and wave crest elevations and recommends designers use the results of that analysis to calculate wave loads directly.

      Wave forces are divided into four categories:
1. Forces from non-breaking waves - can be computed as hydrostatic forces acting against piles.
2. Forces from breaking waves - will be of short duration but high magnitude.
3. Forces from broken waves - are similar to hydrodynamic forces caused by flowing of surging water.
4. Forces from uplift - usually caused by wave runup, deflection, or peaking against the underside of horizontal surfaces.

      The manual recommends the breaking wave load to be used as the design wave load, since it is considered the most severe. Breaking wave loads are divided into those breaking on small diameter vertical elements and those breaking on walls.

Breaking wave loads on vertical piles

      The breaking load on a pile is computed with the following equation and is assumed to act at the still water level.

$$F_{brkp} = \frac{1}{2} C_{db} \gamma D H_b^2 \qquad\qquad \text{Equation 45}$$

where,

F_{brkp} = Drag force acting at the still water level, *lb*

C_{db} = Breaking wave drag coefficient (2.25 for square or rectangular piles and 1.75 for round piles)

D = Pile diameter, ft

H_b = Breaking wave height in feet (0.78 d_s)

γ = Specific weight of water (62.4 lb/ft^3 for fresh water and 64 lb/ft^3 for salt water)

d_s = Design still water flood depth, ft

Breaking wave loads on vertical walls

      The design of walls assumes the vertical wall causes a standing wave to form on the seaward side of the wall, and that the crest of the wave reaches a height of 1.2 d_s above the still water elevation. The breaking wave load per unit length of wall is given by the following equations.

Case 1. Enclosed dry space behind wall

$$f_{brkw} = 1.1C_p\gamma d_s^2 + 2.41\gamma d_s^2 \qquad\qquad \text{Equation 46}$$

Case 2. Equal still water level on both sides of wall

$$f_{brkw} = 1.1C_p\gamma d_s^2 + 1.91\gamma d_s^2 \qquad\qquad \text{Equation 47}$$

where,

f_{brkw} = Total breaking wave load per unit length of wall (*lb/ft*) acting at the still water level

C_p = Dynamic pressure coefficient from Table 6

γ = Specific weight of water (62.4 *lb/ft³* for fresh water and 64 *lb/ft³* for salt water)

d_s = Design still water flood depth in feet

Table 6. Value of dynamic pressure coefficient as a function of probability of exceedance (FEMA, 2000).

Cp	Building type	Probability of exceedance
1.6	Accessory structure, low hazard to human life or property in the event of failure	0.5
2.8	Coastal residential building	0.01
3.2	High-ocupancy building or critical facility	0.001

The resulting static and dynamic pressures are shown on Figure 20.
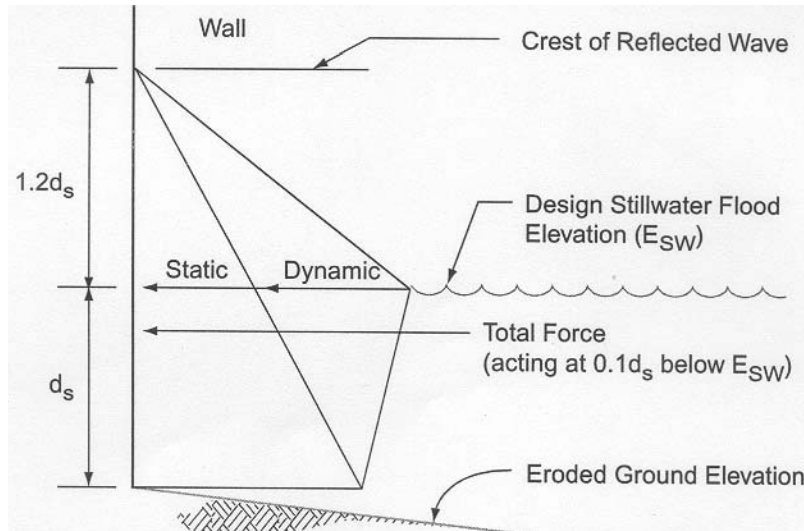
Figure 20. Static and dynamic wave pressure distribution on a vertical wall, source: (FEMA, 2000).

Hydrodynamic loads

The FEMA manual assumes hydrodynamic loads imposed by water velocities lower than 10 ft/sec can be converted to an equivalent hydrostatic load using the following expressions:

$$d_{dyn} = \frac{1}{2} C_d \frac{V^2}{g} \qquad \text{Equation 48}$$

where,

d_{dyn} = Equivalent additional flood depth to be applied to the upstream side of the affected structure, *ft*

V = Velocity of water in ft/sec from Equations 40 through 42

g = Acceleration due to gravity (32.2 *ft/sec²*)

C_d = Drag coefficient (2.0 for square or rectangular piles, 1.2 for round piles or from Table 7 for large obstructions)

$$f_{dyn} = \gamma d_s d_{dyn} \qquad \text{Equation 49}$$

50

where,

f_{dyn} = Equivalent hydrostatic force per unit width (*lb/ft*) due to low-velocity flow acting at the point 2/3 below the still water surface

γ = Specific weight of water (62.4 *lb/ft³* for fresh water and 64 *lb/ft³* for salt water)

The manual recommended the drag coefficient be estimated using Figure 21 and considering: (a) the ratio of the width of the element, *w*, to the height of the element, *h*, for fully immersed elements, or (b) the ratio of the width of the element, *w*, to the still water depth, d_s if the element is not fully immersed in water. The recommended drag coefficients are indicated in Table 7.
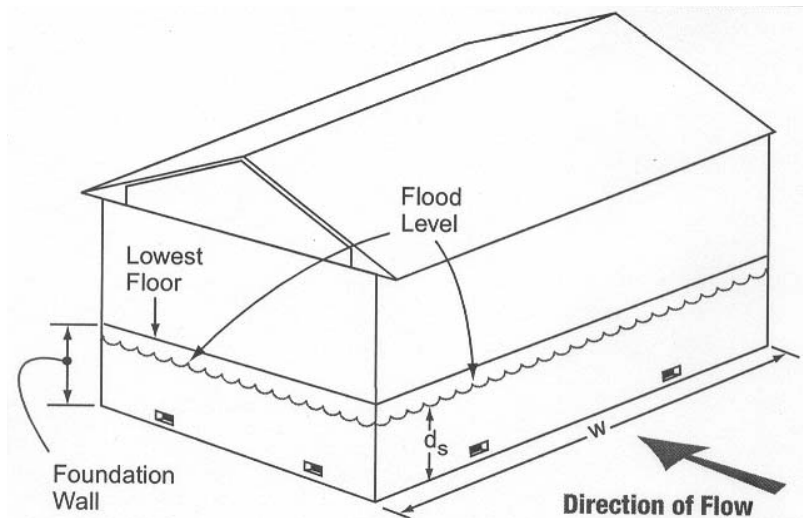
Figure 21. Determination of drag coefficient, source: (FEMA, 2000).

Table 7. Drag coefficients for ratios of w/d_s or w/h.

Width to depth ratio (w/d_s or w/h)	Drag coefficient C_d
From 1-12	1.25
13-20	1.3
21-32	1.4
33-40	1.5
41-80	1.75
81-120	1.8
>120	2.0

For water velocities greater than 10 ft/sec the following expression can be used to obtain the horizontal drag force:

$$F_{dyn} = \frac{1}{2} C_d \rho V^2 A$$

Equation 50

where,

F_{dyn} = Horizontal drag force in lb acting at the still water mid-depth

Cd = Drag coefficient (2.0 for square or rectangular piles, and from Table 7 for larger obstructions)

ρ = Mass density of fluid (1.94 *slugs/ft³* for fresh water and 1.99 *slugs/ft³* for salt water)

V = Velocity of water in *ft/sec* from Equations 40 through 42

A = Surface area of obstruction normal to flow in *ft²* = *wd_s* or *hw*, see Figure 21

Comments

The literature cited in this section indicates that a specific method for the design of bridge superstructures subjected to the action of wave forces is not provided in any of the guidelines. It can also be seen that some available information on this topic is even contradictory.

INFORMATION RELATED TO WAVE FORCES ON BRIDGE SUPERSTRUCTURE

This section includes summaries of research papers, book chapters, and research reports that contain information related to wave forces on elements similar to bridge decks.

Tedesco et al. – Response of structures to water waves – 1999

This section shows a summary of a section of the book Structural Dynamics by Tedesco et al. (Tedesco et al., 1999). The authors indicated that pressure and drag produce the main hydrodynamic forces acting on structures. The interaction between a structure and waves is greatly influenced by the size of the structure relative to the wavelength, L. The following observations hold for a structure such as pile characterized by its diameter, D. If D/L is small then the Morison equation can be used to estimate forces, since wave diffraction is negligible. If D/L is large, diffraction theory is used to estimate forces, since the structure modifies the wave field significantly. When the wave field is not greatly modified by the structure and the drag forces are small, the forces are dominated by inertia and can be estimated by the Froude-Krylov method (Tedesco et al., 1999).

A wave field is said to not be affected by the presence of a structure when the ocean waves just a wavelength away from the structure (50 to 100 pile diameters in the case of the pile) the waves seem to be unaffected by the presence of the structure.

The wave field may be significantly affected by the presence of a structure such as in the case of a floating dock, where some wave energy travels around and under the dock, while an important portion of the incident wave is reflected.

Morison equation

If the diameter of the structure is less than 5% of the wave length the assumption that the wave field is not affected by the structure is reasonable. Some examples of these types of structures include structural elements in oil platforms, piles, pipelines, and moorings. The Morison equation is the most common tool used to estimate the in-line wave force on small bodies.

Consider a horizontal pressure component induced by the wave on a vertical cylinder as indicated in Figure 22. Applying Bernoulli's equation, the fluid pressure is given by:
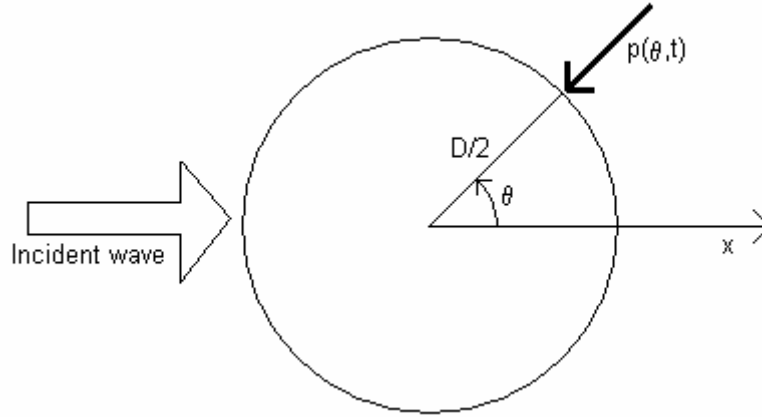
Figure 22. Pressure induced by wave flow through a cylinder (Tedesco et al., 1999).

$$p = -\rho \frac{\partial \phi}{\partial t} - \frac{\rho}{2}\left(u_r^2 + u_\theta^2\right) - \rho g z + C_B \qquad \text{Equation 51}$$

Where ρ and θ are the polar coordinates, u is the water particle velocity, ϕ is the velocity potential, and C_B is the Bernoulli constant. Integrating the pressure over the circumference gives the following force per unit length of cylinder in the wave direction:

$$f_{ix} = -\int_{-\pi}^{\pi} p\left(\frac{D}{2},\theta,t\right)\cos\theta \frac{D}{2} d\theta \qquad \text{Equation 52}$$

Thus the horizontal force per unit length of cylinder is:

$$f_{ix} = \left(1 + C_a\right)\rho \frac{\pi D^2}{4}\frac{du}{dt} \qquad \text{Equation 53}$$

This force is called the inertia force because it is proportional to the acceleration of the fluid. The coefficient C_a is called the added mass coefficient and is equal to one for a vertical circular cylinder. An inertia coefficient that accounts for different geometries is given by:

$$C_m = 1 + C_a \qquad \text{Equation 54}$$

where C_m is called the inertia coefficient.

54

In addition to the inertia forces, drag forces will develop on the structure due to fluid-structure interaction. A drag force will develop from friction between the fluid and the structure, and another force results from a differential of pressure across the structure when the flow separates. The total drag force from the two sources can be written as:

$$f_{dx} = \frac{1}{2}\rho C_d D|u|u \qquad \text{Equation 55}$$

where,

f_{dx} = Drag force per unit length of a cylinder in the direction of flow (x in this case)

C_d = Drag force coefficient

u = Water particle velocities, *ft/sec*

Assuming the drag and inertia forces can be added, the Morison equation is obtained:

$$f_x = f_{dx} + f_{ix} = \frac{1}{2}\rho C_d D|u|u + \rho C_m \frac{\pi D^2}{4}\frac{du}{dt} \qquad \text{Equation 56}$$

In Equation 56 it is assumed the pile is not present when calculating the water particle velocity and acceleration at the center of the pile.

If linear wave theory is used to compute fluid velocity and acceleration at x = 0 (the center of the pile), the Morison equation becomes:

$$f_x = C_d f_{xd} + C_m f_{xm} \qquad \text{Equation 57}$$

where,

$$f_{xd} = \frac{1}{8}\rho D H^2 \omega^2 \frac{\cosh^2[k(h+z)]}{\sinh^2(kh)}|\cos(-\omega t)|\cos(-\omega t) \qquad \text{Equation 58}$$

$$f_{xm} = \frac{\pi}{8}\rho D^2 H \omega^2 \frac{\cosh[k(h+z)]}{\sinh^2(kh)}\sin(-\omega t) \qquad \text{Equation 59}$$

The Keulegan-Carpenter number affects the magnitude of the drag and inertia coefficients shown in previous equations:

$$K = \frac{u_m T}{D} \qquad \text{Equation 60}$$

where K is the Keulegan-Carpenter number, u_m is the magnitude of the horizontal velocity, T is the wave period, and D is the diameter of the structure.

Force coefficients

Inaccurate predictions can be made when using linear wave theory to determine the drag and inertia coefficients. This happens because linear wave theory cannot make predictions for force values above the still water level (SWL), while the largest forces develop near the wave crest in reality. It is common engineering practice to use advanced nonlinear theories such as Stokes 5th or stream function theory.

Marine plants and animals often develop on structural elements. This growth does not contribute to structural stiffness, however, it does increase the weight of structural elements. These biofouling increase the drag and inertia coefficients, as well as the diameter of the structural elements. Examples of these plants and animals range from soft, such as sponges and seaweed, to hard, such as barnacles and mussels. Table 8 illustrates drag and inertia coefficients for typical structural shapes without including any biofouling effects. It should be mentioned that the drag and inertia coefficients depend on the Reynolds number and the Keulegan-Carpenter number (Sarpkaya, 1981; Wilson, 2003). For a dependence on the drag coefficient on the Reynolds number, see Figure 23 (Çengel and Cimbala, 2006).

Table 8. Drag and inertia coefficients for typical geometries, source: (Tedesco et al., 1999).
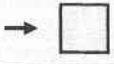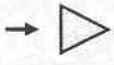
Section Shape	C_d	C_m
→ ☐	2.0	2.5
→ ☐	0.6	2.5
→ ▷	2.0	2.3
→ ◁	1.3	2.3
→ ◇	1.5	2.2
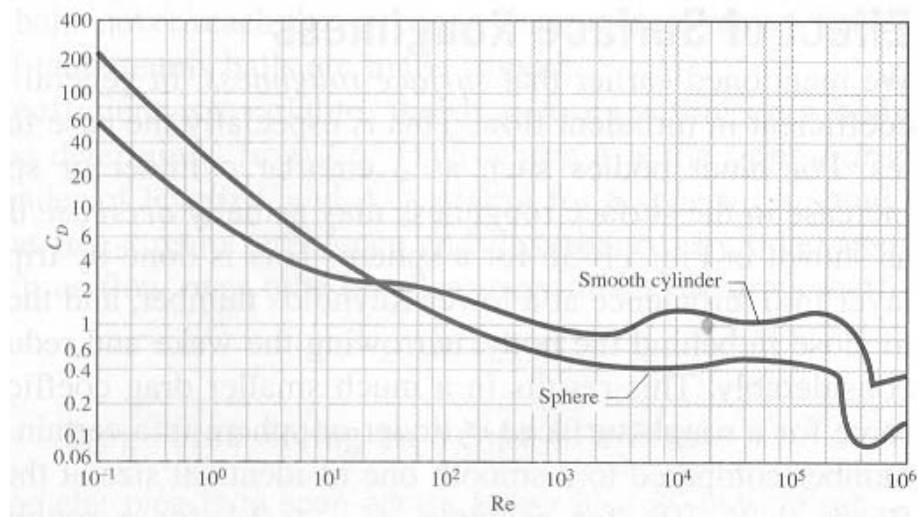
Figure 23. Average drag coefficient for cross flow over a smooth cylinder and a smooth sphere, source: (Cengel and Cimbala, 2006).

Lwin – Floating bridges – 1999

Floating bridges are superstructures typically subjected to sea currents and sea waves. Therefore, as an introduction to the parameters required for the design of bridges exposed to water forces induced by hurricanes, a description of the design factors that are commonly applied to floating bridges will be given in this section.

A large number of bridges span waterways, however, when large bodies of water with considerable depths and soft sea bottom, where conventional piers are impractical, need to be crossed, floating bridges can be cost-effective solutions (Lwin, 1999). Floating bridges have been built for centuries for military operations. Modern floating bridges can be made of concrete, wood, steel, or a combination of materials.

The design of floating bridges needs to conform to AASHTO Bridge Design Specifications as much as possible (Lwin, 1999). The performance of a floating bridge is highly sensitive to environmental forces such as those imposed by waves, winds, and currents.

Winds and waves are the major environmental loads. The environmental loads induce horizontal, vertical, and torsional loads on a floating bridge (Lwin, 1999). These loads are a function of wind speed, wind direction, wind duration, fetch length, channel configuration, and depth. Floating bridges are typically designed for normal storm conditions, which is the maximum storm that is likely to occur once a year. Floating bridges are also designed for extreme conditions, which are caused by the maximum storm likely to occur once in 100 years (Lwin, 1999). Lwin provides some recommendations for load factors to be used in the design of floating bridges following the AASHTO Bridge Design Specifications (Lwin, 1999).

Floating bridges are typically built using a box girder structure, with segments to control progressive failure (Lwin, 1999; Leira and Langen, 1984).

The design of floating bridges may require a dynamic analysis. Leira and Langen used a probabilistic dynamic analysis method to study a floating bridge using finite elements (Leira and Langen, 1984). In this paper the authors modeled the sea waves with a harmonic function.

Shih and Anastasiou – Wave induced uplift pressures acting on a horizontal platform – 1989

A report by Shih and Anastasiou looks at experimental values of wave loads on horizontal platforms (Shih and Anastasiou, 1989). The experimental data is validated through the hindcasting of wave data obtained in Maya Quay, Kobe, during a typhoon in 1964. The authors used their measurements and the best-fit technique to modify Teruaki Furudoi's formula for uplift force:

$$\frac{F_{mean}}{\rho g w H_c c} = 10.91 * \left(\frac{H_u}{d_o}\right) - 10.91 \qquad \text{Equation 61}$$

where,

F_{mean} = Mean impact force

ρ = Specific water density

w = Width of the platform

H_c = Wave crest height above mean water level

c = Clearance of the platform above mean water level

and

$$H_u = H_o \left\{ 1 + \left(\pi H_o \big/ L_o\right) \coth\left(2\pi h_o \big/ L_o\right) \right\} \qquad \text{Equation 62}$$

where,

H_o = Height of incident waves at the off-sea

L_o = Deep water wave length

h_o = Water depth

d_o = Distance between the still water surface and the apron

Equation 62 yielded results compatible with those hindcasted at the site. These being F_{mean} = 5.2 ton/m and F_{max} = 8.0 ton/m. Note when solving for F_{max} to replace F_{mean} with F_{max} and replace 10.91 with 16.67.

The authors also examined three different types of pressure: slow varying positive pressure, P_{+ve}, slow varying negative pressure, P_{-ve}, and impact pressure, P, for different clearance and wave types. These experiments produced maximum values of 1.52 KN, 0.72 KN, and 19.48 KN/m² for P_{+ve}, P_{-ve}, and P, respectively. The authors concluded the slowly varying positive pressure has two components: the hydrostatic head due to the wave crest elevation, and the hydrodynamic head caused by the wave induced fluid motion; although when the platform is free from any lateral constraints, the P_{+ve} is less than the hydrostatic head alone. The slowly varying negative pressure is independent of clearance, but depends greatly on the width of the platform. While the impact pressure, P, is dependent on the wave height, platform clearance, and the properties of the wave impacting the structure.

Suchithra and Koola – A study of wave impact on horizontal slabs – 1995

A paper written by Suchithra and Koola examines the use of stiffeners in deck design and the variation in the slamming coefficient C_s, which is used to find the vertical forces imposed by slamming waves. The vertical force is found using:

$$F_s = \frac{1}{2} C_s \rho A V^2 \qquad \qquad \text{Equation 63}$$

where,

F_s = Slamming force

A = Area of contact

ρ = Mass density of water

V = Vertical water particle velocity

C_s = Slamming coefficient

Equation 63 can only be effectively used if a valid value of C_s is known. The authors obtained experimental values for C_s ranging from 2.5 to 10.2, but also found the coefficient to be dependent on the wave frequency. The authors then defined a modified

slamming coefficient, C_{ns}, to be used for design purposes independent of frequency. This modified slamming coefficient may be found using:

$$C_{ns} = C_s \, d/L \qquad \text{Equation 64}$$

where,

d = Deck clearance

L = Deep water wave length

A mean value of 1.7 was obtained for C_{ns}, which could be used in design due to its frequency independence (Suchithra and Koola, 1995).

Bea et al. – Wave forces on decks of offshore platforms – 1999

Isaacson and Prasad stated that the total forces imposed on an offshore platform deck could be formulated as (Isaacson and Prasad, 1992):

$$F_{tw} = F_b + F_s + F_d + F_l + F_i \qquad \text{Equation 65}$$

where,

F_b = Buoyancy force (vertical)

F_s = Slamming force

F_d = Drag (velocity-dependent) force

F_l = Lift (velocity-dependent, normal to wave direction) force

F_i = Inertia (acceleration dependent)

The force idealized by Isaacson and Prasad is shown in Figure 24.

Slamming force

A horizontal slamming force can be estimated with the expression (Bea et al., 1999):

$$F_s = 0.5C_s \rho A u^2 \qquad \text{Equation 66}$$
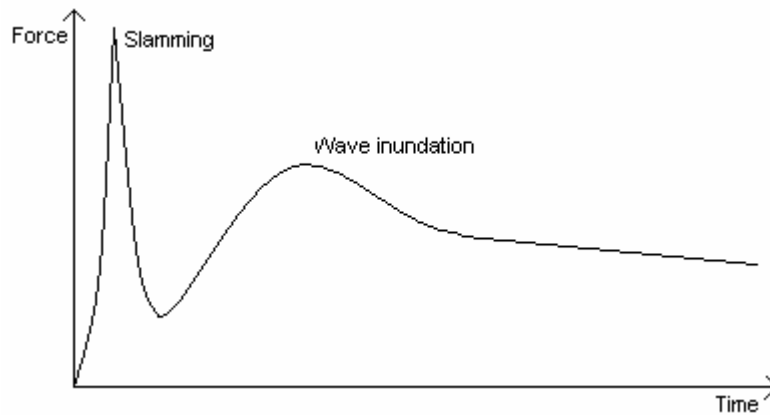
Figure 24. Idealized wave force on a platform deck.

where,

F_s = Slamming force

C_s = Slamming coefficient

ρ = Mass density of seawater (= 1.99 *slugs/ft³* for seawater)

A = Vertical deck area subjected to the wave crest

u = Horizontal fluid velocity in the wave crest

Isaacson and Prasad asserted that C_s could vary approximately between π and 2π.

According to Bea et al., the effective slamming force can be obtained by including a dynamic load factor:

$$F_{se} = F_e F_s$$ Equation 67

where,

F_{se} = Effective slamming force

F_e = Dynamic load factor

F_s = Slamming force

The value of the dynamic load factor depends on the relative values of the duration of loading and the period of vibration of the structure. Bea et al. indicate that the dynamic load factor is equal to:

$$DAF = 2\pi\alpha\left(t_d / T_n\right)$$
Equation 68

where,

t_d = duration of the impact loading

T_n = natural period of the deck

α = reflects the time-magnitude characteristics of the impact loading ($\alpha = 0.5$ for triangular loading and $\alpha = 2/\pi$ for half-sine loading).

Inundation forces

The horizontal drag force can be estimated with the equation:

$$F_d = 0.5\rho C_d A u_h^2$$
Equation 69

where,

F_d = Horizontal drag force

C_d = Drag coefficient

A   = Horizontal area

u_h = Horizontal velocity of water particles

The vertical lift force can be found with the expression:

$$F_l = 0.5\rho C_l A u_v^2$$
Equation 70

where,

F_l = Vertical lift force

C_l = Lift coefficient

A   = Vertical area

u_v = Vertical velocity of water particles

The horizontal inertial force can be determined as:

$$F_i = \rho C_m V a \qquad \text{Equation 71}$$

where,

F_i = Inertial force

C_m = Inertia coefficient

V = Volume of deck inundated

a = Horizontal acceleration of water particles

McConnell et al. – Piers, jetties, and related structures exposed to waves – 2004

A research report by McConnell et al. presents a methodology to estimate wave forces on horizontal elements (McConnell et al., 2004). The authors adopt the Rayleigh distribution as a first approximation to the distribution of individual wave heights. With this assumption, the most probable value of the maximum wave height H_{max} can be estimated with the relationship:

$$\left[\frac{H_{max}}{H_{1/3}}\right]_{mode} \approx 0.706\sqrt{\ln N_z} \qquad \text{Equation 72}$$

where,

H_{max} = Maximum wave height

$H_{1/3}$ = Significant wave height

N_z = Number of waves (can be calculated knowing the wave period and assuming a storm duration)

The authors follow Stansber's approximation to estimate the crest height in deep water as:

$$\eta_{max} = \frac{H_{max}}{2}\exp\left(\frac{2\pi}{L_m}\frac{H_{max}}{2}\right) \qquad \text{Equation 73}$$

where,

η_{max} = expected maximum crest elevation, ft

L_m = Wave length, *ft*

H_{max} = Maximum wave height, *ft*

McConnell et al. report the results of a series of experiments made on a model of a platform deck. The model was designed to resemble the configuration and dimensions of a typical platform. The model was made to a scale of 1:50 of a typical offshore structure. The waves used to test the specimen were also representative of an offshore structure.

The model was tested with three configurations: (a) deck with beams, (b) flat deck (no beams), and (c) deck with beams and side panels. The parameters used in the test modelled the following conditions: H_s = 2.5 to 5.5 m, T_m = 5 to 15 s, water depth 18.75 and 15 m, clearance 0.25 to 4 m, relative water depth (h/L_m) = 0.48, and sampling frequency 40 Hz.

The authors recorded the three force parameters defined next and shown in :

F_{max} = Impact force

$F_{qs+,\ v\ or\ h}$ = Maximum positive (upward or landward) quasi-static force

$F_{qs-,\ v\ or\ h}$ = Maximum negative (downward or seaward) quasi-static force
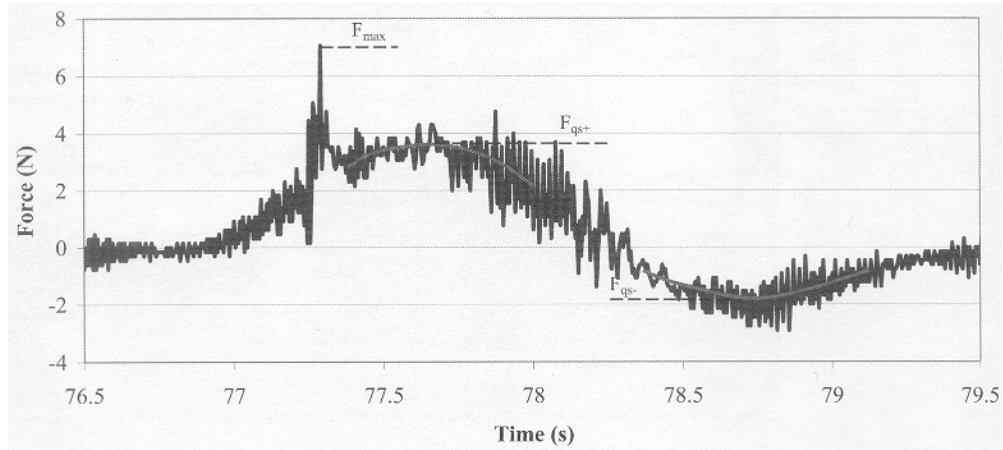
Figure 25. Force parameters, source: (McConnell et al., 2004).

The authors modelled the design wave with a maximum crest elevation as shown in Figure 26. According to this diagram, the hydrostatic pressures acting on the side and bottom of a deck are:

$$p_1 = (\eta_{max} - b_h - c_1)\rho g \qquad \text{Equation 74}$$

$$p_2 = (\eta_{max} - c_1)\rho g \qquad \text{Equation 75}$$

where,

p_1 = Pressure at the top of the deck

p_2 = Pressure at the bottom of the deck

b_w = Deck width

b_h = Deck height

b_l = Deck length

c_1 = Clearance

η_{max} = Maximum wave crest elevation

Thus, the hydrostatic horizontal wave force is:

$$F_h^* = b_w \left(\eta_{\max} - c_1 \right) \frac{p_2}{2} \qquad \text{for } \eta_{\max} \le c_1 + b_h \qquad \text{Equation 76}$$

$$F_h^* = b_w b_h \frac{p_1 + p_2}{2} \qquad \text{for } \eta_{\max} > c_1 + b_h \qquad \text{Equation 77}$$

and the hydrostatic vertical wave force is:

$$F_v^* = b_w b_l p_2 \qquad \text{Equation 78}$$
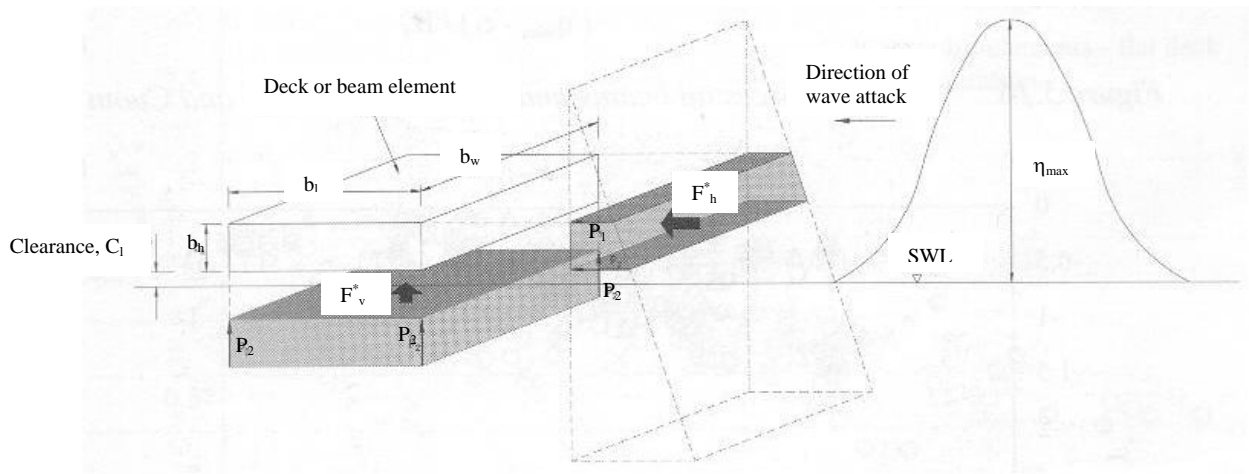
Figure 26. Definition of wave forces, modified from: (McConnell et al., 2004).

According to the experimental studies carried out by the authors, the ratio of the measured wave forces (F_{qs+} or F_{qs-} as defined in Figure 25) to the hydrostatic forces (F_h^* or F_v^*) for different ratios of maximum freeboard (η_{max}-c_1) to significant wave height are given in a set of plots. The forces described are the average of the highest four values recorded in 1000 waves ($F_{1/250}$). For the case of upward forces on beams and decks (ratio of F_{qs+} to F_v^*) the maximum-observed ratio of wave load to hydrostatic force is 4.5. For downward forces (ratio of F_{qs-} to F_v^*) the maximum-recorded ratio is 2.3. The maximum ratio for horizontal forces (ratio of F_{hqs} to F_h^*) is approximately 11.

The authors also measured impact wave forces on the model. The maximum values recorded were as follows: the ratio of the maximum observed vertical impact force over the quasi-static wave force (ratio of F_{max} to F_{vqs+}) was approximately 5, following the definitions of Figure 25. As far as the horizontal force is concerned, the maximum observed impact ratio (ratio of F_{max} to F_{hqs+}) was approximately 7.

The authors indicate that according to laboratory studies vertical loads can be higher than horizontal loads.

From the results of their experiments the authors found the following equations based on the best-fit trend to the experimental data.

For vertical forces:

$$\frac{F_{vqs(+or-)}}{F_v^*} = \frac{a}{\left[\dfrac{\eta_{max} - c_l}{H_s}\right]^b}$$

Equation 79

The best-fit coefficients for upward vertical forces (seaward beam and deck) were $a = 0.82$ and $b = 0.61$, and for downward vertical forces (seaward beam and deck) the coefficients were $a = -0.54$, $b = 0.91$.

For horizontal forces:

$$\frac{F_{hqs(+or-)}}{F_h^*} = \frac{a}{\left[\dfrac{\eta_{max} - c_l}{H_s}\right]^b}$$

Equation 80

The best-fit coefficients for the case of shoreward horizontal forces (seaward beam) were $a = 0.45$ and $b = 1.56$, while for seaward horizontal forces (seaward beam) were $a = -0.20$ and $b = 1.09$.

Goda – Random seas and design of maritime structures – 2000

Goda presents an overview of the development of wave pressure formulas (Goda, 2000). The formula proposed by Hiroi in 1919 yields a pressure as a function of wave height:

$$p = 1.5\rho g H$$
Equation 81

where,

p = Pressure assumed to act uniformly over the full height of an upright section, or to an elevation of 1.25 times the wave height above the still water level, whichever is less

ρ = Density of seawater

g = Acceleration of gravity

H = Incident wave height

Where wave information was scarce, Hiroi recommended using a design wave height of 0.9 times the water depth. During the development of design equations engineers debated whether to use $H_{1/3}$, $H_{1/10}$, or H_{max} as the design wave, concluding that H_{max} should be substituted in the wave pressure formulas.

The wave pressure distribution proposed by Goda is illustrated in Figure 27. This figure helps clarify the meaning of the terms involved in the pressure coefficients proposed by the author. The equation is applicable to breaking and non-breaking waves. The terms shown in the figure denote the following: h, water depth in front of the breakwater, d, depth above the armor layer of the rubble foundation, h', distance from the design water level to the bottom of the upright section, and h_c, crest elevation of the breakwater above the design water level.
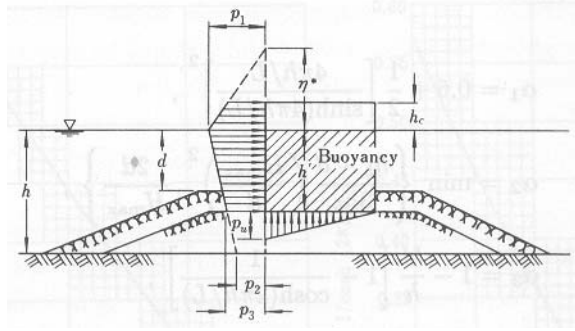
Figure 27. Wave pressure distribution on the vertical section of a breakwater, source: (Goda, 2000).

Goda specifies that the highest wave in the design sea state should be used. Its height should be taken as $H_{max} = 1.8\ H_{1/3}$ seaward of the surf zone, whereas within the surf zone the height should be taken as the highest random breaking wave H_{max} at the location at a distance $5H_{1/3}$ seaward of the breakwater. $H_{1/3}$ should be estimated at the depth of the location of the breakwater. The period of the highest wave is taken as that of the significant wave: $T_{max} = T_{1/3}$.

Goda specifies that the elevation to which the wave pressure is exerted be:

$$\eta^* = 0.75(1 + \cos\beta)H_{max}$$ Equation 82

where,

β = Angle between the direction of wave approach and a line normal to the breakwater. Due to the uncertainty of the wave direction, the principal wave direction should be rotated $15°$ toward the line normal to the breakwater.

The wave pressure on the front of a vertical wall is thus:

$$p_1 = \frac{1}{2}(1 + \cos\beta)(\alpha_1 + \alpha_2 \cos^2\beta)\rho g H_{max}$$ Equation 83

$$p_2 = \frac{p_1}{\cosh(2\pi h/L)}$$ Equation 84

$$p_3 = \alpha_3 p_1$$ Equation 85

where,

70

$$\alpha_1 = 0.6 + \frac{1}{2}\left[\frac{4\pi h/L}{\sinh(4\pi h/L)}\right]^2$$

Equation 86

$$\alpha_2 = \min\left\{\frac{h_b - d}{3h_b}\left(\frac{H_{max}}{d}\right)^2, \frac{2d}{H_{max}}\right\}$$

Equation 87

$$\alpha_3 = 1 - \frac{h'}{h}\left[1 - \frac{1}{\cosh(2\pi h/L)}\right]^2$$

Equation 88

h_b = water depth at the location at a distance $5H_{1/3}$ seaward of the breakwater

L = Wave length at the structure

The previous equations are assumed to hold even in the case of wave overtopping.

The buoyancy pressure is calculated for the displaced volume of the structure in still water below the design water level. The uplift pressure acting at the bottom of the structure is assumed to have a triangular distribution with toe pressure equal to:

$$p_u = \frac{1}{2}(1 + \cos\beta)\alpha_1\alpha_3\rho g H_{max}$$

Equation 89

H_{max} is used in the previous equation based on the philosophy that a breakwater should be designed to be safe against a wave with the largest pressure among storm waves. Goda recommends a value of H_{max} = 1.8 $H_{1/3}$ based on performance of many prototype breakwaters. However, the design engineer could select H_{max} to have a different value. The criterion used in deriving the equation proposed by Goda recognizes that the greatest wave pressure is exerted not by waves just breaking at the site, but by waves which have already begun to break at a short distance seaward of the breakwater, midway through the plunging distance. The value of the empirical coefficient α_1 in the pressure intensity p_1 has been determined based on tendency for wave pressure to increase with the wave period. The equation for coefficient α_2 represents the tendency of

the pressure to increase with the rubble foundation height. Coefficient α_3 was derived assuming a linear pressure variation between p_1 and p_2 along a vertical wall.

Goda also mentioned that the wave pressure exerted on the upright section of a vertical breakwater is approximately proportional to the height of the wave incident on the breakwater, and is to some extent influenced by the wave period, the seafloor slope, and the shape and dimensions of the rubble mound foundation among other factors. Laboratory tests indicated that the breaking wave pressure increases as the seafloor slope becomes steeper. The wave pressure and the width of the upright section of the breakwater decrease gradually as the incident wave angle decreases.

Goda also addressed the topic of impulsive wave pressure. He states that the impulsive pressure has a very short duration, although it may rise to over an order of magnitude above the hydrostatic pressure corresponding to the wave height. The author states that with an increase in the incident angle of the wave, the impulsive pressure decreases rapidly. A questionnaire based mostly on the work of Mitsuyasu is shown in Figure 28 to evaluate the danger of impulsive breaking wave pressure (Mitsuyasu, 1962). The angle between the breakwater longitudinal axis and the wave longitudinal axis is called the angle of incidence. Goda explains that a Japanese document written by Tanimoto suggested that if the angle of incidence is greater than 20°, the danger of impulsive breaking wave pressure is small (Tanimoto, 1976).
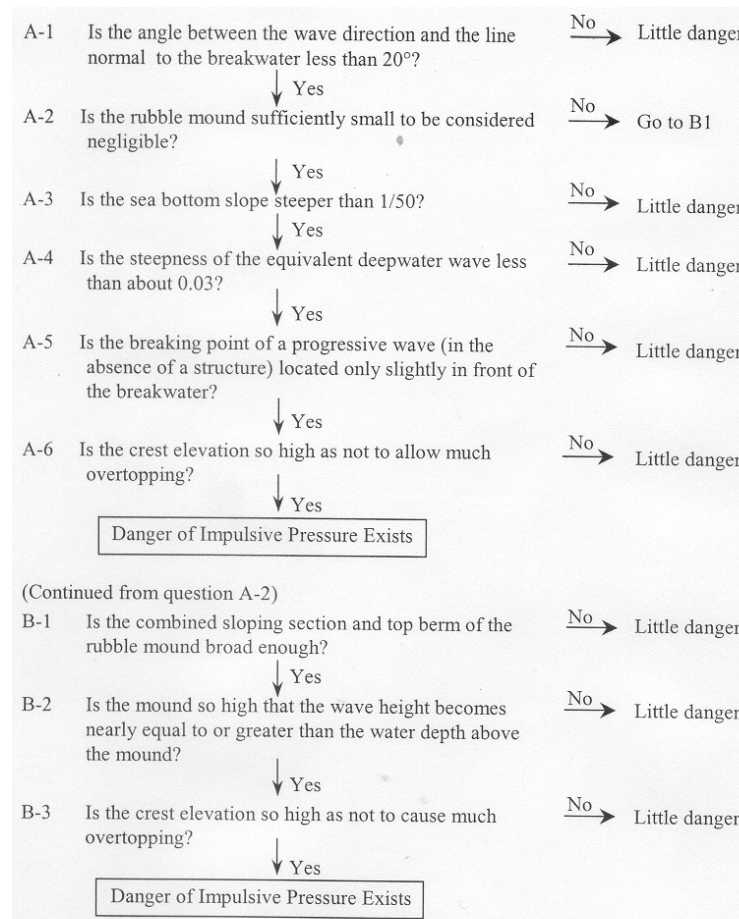
Figure 28. Questionnaire to evaluate the danger of impulsive wave pressure, source: (Goda, 2000).

Faltinsen – Sea loads on ships and offshore structures – 1990

Faltinsen indicates that the significant wave height can be larger than 2 m for 60% of the time in the North Sea area (Faltinsen, 1990). Wave heights larger than 30 m are possible. The mean period can range from 15 to 20 sec in extreme weather conditions and is seldom below 4 sec. The author points out that viscous effects and potential flow effects may be important in the determination of the wave induced motions and loads on maritime structures. Figure 29 can be used to make quick estimates as to when viscous effects and different potential flow effects are important. Regarding engineering tools, model tests are shown to have problems with scaling test results,

while computer programs are having an important modelling role in calculating wave-induced motions and loads on ships and offshore structures. However, the author indicates that more theoretical work is still needed on separated viscous flow and extreme wave effects on ships and offshore structures.
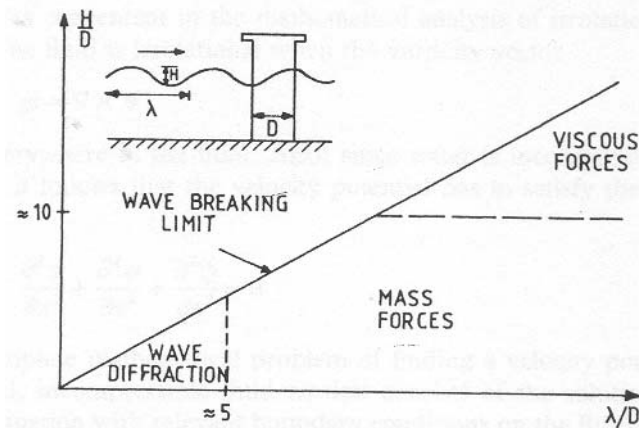
Figure 29. Relative importance of viscous drag, mass, and diffraction forces on marine structures, source: (Faltinsen, 1990).

Faltinsen studied the effects of water impact. He states that the duration of slamming pressure is in the milliseconds range. The slamming pressure is highly localized, and the position where high slamming occurs changes with time. The author presents a derivation to obtain a slamming pressure for a circular cylinder impacting a body of water at rest. Assuming irrotational flow and incompressible fluid he presents an equation for the hydrodynamic pressure and finds a slamming coefficient to be equal to π. However, the author reports that an experimental study by Campbell and Weynberg reports a value of 5.15 at the time of impact (Campbell and Wyenberg, 1980). The author indicates that it may be valid to use only a fraction of the slamming loads because, the derivations presented assumed fluid incompressibility, and when compressibility is accounted for, the pressure has a peak value. This rationale is supported by the work of Hagiwara and Yuhara, where the authors indicate that the peak value of the slamming pressure gives a conservative estimate of the load distribution in

the design of structural parts against slamming loads (Hagiwara and Yuhara, 1976). Hagiwara and Yuhara found that by introducing an equivalent static pressure in analyzing the strain of a rectangular panel due to slamming load, the equivalent static pressure was approximately one third of the maximum impact pressure.

Hinwood – Design for tsunamis – coastal engineering considerations – 2005

Sliding of tectonic faults in the ocean is the main origin of tsunami waves. Although it is not very likely that the Texas or U.S. Atlantic coasts will experience tsunami waves, it is possible. Searching on the NOAA/NGDC world tsunami database it can be seen that 12.2 m high tsunami waves were recorded on the coast of Portugal on November 1, 1755 (NOAA/NGDC-2, 2006). A tsunami wave with the same height was recorded on the coast of Ireland on November 21, 1894. Hinwood indicates that neglecting the small loss of energy with distance travelled by a wave, results in a small wave height reduction. In deep water a small tsunami travels at the speed:

$$c = \sqrt{gd} \qquad \text{Equation 90}$$

where g is the acceleration of gravity, and d is the ocean depth. In mid ocean with depths of 16400 ft, c = 500 mph, and for a typical shore depth of 164 ft, c = 50 mph. The author presents an analysis of wave forces on coastal structures, using the same equations given by Bea (Bea et al., 1999). The horizontal force contains a hydrostatic component, owing to water gradients at both sides of the structure. The horizontal force also has a drag, impact, and inertia components. The vertical force has three components: a buoyancy term, a vertical dynamic lift force term, and a negative term (downward force) owing to the weight of water trapped on the structure after the wave passes (Hinwood, 2005).

Kaplan – Wave impact forces on offshore structures – 1992

Kaplan presents a theoretical method to predict forces on horizontal cylinders and on flat plate decks (Kaplan, 1992). For a horizontal cylinder Kaplan proposed to estimate the vertical force per unit length of cylinder with the expression:

$$F_z = \rho g A_i + (m_3 + \rho A_i)\ddot{\eta} + \frac{\partial m_3}{\partial z}\dot{\eta}^2 + \frac{\rho}{2}\dot{\eta}|\dot{\eta}|d\left(\frac{z}{r}\right)C_{Dz}\left(\frac{z}{r}\right)$$

Equation 91

where,

F_z = Vertical force per unit length

ρ = Water density

g = Acceleration of gravity

A_i = Immersed cross sectional area of the cylinder

m_3 = Vertical added mass

z = Immersed depth of cylinder

$\dot{\eta}$ = First derivative of wave crest elevation with respect to time

$\ddot{\eta}$ = Second derivative of wave crest elevation with respect to time

r = Radius of cylinder

d = Cylinder diameter

C_{Dz} = Drag coefficient for vertical flow (varies with immersed depth of the cylinder)

Figure 30 illustrates the definitions used by Kaplan for z, r, A_i, H, and η used in Equation 91.
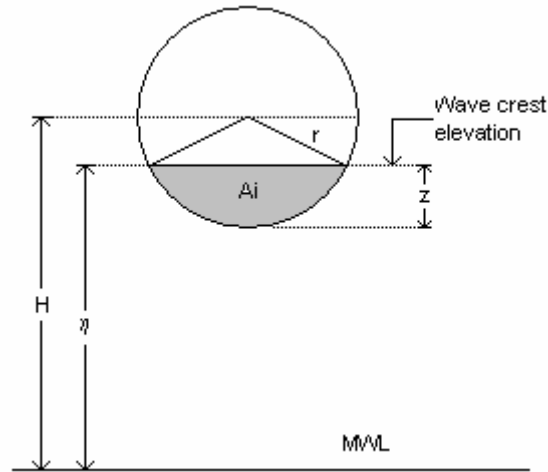
Figure 30. Definitions of z, r, A_i, H, and η.

The first term in Equation 91 is the buoyancy force, the term $\rho A_i \ddot{\eta}$ is due to the effect of the spatial pressure gradient in the waves, the terms including m_3 are obtained from the time rate of change of vertical fluid momentum, the last term is the drag force component.

The horizontal force produced on a cylinder by waves is given by:

$$F_y = \left(\rho A_i + m_2\right)\dot{v} + \frac{\partial m_2}{\partial z}\dot{\eta}v + \frac{\rho}{2}v|v|h\left(\frac{z}{r}\right)C_{Dy}\left(\frac{z}{r}\right)$$

Equation 92

where,

m_2 = Horizontal added mass (depends on the level of immersion)

v = Horizontal wave orbital velocity

h = Cylinder diameter

C_{Dz} = Drag coefficient for lateral flow (varies with immersed depth of the cylinder)

Kaplan also proposes the following expression to be used to compute the vertical impact force acting underneath a flat rigid deck of negligible thickness

$$F_z = \left(\rho\frac{\pi}{8}c^2\ddot{\eta} + \rho\frac{\pi}{4}\dot{\eta}c\frac{\partial c}{\partial t} + \frac{\rho}{2}\dot{\eta}|\dot{\eta}|cC_D\right)b$$

Equation 93

where c is the wetted length, and b is the plate width.

The author presents a comparison of horizontal forces obtained from an analysis using the equations proposed and measurements at an offshore test structure, showing reasonable agreement for the case studied. An analysis of the vertical force on a flat plate presented by the author reveals that the shape of the force time history obtained using Equation 93 might differ from field measurements having high negative impact pressures.

Overbeek and Klabbers – Design of jetty decks for extreme vertical wave loads – 2001

A paper written by Overbeek and Klabbers examines the design of two jetty platforms built on the island of St. Vincent in the Caribbean. One was a container jetty, placed 8.2 ft above the still water level, and the other was a cruise berth, placed below the maximum expected hurricane wave level (Overbeek and Klabbers, 2001).

The authors conducted a literature search for design considerations, from which they decided to use two design equations for the projects.

For the impact pressure, assumed over the first 3 ft of the wave front:

$$P_{ve} = c\rho g H_{max} \hspace{4cm} \text{Equation 94}$$

For the slow varying pressure, assumed acting over the immersed portion of the structure:

$$P_{ve} = 1.0\rho g \left(H_{cr} - d_c\right) \hspace{3cm} \text{Equation 95}$$

where,

P_{ve} = Vertical wave pressure

c = Wave impact constant, the authors used a value of 1.5

ρ = Specific density of water

g = Acceleration of gravity

H_{max} = Maximum wave height

H_{cr} = Wave crest above still water level

d_c = Height of the bottom of the deck above still water level

Equations 94 and 95 evolved from the fact that the pressure induced by waves varies as sketched in Figure 31. In order to avoid air entrapment the authors designed the cruise berth decks with the beams running only parallel to the berthing line, to avoid the entrapment of the waves in a beam grid. They also placed gaps in the deck in the transverse direction 2 in. wide every 6.5 ft. These gaps were covered with unanchored T-shaped timber strips to allow them to be blown out in the presence of the design waves.
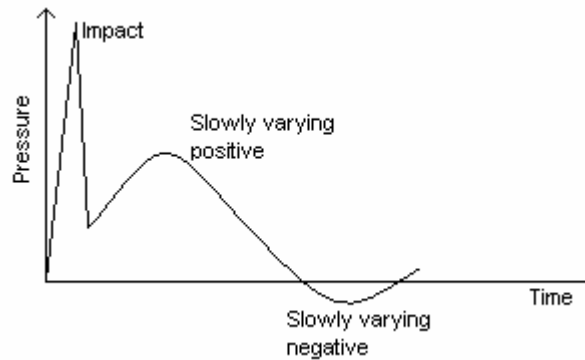
Figure 31. Wave-induced pressures.

When Lenny, a category 4 hurricane, hit the cruise berth the authors concluded that design wave conditions were met. Although some structural damage was done, the structure could be easily restored. Some lightly anchored slabs were washed away by the storm. The authors estimated the pressure that caused the slabs to be detached from the structure was produced by an impact factor, c, of 3 or higher.

Chan et al. – Breaking-wave loads on vertical walls suspended above mean sea level – 1995

A laboratory experiment conducted by Chan et al. at the Hydraulics Laboratory in Singapore examined the forces produced by plunging waves on a suspended vertical wall. The authors intended to explore the impact pressures produced by breaking waves on suspended structures, such as facial beams of piers and wharves. The authors emphasize that extension of the design methodology used in the Shore Protection Manual (now Coastal Engineering Manual) for surface-piercing vertical walls to suspended structural elements would be inaccurate due to the significant difference in wave-structure interactions during wave action. The authors produced three types of waves during the experiment: (1) waves with an inclined wave front prior to jet formation, (2) an almost vertical wave front at the start of jet formation, and (3) a curved wave front after jet formation. Figure 32 illustrates the wave profiles as they impact the suspended wall.
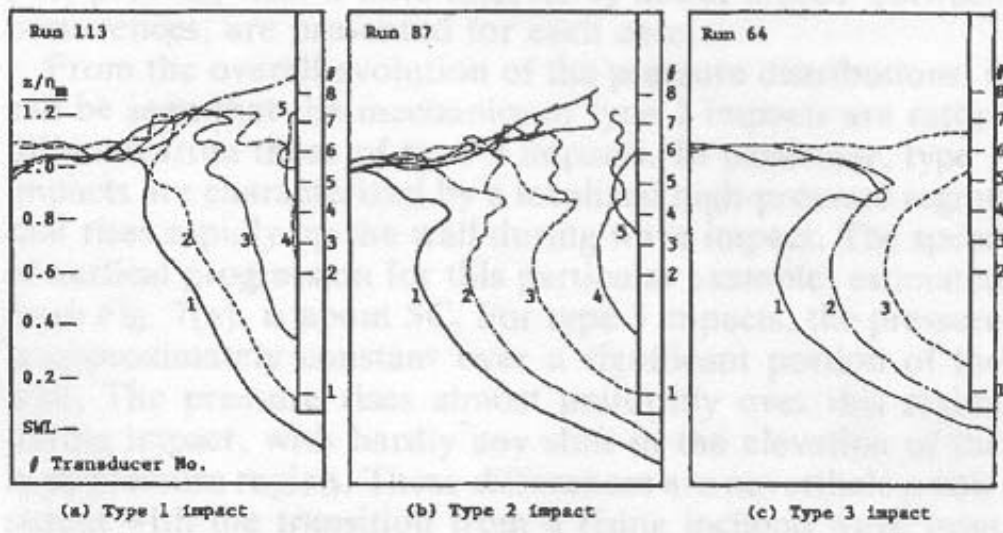
Figure 32. Incident wave profiles, source: (Chan et al., 1995).

On the right of Figure 32 a scale indicates the location of 8 sensors used on the hanging wall to measure wave pressures for each wave profile. Figure 33 shows the simultaneous records captured at the 8 sensor locations at impact.
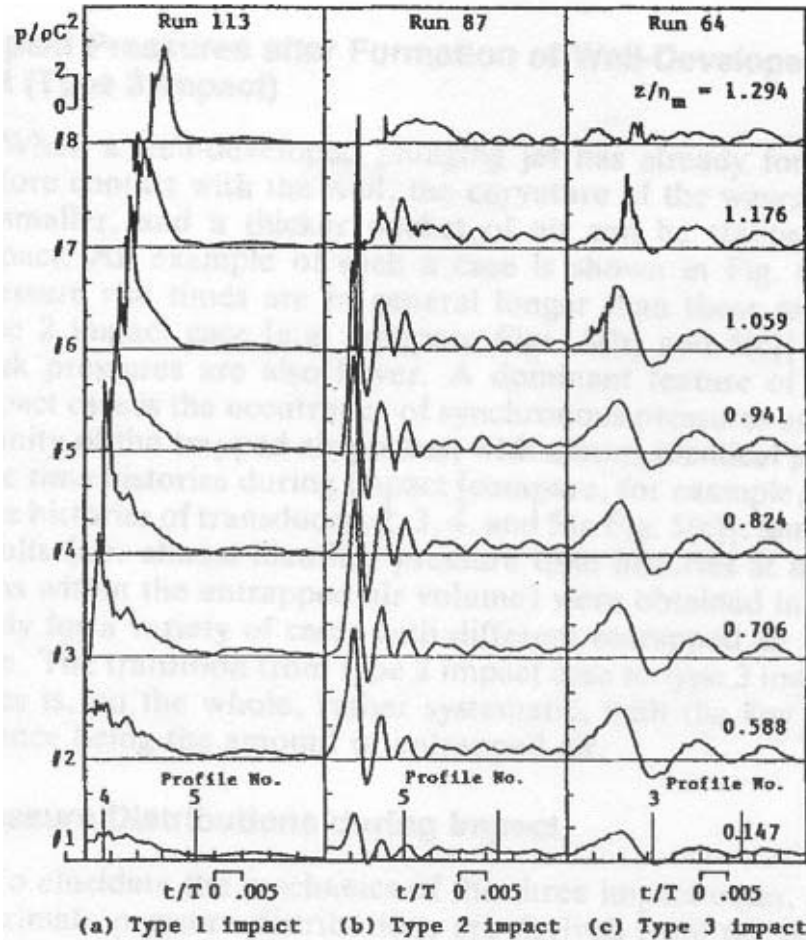
Figure 33. Three examples of simultaneous pressure records at impact, source: (Chan et al., 1995).

The records shown in Figure 33 indicate that the type I impact wave generates maximum pressures on the order of 10 ρC^2, where ρ is the density of water and C is the characteristic phase speed of incident waves. Similarly, the type II impact wave produces maximum pressures of 12 ρC^2. While the type III wave impact generates maximum impact pressures of approximately 4 ρC^2. Although wave profile type I produces large pressures, the largest forces produced by this wave profile are

approximately 3 $\rho C^2 \eta_m$, where η_m is the maximum crest elevation of a plunging wave in the absence of the wall. A similar value was obtained for the total force generated by the wave profile type III. Wave profile type II, however, produced a much larger force, namely 7 $\rho C^2 \eta_m$. This behavior is explained by the following reasons: wave type I produces large pressures, but since the peak pressures at different heights of the wall (sensor locations 1 through 8) are asynchronous, the resultant peak force is not very large. Wave profile type II produces large pressures simultaneously on most of the wall surface, thus generating the largest peak force. Wave profile type III generates synchronous peak pressures on most of the wall surface, although their magnitude is low due to cushioning of the pressure by large amounts of entrapped air between the plunging wave and the wall. A time history of the three impact forces on the wall is depicted in Figure 34.
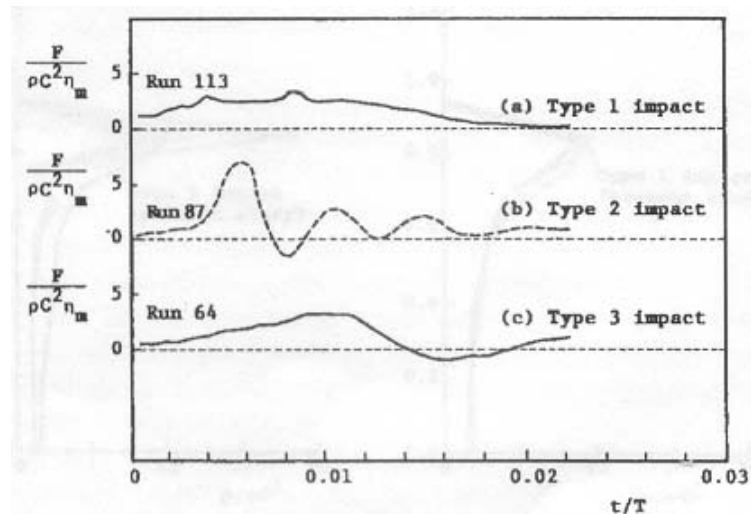
Figure 34. Horizontal force time histories, source: (Chan et al., 1995).

Pressure distributions captured along the wall height are presented in Figure 33. The pressure distributions suggest that the impact is more impulsive over the upper half of the wall; that is the region spanning from incident crest level to 0.5 η_m. The ordinates of Figure 35 indicate the distance above still water level, z, as a fraction of the maximum crest elevation, η_m.
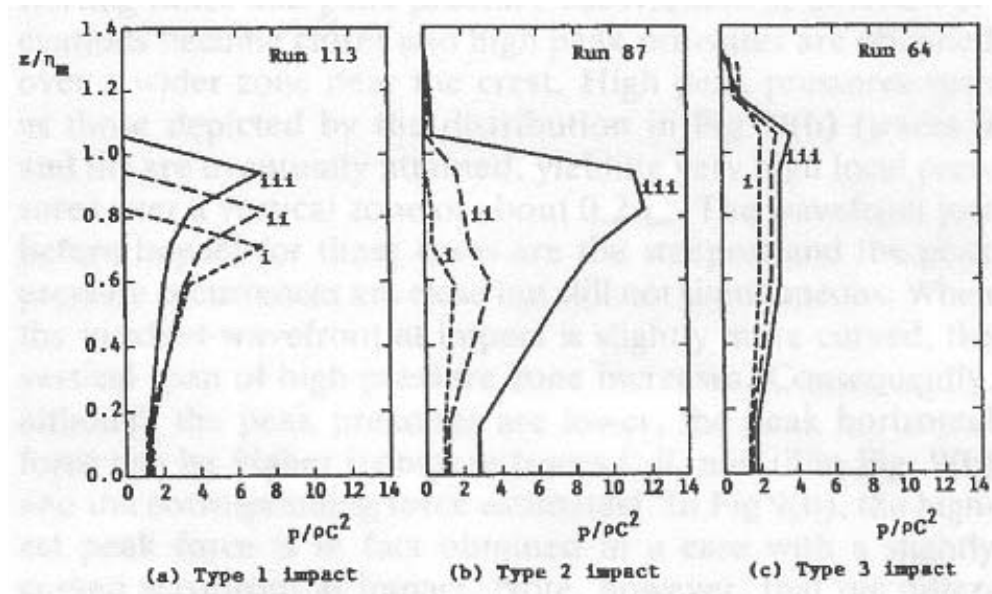
Figure 35. Sequential evolution of pressure distributions (i, ii, iii) for the three types of wave impact profiles, source: (Chan et al., 1995).

Weggel – Discussion of paper: breaking-wave loads on vertical walls suspended above mean sea level – 1997

Weggel presents experimental results similar to those reported by Chan et al. (Weggel, 1997). Weggel also presents a model for the pressure distribution on a vertical suspended wall as depicted in Figure 36. The author assumes the pressure distribution to be parabolic and concentrated near the wave crest. The pressure is zero at the wave crest, increasing parabolically downward, with the maximum pressure point located at a distance of 80% of the wall's height, above the bottom. The pressure distribution proposed is zero at and below 60% of the wall's height.
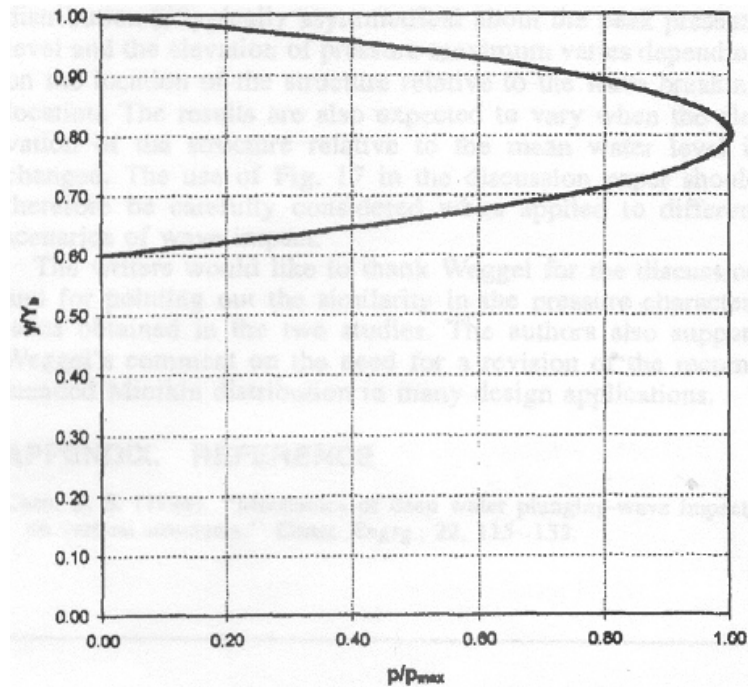
Figure 36. Pressure distribution on a vertical wall due to wave impact suggested by Weggel, source: (Weggel, 1997).

Aagaard and Dean – Wave forces: data analysis and engineering calculation method – 1969

The paper presents a method to compute wave forces on offshore structures (Aagaard and Dean, 1969). The authors use Morison's equation to compute the forces on the cylindrical elements of the platform. Once the design wave is defined in terms of wave height, wave period, and water depth, the authors calculate the kinematic flow field using a stream function to represent nonlinear ocean waves proposed by Dean (known as stream function theory). The authors used measured wave force and wave profile data and used the mathematical model to find empirical coefficients for drag and inertia. These drag and inertia coefficients were obtained by correlating measured wave forces with computed instantaneous horizontal particle velocities and accelerations. The authors show that the inertia coefficient varies between approximately 1 and 1.6 for Reynolds numbers approximately between 1.8×10^4 and 2.0×10^6. The drag coefficient

84

recommended for design has a constant value of 1.2 and 1.35 for in-line forces for Reynolds numbers below 2.0×10^5 and 0.55 above 6.0×10^6, and has a smooth variation in between. The authors mentioned that the values given are "representative of average wave forces and are used in calculating wave forces for wave heights ranging to near-breaking, for all wave periods, for all water depths, for all phase and elevation positions in the wave, and for all piling diameters commonly used in wave force calculations for offshore structures." The pipe diameters used in the study ranged from 2 ft to 4 ft and at water depths from 33 ft to 100 ft.

The wave force was estimated using a computer program. The authors indicate that it is common practice in the offshore industry to compute wave forces at a number of locations on the structure within the wave to allow for smooth interpolation. The computer output includes surface wave profile, local forces at predetermined elevations and phase positions, and total force and moment about the base of the structure. The authors indicate that calculated distributed forces and average measured values agree within ± 10%. The authors indicate that other mathematical models may yield different drag and inertia coefficients yet produce valid computed forces.

Tickell – Wave forces on structures – 1993

Tickell summarizes information available to obtain design forces for coastal structures (Tickell, 1993). The author states that the design may use deterministic (long-crested regular) waves, but storm waves are random and short crested. The author presents a derivation of Morison's equation applied to slender cylinders where D/L is less than 0.2, indicating that for higher ratios of D/L diffraction effects are important. Where D is the diameter of the cylinder and L is the wavelength. The hydrodynamics of wave-current interaction cited by Tickell include studies by Hedges and Barltrop et al. (Hedges, 1987; Barltrop et al., 1990). When a current acts on the structure, the drag and inertia coefficients need to be modified. Tickell ends the chapter with a summary of

wave loading on walls. The author points out that a useful method to compute non-breaking wave forces on vertical walls is described in the Shore Protection Manual (SPM, 1984) assuming a pressure distribution shown in Figure 37. The incremental pressure at the sea bottom is equal to:

$$p_1 = 0.5(1 + H_r/H_i)\rho g\, H_i/\cosh(kd) \qquad \text{Equation 96}$$

where H_r is the reflected wave height, and H_i is the incident wave height.
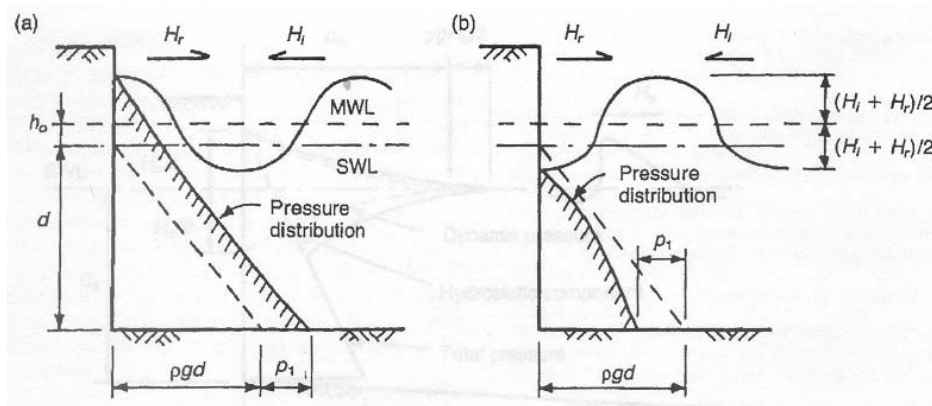
Figure 37. Non-breaking wave forces on a vertical wall (a) crest on wall (b) trough on wall, source: (Tickell, 1993).

For breaking waves Tickell suggests the use of the procedure followed by the Shore Protection Manual, based on Minikin's method, assuming the pressure distribution indicated in Figure 38. The dynamic pressure component is given by

$$p_m = 0.5 C_i \rho u_b^2 \qquad \text{Equation 97}$$

where u_b is the characteristic velocity of the breaking wave, and C_i is an impact coefficient.

It should be mentioned that Minikin's method is no longer recommended in the Coastal Engineering Manual, since it is considered to yield overconservative estimates of wave pressures.
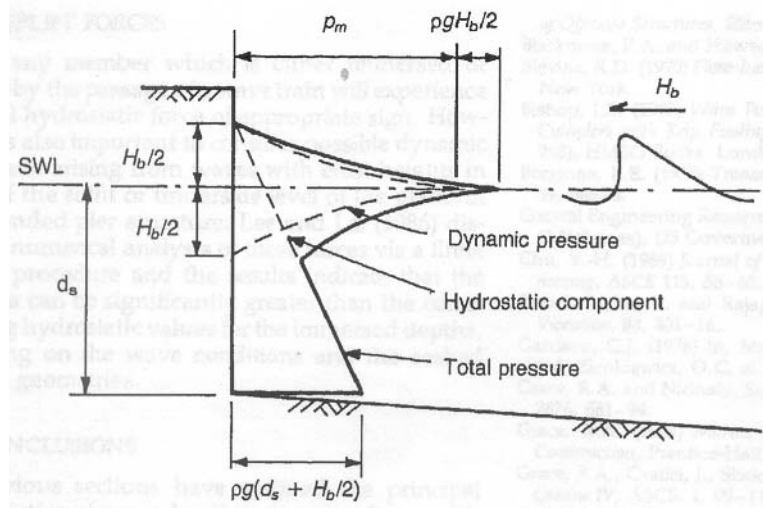
Figure 38. Breaking wave forces on a vertical wall, source: (Tickell, 1993).

For broken waves, the author describes the method used by the Shore Protection Manual, giving a dynamic pressure on the wall of:

$$p_m = 0.5\rho c^2$$ Equation 98

where c is the wave celerity. The dynamic pressure is assumed to act uniformly from the still water level (SWL) to $h_c = 0.78\ H_b$, where H_b is the height of the breaking wave. To this dynamic pressure a hydrostatic pressure distribution is added having a zero value at h_c above SWL and a pressure of $\rho g(h_c + d_s)$ at the sea bed, where d_s is the depth of water at the wall.

Denson – Wave forces on causeway-type coastal bridges – 1978

Due to observed damage caused by hurricane Camille to the St. Louis Bay and Biloxi Bay bridges, Denson initiated a research on the effects of wave forces on bridge superstructures (Denson, 1978). Denson noted that hurricanes could produce extreme wave forces due to a general rise in water elevation (storm surge) accompanied by superimposed surface waves. Denson noted that perhaps most of the damage to the two bridges mentioned was due to vertical forces that exceeded the weight of the bridge superstructure. The effects of horizontal drag forces were evident in horizontal

87

displacement of bridge sections on the Biloxi Bay Bridge. It is mentioned that bridge retrofit required extensive repairs. Another problem was anchorage failure at the superstructure-substructure connection. Denson built a 1:24 scale Plexiglass model of the bay St. Louis Bay bridge. The bridge model was subjected to trochoidal waves with a period of 3 seconds. However, no further details on the wave type and the reason for using a period of 3 seconds are given in the report. Isaacson and Sarpkaya indicate that the physical realization of trochoidal waves seldom occurs. Isaacson and Sarpkaya state that an example of the development of a trochoidal wave is when waves are progressing against a wind that induces a vorticity within the fluid in the opposite sense of the particle motions (Issacson and Sarpkaya, 1981). The angle of wave attack in Denson's model was 90 degrees (direction of wave propagation normal to bridge longitudinal axis). The author presented the results of the tests in dimensionless format. Five incremental test values were used for water depth. Five wave heights were used for each test condition, with heights ranging from nearly zero to breaking height. Five different deck clearances were also investigated, ranging from submerged-deck to deck placed above still water level. The results are presented for three different quantities per unit length of bridge, namely: rolling moment, lift force, and drag force.

Rolling moment per unit length

From the results presented it can be observed that overturning moments tend to be higher for deck locations near or below the surface water level, than for decks placed above the water level. As the value of the variable *h/W* (ratio of bridge deck height measured from sea bottom to deck width) decreases (as the deck is located closer to the sea bottom), there is no discernible difference between the moments measured for different values of the *h/D* variable (ratio of bridge deck height measured from sea bottom to water depth).

Lift force per unit length

For high values of the *h/W* variable the lift forces are lower for decks placed above water level than for decks placed near or below water level. As the variable *h/W* is

reduced, the lift force is reduced with respect to values measured for high values of *h/W*. For example, if the *h/W* values are reduced from 0.64 to 0.38 the lift force is reduced to approximately 60%. As the variable *h/W* increases, the lowest lift force values are obtained at elevated decks.

Drag force per unit length

By reducing *h/W* from 0.64 to 0.38 the drag force is also reduced to approximately 60%. That is, the drag force is reduced as *h/W* is reduced. The moment, lift, and drag forces always increase with increasing values of the wave height to water depth ratio. The lift force tends to be between 5 and 7.5 times the value observed for the drag force.

The tests were conducted on two sets of bridge decks consisting of seaward and landward lanes supported independently. Since the waves were moving from sea toward land, the moment, lift, and drag forces in general, tend to be smaller for the landward sections, with some exceptions. The moment and lift force values recorded for landward sections were approximately 75% of those observed on the seaward sections.

Design procedure

Denson proposed the following design method using his results:

1. Define the bridge geometry and height above sea bottom.
2. Estimate the maximum water depth including storm surge.
   a. The previous two steps define *h/W* and *h/D*.
3. Find the maximum value of moment, lift, and drag from the figures presented in the report, using a value of wave height to water depth ratio of 0.7.

Figure 39 shows a typical plot of the results presented in the report. The quantities *h/D* and *h/W* have been defined before, and *r* is the correlation coefficient obtained using a least square approximation with a third degree polynomial. *H/D* is the ratio of wave height to water depth, and the overturning moment, *M*, is

89

nondimensionalized by dividing it by the specific weight of water, γ, and by the width of the bridge deck, W, raised to the third power. In this case M has units of *lb-ft/ft*, γ has units of *lb/ft³*, and W has units of *ft*.
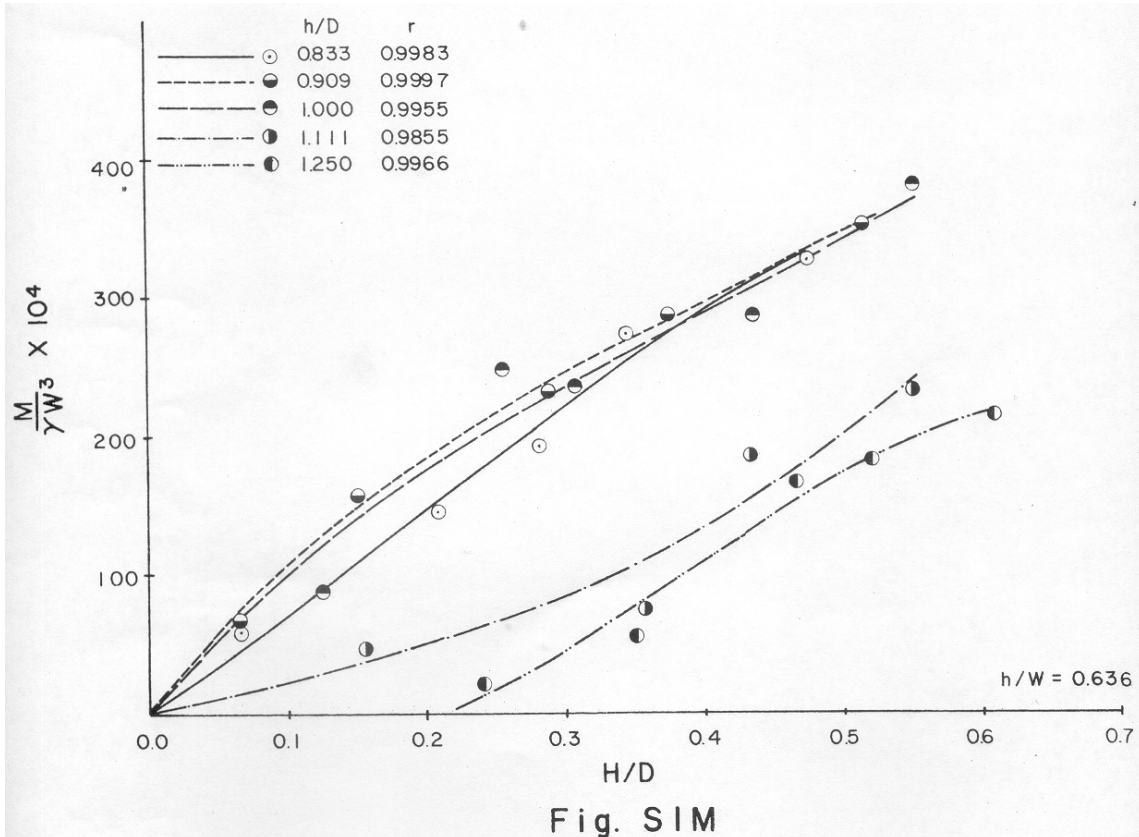
Figure 39. Results for overturning moments, *M*, of seaward deck under condition 1, source: (*h/W* = 0.636), (Denson, 1978).

Denson – Wave forces on causeway-type coastal bridges: effects of angle of wave incidence and cross-section shape – 1980

The author carried out a set of tests on two model specimens of bridge sections. One was a model scaled to 1:24 of the Bay St. Louis Bridge located in Mississippi on U.S. HW 90, heavily damaged by hurricane Camille in 1969, which developed a storm surge of nearly 20 ft. The bridge consists of two separate bodies (seaward and

landward), each having a 48 ft span and a two-lane beam and slab cross-section with four beams each. The width of the deck, *W,* of this study refers to the width of a two-lane section supported by four beams. The other was a trapezoidal box girder section built to a 1:24 geometric scale. The bridges were fixed in a tank at a constant height above the floor, subjected to waves with a period of 3 seconds. The bridge sections were supported on piles to simulate bridge conditions, and subjected to waves of five different heights, using five different mean water levels. The bridge models were tested under five different angles of wave attack (angle between longitudinal axis of bridge and direction of wave travel), namely: 30º, 45º, 60º, 75º, and 90º. The following quantities were measured: rolling, pitching, and yawning moments, a well as transverse and longitudinal drag forces, and lift forces.

The author includes a section in which he describes a survey being given to bridge engineers in 22 states. Out of 20 states replying, 6 reported damage observed on coastal bridges, and 17 states reported bridges located in areas susceptible to damage. After the questionnaire was received, two bridges were destroyed by hurricane-type waves and winds: the Hood Canal floating bridge in Washington and the Dauphin Island causeway in Alabama. Hood Canal floating bridge was damaged in 1979 by a cyclone with average winds of 80 mph and wind gusts of 115 mph. Dauphin Island causeway lost many spans to hurricane Frederic in 1979 with recorded wind gusts reaching 145 mph and an estimated storm surge of 13 ft. The damaged caused on the St. Louis Bay Bridge and Dauphin Bay Bridge was horizontal transport due to hydrodynamic lifting and drag forces.

Denson makes a more detailed description of the method used to measure the waves and forces than used in his 1978 study. The author describes the design method that could be followed using his report, which is essentially the same method described for the 1978 report. There are some differences between this project and the 1978 study. The model with slab and beams used in this study has end diaphragms, while the model

used in the 1978 study did not have end diaphragms. This fact is not specified in the 1978 document. The forces reported in the 1978 study are given in units of force per unit length, while the forces in this study are given in units of force. The 1980 study makes a comparison of the two studies by listing maximum measured lift and drag forces, as well as overturning moments for the 90 incidence waves. However, the results presented in the report could not be verified from the information given on the plots where they were extracted, neither for the 1978 study nor for the 1980 study.

The report compares the values of the vertical lift force obtained for the slab-beam bridge with the box-girder bridge. The values for the seaward bridge sections of the non-dimensionalized lift force coefficients ($Fz/\gamma W^3$) are summarized in Table 9. The lift force, Fz, has units of lb, the density of water, γ, has units of lb/ft^3, and the width of the bridge, W, has units of ft. The values of the lift force coefficients presented in the comparison given in the report are different from the values read from the plotted results shown in appendices B and C of the report. Thus, the values given in Table 9 are those obtained directly from the appendices.

Table 9. Values of coefficient Fz/GW³x10³ for different angles of wave incidence

Angle of incidence	Slab-beam bridge		Box girder bridge	
	Positive	Negative	Positive	Negative
30°	183	128	307	
45°	237	149	392	
60°	184	165	469	Negligible
75°	267	156	548	
90°	267	146	857	

Table 9 shows that the negative force coefficients are nearly independent of angle of wave incidence. The lift force magnitude increases for the box girder section as the angle of wave incidence approaches 90°. However, no conclusions can be drawn for the lift force acting on the slab-beam bridge section. Denson mentions that in order to compare the values of the slab-beam section with the box girder section the slab-beam values need to be multiplied by two to account for span length. The report indicates that

doing that elicits a similar behavior between the box girder section and the slab-beam section. However, that could not be verified using the values from Table 9.

Wang – Water wave pressure on horizontal plate – 1970

The paper is mainly concerned with the uplift pressure induced by waves on the underside of a horizontal plate placed either at mean water level or above mean water level. The author asserts that the uplift pressure has a slowly varying component and an impact component. The author explains that the impact pressures produced by waves as they come in contact with horizontal and vertical barriers are different. It is pointed out that the impact on the underside of a deck is produced by the change of momentum of the fluid flow. While the impact produced on a vertical wall is produced by the collapse of an air layer. Wang presents a set of equations for a standing wave system (waves typically generated by wind). The author used the assumption proposed by von Kármán, that affirms that the mass responsible for impact under a flat plate fixed near the water surface is the mass of water enclosed in a semi-cylinder of diameter, 2*S*, and length, *b*, as depicted in Figure 40.
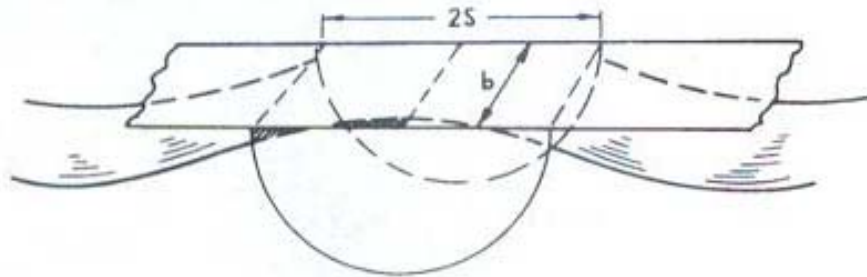
Figure 40. Profile of standing wave modified after contact with a horizontal flat plate, source: (Wang, 1970).

The impact pressure computed is given by:

$$\frac{p_i}{\gamma} = \frac{\pi}{2g} v^2 \delta$$

Equation 99

93

where,

p_i = Impact pressure

δ = Factor that depends on the shape and degree of asymmetry of the incident wave

γ = Specific weight of water (lb/ft^3)

g = Acceleration of gravity (ft/sec^2)

v = Vertical velocity of water particles at the surface of the plate (ft/s)

The author carried out a series of experiments in a 90 ft square basin. By inserting a plunger into the water, and by retrieving it out of the water, dispersive waves were generated for the tests. The waves generated by this method are akin to dispersive waves produced by an explosion rather than to standing waves generated by wind during a storm. As such, the period and wave length of the dispersive waves generated were variable and difficult to measure. The plate was placed at several distances from the water surface that ranged from 0 to 1.5 in.

It was observed that the wave pressure depends on the characteristics of the wave at the moment of impact. Impact pressures are likely to be produced by waves of moderate steepness preceded by a trough located below the deck. Steep waves or waves preceded by a trough located below the deck are not likely to produce impact. After waves break, the water motion is mainly horizontal, and the uplift pressure is nearly hydrostatic. No impact was observed for this wave condition.

The author compared measured pressures with the following equation derived to obtain impact uplift pressure induced by dispersive waves.

$$\frac{p_i}{\gamma} = \pi \left[1 - \left(\frac{d}{T_r A} \right)^2 \right]^{1/2} T_r A \tanh \sigma \qquad \text{Equation 100}$$

where,

p_i = Impact pressure

γ = Specific weight of water (lb/ft^3)

A = Wave amplitude

d = Clearance between still-water level and deck underside

σ = $2\pi h/\lambda$

h = Water depth

λ = Wave length

T_r = Transmissibility = H/H_I (Attenuation of incident wave height by the presence of the deck)

$$T_r = \frac{1}{\left\{1 - \left[\dfrac{\pi B}{\lambda}\left(1 - \dfrac{2d}{H_I}\right)\right]^2\right\}^{\frac{1}{2}}} \qquad \text{Equation 101}$$

H_I = Height of incident wave (before reaching the plate)

H = Wave height at a given location landward of location where H_I was measured

B = Length of plate from leading edge to point where H needs to be determined

The experimental observations did not agree with predictions made by Equation 101 modified as shown below. Thus, upper bound values were proposed for the ordinate, Y, shown in Equation 102 by the author as 3.14 for a constant water depth study and 4.5 for shoaling water.

$$Y = \frac{p_i}{\gamma\left[1 - \left(\dfrac{d}{T_r A}\right)^2\right]^{\frac{1}{2}} T_r A} \qquad \text{Equation 102}$$

The durations of impact observed in the study varied from 6 msec to 16 msec, with an average of 11 msec. Measured slowly varying pressures were one to two times the hydrostatic pressure.

El Ghamry – Wave forces on a dock – 1963

The study by El Ghamry was one of the earliest of its type (El Ghamry, 1963). The author studied uplift pressures, uplift forces, reactions, and moments on a dock, induced by waves generated in a flume (105 ft long, 1 ft wide, and 3 ft deep). Fresh water was used in the experiments. The dock was made of aluminum and was 4 ft long, 1 ft wide, and ¼ in. thick. Several test cases were investigated by the author: one involved no breaking waves allowing an air gap underneath the deck, another case involved breaking waves with 1:3 and 1:5 beach slopes, some other variations with and without air gap under the deck were also studied. The waves used in the study were monochromatic with varying periods and heights.

The force and pressure records have a periodic shape that depends on wave period, T, and the deck clearance above the mean water level. The author made an attempt to predict the uplift pressures using Stoker's theory. However, since Stoker's theory predicts a sinusoidal shape for the waves, and the wave records were not symmetric, discrepancies were found. An approximation was, however, obtained for the uplift force and downward force using Stoker's theory by employing curve fitting to the data recorded and the parameters of Stoker's theory. The following equations resulted for uplift force and downward force, respectively, for the case of a deck placed at the still water level:

$$F_1 = C_1 C_2 \frac{\rho_f g \lambda H}{2}$$
Equation 103

where,

F_1 = Uplift force

$$C_1 = \sqrt{1 + \frac{3r^2}{1+r^2}}$$
Equation 104

r = $\pi \lambda / L$

and ρ_f is the mass density of the fluid, g is the acceleration of gravity, λ is the length of the dock, H is the wave height, L is the wave length, C_2 is a correction factor obtained from Figure 41, and

$$F_2 = C_4 \rho_f gHL$$
Equation 105

where F_2 is a downward force, and C_4 is a function of wave steepness and can be obtained from Figure 42.
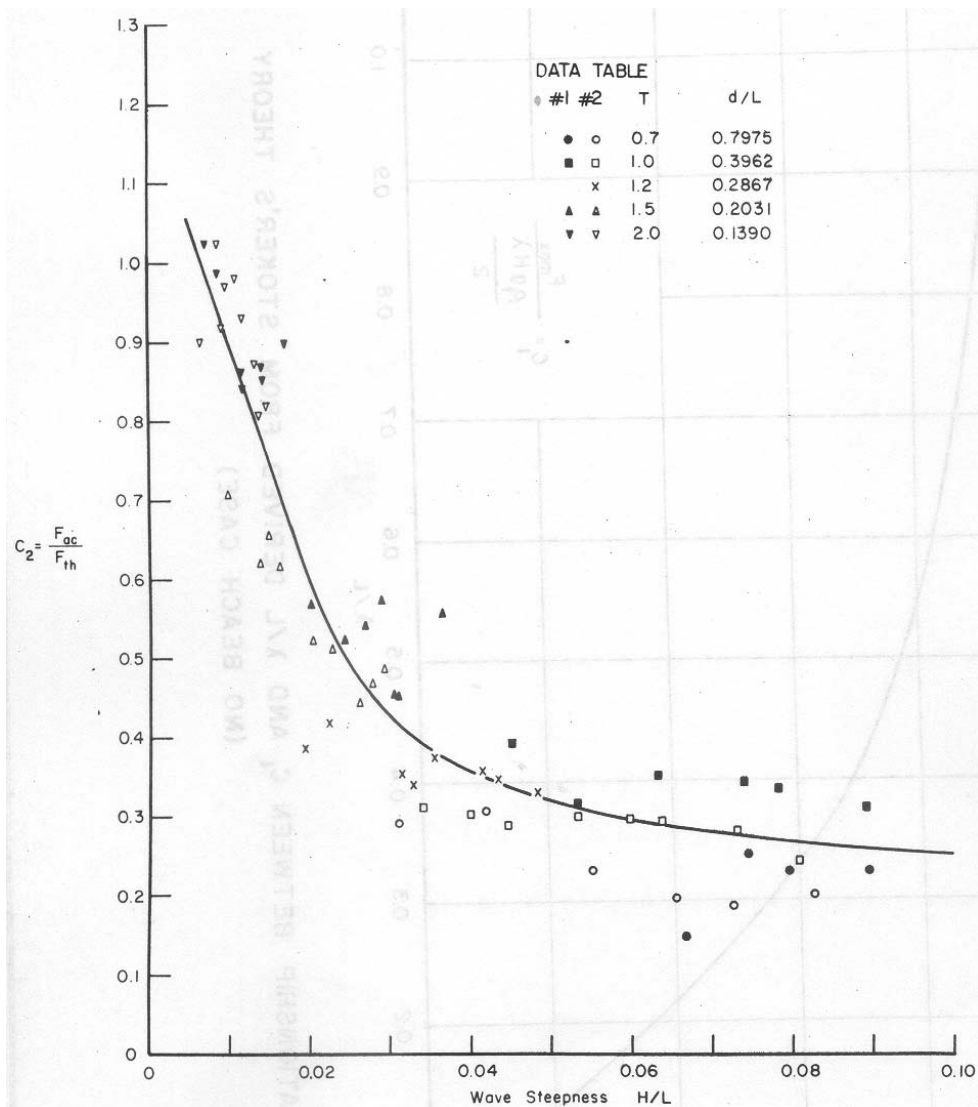
Figure 41. Relationship wave steepness and C_2 – no beach case, source: (El Ghamry, 1963).

97
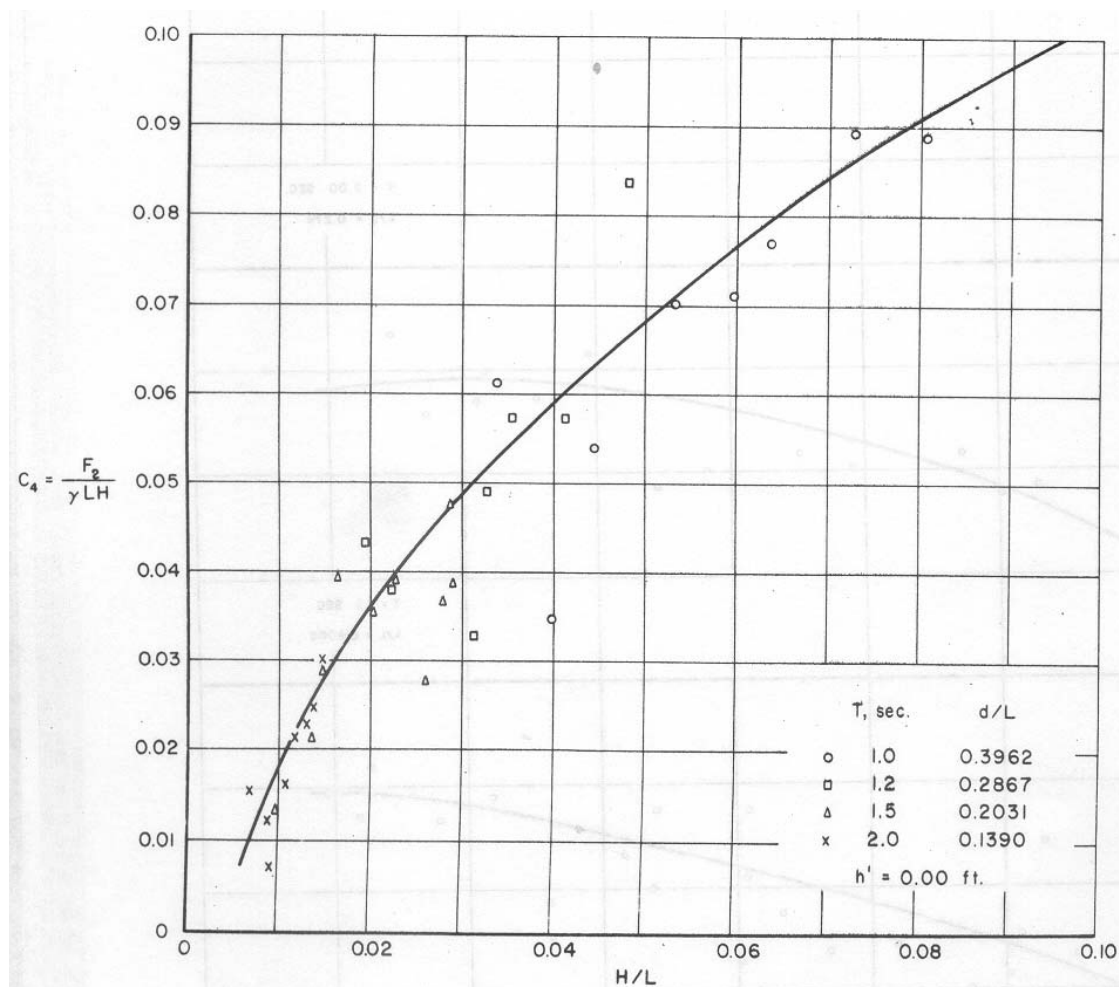
Figure 42. Relationship between H/L and C4 – no beach case, source: (El Ghamry, 1963).

It should be mentioned that the plots show considerable scatter. The author mentions that extraordinary high pressures were rarely recorded.

The author characterized the peak pressures statistically, finding that the distribution was close to the normal distribution. Likewise, the maximum uplift force could be approximated by the Rayleigh distribution. The author presents a design method for cases when the deck is placed above the still water level, for known incident wave characteristics. The author indicated that the uplift force for the case when there was no air gap under the deck, developed forces that are an order of magnitude greater

than for cases when there was room for the air to escape. On few instances the uplift force was as high as 100 times that of the no air entrapment case.

Douglass et al. – Wave forces on bridge decks – 2006

Douglass et al. carried out a literature review of wave forces on bridge decks, investigated the causes of failure of the U.S. HW 90 Bridge across Biloxi Bay after it was hit by hurricane Katrina, presented the results of some laboratory experiments, and proposed a method to estimate wave forces on bridge decks (Douglass et al., 2006). The researchers assumed the wave and surge conditions at the bridge site when hurricane Katrina crossed the area where as follows:

- Significant wave height $H_s = 6.2$ ft
- Wave period $T = 5$ sec
- Water depth $d = 16$ ft
- Storm surge $\overline{\eta} = 12$ ft

The authors presented an appendix with the computation of forces estimated by different methods available for a case study involving the failure loads of the bridge on U.S. HW 90, across Biloxi Bay. The authors computed the weight of the span to be 340 kips. The results presented by the authors are summarized in Table 10. The forces estimated by a method proposed by the authors are also included in Table 10.

Table 10. Summary of results obtained by Douglass et al. (2006).

Method	Uplift Force (kips)	Lateral Force (kips)
McConnel et al., avg. values, 2004	520	165
Bea et al., 1999	inertia + drag	inertia + drag + slamming
	320 + 130 = 450	430 + 40 + 250 = 720
Denson, 1978	50	9
Denson, 1980	710	150
Douglass et al., 2006	440	230

Our research team examined and verified most of the results. However, it can be noted that discrepancies between the results obtained by different methods are due to the geometry of the sections used to develop the equations. For example, the geometry used in Denson's study has a shallower section and less beams than the Biloxi Bridge, thus lower lateral force values are obtained from Denson's equations. It should be mentioned that the values reported by Denson's study are maxima, while the values computed by Douglass et al., when using McConnel et al.'s equations, are average (Denson, 1980; McConnel et al., 2004). For the results of both studies to be comparable, the values obtained using the McConnel et al. study should be multiplied by the coefficients for upper limit recommended by McConnel et al. (approximately 1.5 for vertical forces and 2 for lateral forces). It should be mentioned that the studies carried out by McConnel et al., El Ghamry, and Denson show considerable scatter in the data (McConnel et al. 2004; El Ghamry, 1963; Denson, 1980). The values computed by our research team using the equations given by some of the studies are presented in Table 11.

Table 11. Uplift force and lateral force estimated by various methods.

Method	Uplift Force (kips)	Lateral Force (kips)
McConnel et al., upper values, 2004	568	165
Bea et al., 1999	inertia + drag	inertia + drag + slamming
	320 + 130 = 450	430 + 40 + 125 = 595
Denson, 1978	50	9
Denson, 1980	710	150
Douglass et al., 2006	440	230
El Ghamry, 1963	332	N.A.

An approximate analysis employing the study made by El Ghamry for the same bridge using the same wave conditions was made by our research team and is presented next (El Ghamry, 1963).

Equation 106 was needed to estimate uplift force for a deck placed above the still water level:

$$F_1 = C_1 C_2 C_3 \frac{\rho_f g \lambda H}{2}$$

Equation 106

where,

λ = Length of dock (in our case width of deck) = 33.3 ft

ρ_f = Mass density of fluid = 2 slugs/ft^3

g = Acceleration of gravity = 32.2 ft/sec^2

L = Wave length = 104 ft (using same value estimated by Douglass et al.)

λ/L = 33 ft / 104 ft = 0.32, so from Figure 21 of El Ghamry, $C_1 = 1.6$

H/L = Wave height over wave length = 10.4 ft / 104 ft = 0.1, so from Figure 22 of El Ghamry, $C_2 = 0.25$

d/L = Water depth over wave length = 16 ft / 104 ft = 0.15

h' = 1 ft (Clearance between still water level and lower level of the deck)

$\Delta H'$ = $H/2 - h'$ = 10.4 ft /2 – 1 ft = 4.2 ft

$\Delta H' / H$ = 4.2 ft / 10.4 ft = 0.40, so from Figure 24 of El Ghamry, $C_3 = 1.1$

The values listed above were used in Equation 106 to give,

$$F_1 = (1.6)(0.25)(1.1)\frac{\left(2 \frac{slugs}{ft^3}\right)\left(32.2 \frac{ft}{sec^2}\right)(33 ft)(10.4 ft)}{2}\left(\frac{52 ft \cdot long}{1 ft \cdot wide}\right) = 255 kips$$

Equation 107

Using a factor of safety recommended by El Ghamry of 1.3, the total uplift force was calculated to be: 255 * 1.3 = 332 kips. Equation 107 was multiplied by 52, the length of the Biloxi Bay Bridge and divided by 1 ft, the width of the dock used in El Ghamry's study. Notice that the model studied by El Ghamry did not have beams under the plate.

DESIGN GUIDELINES FOR WAVE FORCES ON BRIDGE SUBSTRUCTURE

The design of a bridge substructure spanning a body of water always accounts for water flow forces imposed on the substructure and potential resulting scour. This section

contains a brief description of current bridge design aids and specifications used in the design of bridge substructures subjected to water flow forces.

A critical aspect of the design of a bridge spanning a waterway is the design of the bridge substructure against scour and the design of the foundation to sustain forces from stream flow, debris, and ice. For this type of design there are a number of sources available, such as Chapter 7 of the Shore Protection Manual (SPM, 1984), Evaluating Scour at Bridges (FHWA, 2001), Stream Stability at Highway Structures (FHWA, 1991), Section 8.9 Bridge Scour of the TxDOT Hydraulic Design Manual (TxDOT, 1997). It is worth mentioning that scouring around the foundation of bridges is the most prevailing source of failure of bridges subjected to floods and other actions of water (Hamill, 1999).

Field inspection of the structure of bridges recently damaged by hurricanes shows that bridge foundations were not a major source of damage. After being inspected by structural divers, it was concluded that the foundation of the bridge on I-10 across Lake Pontchartrain in New Orleans did not show scour problems although the superstructure was badly damaged by hurricane Katrina in 2005. A similar situation was identified during a field visual inspection by our research team to the bridge on U.S. highway 90 across St. Louis Bay in Mississippi. By inspecting photographs of the Biloxi Bay Bridge, the same observation can be made, since most of the piers remained vertical after hurricane Katrina struck the area.

Section 3.7.3.1 of the AASHTO Bridge Design Manual contains an equation to compute the stream pressure acting along the longitudinal axis of a pier (AASHTO, 2004):

$$p = \frac{C_D V^2}{1000} \qquad\qquad \text{Equation 108}$$

where,

p = lateral pressure, *ksf*

C_D = drag coefficient for piers, depends on the shape of piers and whether debris is lodged against a pier, varies from 0.7 and 1.4

V = design velocity of water for the design flood in strength and service limit states and for the check flood in the extreme event limit state, *ft/sec*

Table 12 presents a list of some sources of information available for substructure design. The design of piers, abutments/retaining walls that transfer loads onto spread footings, driven piles, and drilled shafts and the water related forces acting on them are discussed in documents about substructure design (Anderson, 1995), publications of the Federal Highway Administration (FHWA, 2001; FHWA, 2004), and the Coastal Engineering Manual (CEM, 2006).

Table 12. Substructure design methods

Stream Pressure	Method applies pressure $P = C_D\,V^2$ in the direction of flow against substructure.	P = stream pressure C_D = drag coefficient V = velocity of water.	(Xanthakos, 1995), p. 93
Scour	Method applies several equations toward designing bridges to resist scour.	Flood event, discharge, water surface profiles flood history, watershed characteristics, bridge location and erosion history.	(FHWA, 2001)
Earth pressure due to ponding	Applies earth pressure, static water pressure, and passive pressure to retaining wall or abutment. Checks are made for sliding, overturning, and bearing capacity. Flow net analyses are employed.	Hydrostatic pressure, earth pressure.	(Xanthakos, 1995), p. 418
Uplift	Applies water table at the underside of superstructure (foundation submerged) and computes uplift based on the parameters listed.	Hydrostatic pressure, dead weight of superstructure and diaphragm walls, friction, pile, or shaft characteristics.	(Xanthakos, 1995), p. 433, 633
Breakwater design (buoyancy)	Applies wave pressure by striking waves to structures that are submerged.	Height of water, velocity of propagation, maximum velocity, empirical constant, acceleration due to gravity.	(Anderson, 1984), p. 254
Scour and scour depth	Presents design guidelines toward predicting different types of scour and scour depth.	Velocity of flow, channel characteristics, flow path, water level, river bed characteristics, pier configuration/inclination to flow, volume of debris.	(Xanthakos, 1995), p. 180
Shore protection (revetments)	Guidelines for using revetments.	Revetment type (rigid or flexible) water/wave height channel slope and characteristics.	(FHWA, 2004), pp. 7.10

DESIGN GUIDELINES FOR WAVE FORCES ON BRIDGE REVETMENTS

A well-known source to verify the stability of channel revetments or to design channel revetments is the Coastal Engineering Manual of the U.S. Army Corps of Engineers (CEM, 2006).

V. RELEVANT BRIDGE DESIGN PARAMETERS

This section describes the main forces induced by waves on bridge superstructures and the parameters needed to estimate those forces. This is followed by a list of methods available to predict storm surge. Finally, a list of compiled meteorological and oceanographic parameters is presented.

FORCES INDUCED BY WAVES ON A BRIDGE SUPERSTRUCTURE

Some of the most important parameters that must be used in designing bridge superstructures in coastal areas are the resultant forces acting on the bridge superstructure due to hurricane effects. These force resultants are depicted in Figure 43.
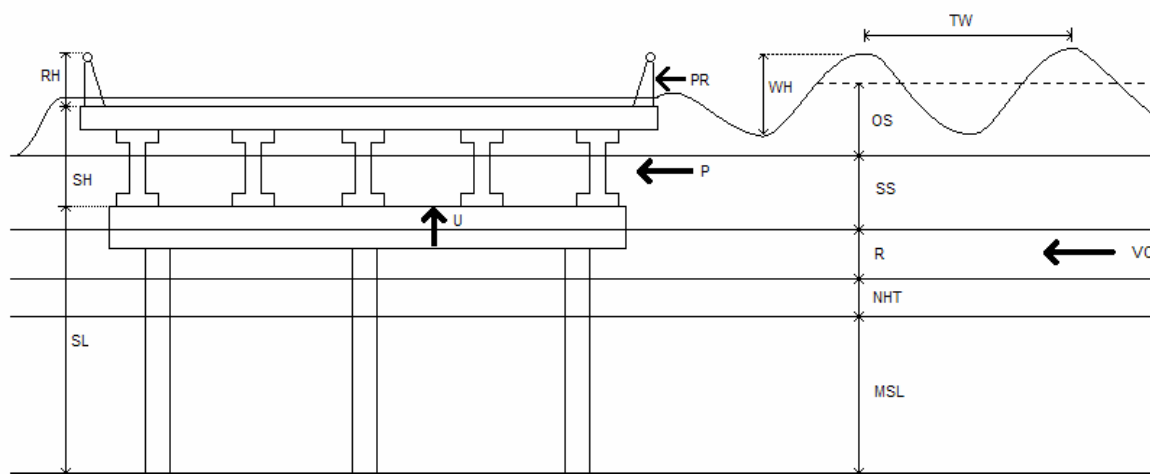
Figure 43. Parameters affecting bridge superstructure design.

The superstructure force resultants can be written as a function of the following parameters:

$$P = f(MSL, NHT, R, SS, OS, WH, TW, VC, DC, SH, SL, SG) \qquad \text{Equation 109}$$

$$U = f(MSL, NHT, R, SS, OS, WH, TW, WB, SH, SL, SG, TA) \qquad \text{Equation 110}$$

$$PR = f(MSL, NHT, R, SS, OS, WH, TW, VC, SH, SL, SG, RH, RG) \qquad \text{Equation 111}$$

where,

P	= Superstructure lateral force	
U	= Uplift force	
PR	= Rail lateral force	

FORCE DESIGN PARAMETERS

Table 13 presents a list of hurricane force design parameters. This list of parameters has been determined considering the importance or influence of each parameter on the design of bridge superstructures. Figure 43 shows a graphical description of the bridge superstructure design parameters.

Available methods used to predict storm surge

Storm surges are created from extreme winds and a drop in atmospheric pressure. This change in pressure creates a bulge in the surface causing the water level to rise. This relationship is plotted in Figure 44 below (Simpson and Riehl, 1981).
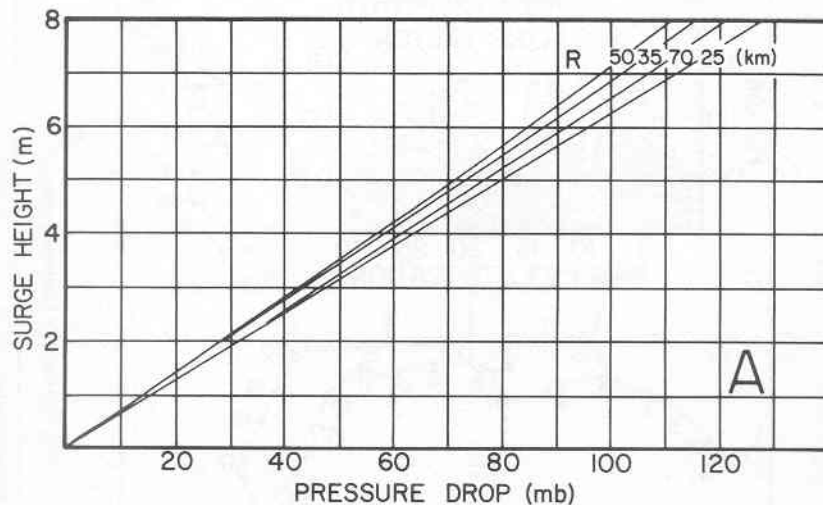
Figure 44. Relationship between pressure drop and surge, source: (Simpson and Riehl, 1981).

Table 13. List of hurricane force design parameters

Parameter	Symbol	Units	Depends on
Mean sea level	MSL	in.	Measurable parameter
Normal high tide	NHT	in.	Measurable parameter
Storm surge	SS	in.	Can be predicted with model knowing: Maximum WS, bathymetry/hydrography, forward speed of storm, central pressure of storm, atmospheric pressure difference, earth's rotation, radius of maximum winds, and storm track[1]
Obstacle surge	OS	in.	Can be predicted with model knowing: SL, SH, RH, bridge geometry, bridge length, design storm[1]
Rain	R	in.	This factor may not be critical
Wave height	WH	in.	Measurable parameter
Period of wave	TW	sec	Measurable parameter
Velocity of current	VC	in./sec	Can be predicted with model knowing: SS, tide changes, wind speed (WS) and direction, and bathymetry[1]
Wave celerity	c	ft/sec	Wave theory
Horizontal and vertical wave particle velocities	u, w	in./sec	Wave theory
Horizontal and vertical wave particle accelerations	du/dt, dw/dt	ft/sec^2	Wave theory
Drag coefficient	DC	None	Bridge geometry
Superstructure height	SH	in.	Bridge geometry
Superstructure level	SL	in.	Bridge geometry
Superstructure geometry	SG	None	Bridge geometry
Weight of bridge	WB	lb	Materials densities, bridge geometry
Trapped air	TA	None	Air tightness under beams
Rail height	RH	in.	Bridge geometry
Rail geometry	RG	None	Bridge geometry

[1] The parameters to be used will depend on the method used to predict the storm surge, obstacle surge, and velocity of current.

The design of a coastal bridge to withstand a marine storm such as a hurricane requires estimating the design storm surge elevations and the design storm wind velocity. Edge et al. described a procedure that can be used to estimate storm surge elevations and the design velocity for bridge scour computations in estuaries (Edge et al., 1998).

The U.S. Corps of Engineers surge database can be used to make storm surge predictions in a given area, since it contains hydrographs for 143 actual hurricanes recorded over 104 years (Scheffner et al., 1994). Storm forecasting information can also be obtained in a report of the Weather Bureau (Harris, 1959).

Some methods available for predicting storm surge are listed below:

1. Historical data probability analyses
2. Synthetic storm surge hydrograph method
3. FEMA surge model
4. Sea, Lake, and Overland Surges from Hurricanes (SLOSH) model
5. Advanced Circulation (ADCIRC) model
6. FDEP Storm Surge Model

1. Historical data probability analyses

This method predicts surge elevations and potential duration by applying stochastic approaches to historical water level or storm records. The lack of historical data is a major hindrance for this application. The historical method requires the following data as input: historical water level or storm records (maximum wind speed, barometric pressure, duration, category, etc.). The outputs obtained from this method are surge elevations and potential duration (FHWA, 2004).

2. Synthetic storm surge hydrograph method

This is a deterministic method that provides a way to obtain time-dependent surge values for analysis of unsteady flow. Estimates predicted by this method are typically conservative. This method requires the following information: radius of maximum winds, forward speed of the storm, peak storm surge elevation, and time of peak surge. The output is a series of time-dependent surge values (FHWA, 2004).

3. FEMA SURGE model

This method was developed by the Federal Emergency Management Agency and is used in Flood Insurance Studies. It has a meteorological, hydrodynamic, and statistical model. The statistical model gives the storm surge frequency using synthetic storms (Sheppard and Miller, 2003).

Historical storms are used to develop synthetic storms. The meteorological storm model provides the magnitude and distribution of the wind velocity, and atmospheric pressure of synthetic storms. This model also gives shear stress and pressure gradient to be used in the hydrodynamic model, whose results in turn provide the storm surge. Although the hydrodynamic model does not explicitly include the dynamic wave setup and astronomical tides, the influence of wave setup can be approximated through the calibration process if the storm surge elevation data is available. The effect of astronomical tides on the other hand is accounted for by simulating a range of tidal phases for each storm event.

The hydrodynamic model simulates storm surges using a 2-D, depth-integrated finite difference model. The input data for this model is: offshore bathymetry, coastal configuration, boundary conditions, bottom friction, other resistance coefficients (e.g., flow drag caused by obstacles protruding through the water column), surface wind stress, and atmospheric pressure distribution of the hurricanes. The output of this model includes: maximum storm surge and storm surge frequency of occurrence for different locations.

4. NOAA SLOSH model

This is a 2-D, depth averaged, finite difference model developed and run by the National Hurricane Center (NHC) of the National Oceanographic and Atmospheric Administration (NOAA) to estimate storm surge heights and winds resulting from historical, hypothetical, or predicted hurricanes. The numerical model SLOSH can estimate peak storm surge elevations (surge plus tide) based on hurricane severity

(category 1-5) (SLOSH, 2006). The governing equations solved by this model are the same as those solved by the 2-D Florida Department of Environmental Protection storm surge model. The data required for this model are: barometric pressure, storm size, storm forward speed, storm track, and wind speed (Sheppard and Miller, 2003). Output from this model includes: storm surge heights resulting from historical, hypothetical, or predicted hurricanes.

5. U.S. Army Corps of Engineers (ADCIRC model)

This model was developed between July 1988 and September 1990 for the purpose of generating a database of harmonic constituents for tidal elevations and currents along the U.S. coasts. It is also applied to compute frequency indexed storm surge hydrographs with the use of tropical and extra-tropical global boundary conditions.

ADCIRC is a 2-D, depth-integrated model with free surface displacement and depth-averaged velocity as output. Finite element methods and finite difference methods are used to discretize the 2-D equations in space and time. The solution of the depth-integrated continuity equation gives the elevation, whereas the solution of the 2-D depth-integrated momentum equation gives the velocity. The boundary conditions for this model are: specified elevation (harmonic tidal constituents or time series), specified normal flow (harmonic tidal constituents or time series), zero normal flow, slip or no slip conditions for velocity, external barrier overflow out of the domain, internal barrier overflow between the sections of the domain, surface stress (wind and/or wave radiation stress), atmospheric pressure, and outward radiation of waves (Sommerfield condition).

The input data for the model includes: boundary conditions, storm size, astronomical tide, wind pressures, tidal data, bathymetric data, and topographic data. The output data includes: free surface displacement, depth averaged velocity, frequency indexed storm hydrographs, and database of harmonic constituents for tidal elevation and current.

6. Florida Department of Environmental Protection (FDEP) storm surge model

This model is capable of one-dimensional (1-D) and two-dimensional modeling and was developed originally for establishing the location of the Florida Coastal Construction Control Line. For this purpose, the model used bathymetric and topographic data as its input. NOAA's HURDAT data from the Atlantic and Gulf of Mexico were used to synthesize hurricanes representative of the most probable hurricanes of the area.

The 2-D model uses an implicit finite difference method to find the solution of the governing equation. Barometric pressure, Coriolis acceleration, the components of the slope of the water surface, boundary conditions, surface wind, and bottom friction shear stresses are incorporated in this model. Both astronomical tides and available hurricane storm surge are given appropriate weight. From the available NOAA's data, the probability distributions for the hurricane parameters such as maximum wind speed, hurricane speed, radius to maximum wind speed, barometric pressure, phase with astronomical tides, etc., are established. The results of the 2-D model synthetic hurricanes are then used to configure and calibrate the 1-D model. This 1-D model, when run for the storms anticipated in 2000 years for a particular site, gave sufficient data to determine storm surge elevations for return periods up to 500 years. Since the astronomical tide phase was considered to be a parameter in Monte Carlo simulation, it is accounted for in the statistics for the various return interval events (Sheppard and Miller, 2003).

Maximum dynamic wave setup across the surf zone is calculated using the maximum deep-water significant wave height. Because of the variation of deep-water significant wave height with wind speed and that of wind speed with time, the dynamic wave setup is time dependent. Therefore, the storm surge due to wind stress, barometric pressure, and the effect of astronomical tide is added to the value of maximum dynamic wave setup calculated at each time step to yield the total storm tide history.

Input data required by the model includes: bathymetric data, topographic data, atmospheric pressure, storm forward speed, astronomical tide, storm size, the components of the water slope, boundary conditions, bottom friction shear stresses, surface wind shear stresses. The output data includes: storm surge elevations and maximum dynamic wave setup across the surf zone.

Another alternative to estimate the storm surge is to use the software ACES (Automated Coastal Engineering Systems), which uses the CEDAS (Coastal Engineering Design and Analysis System) interface to access underlying collection of coastal engineering design and analysis technologies, prepares various and often large input data sets, and visualizes results. Veritech Incorporated developed this software (CEDAS, 2006). The user of this software begins with an analysis of historical events, after a database of storm events for the project site is selected. Then, the events are parameterized according to their characteristics and impacts. An example of a tropical storm input vector includes the following parameters: central pressure deficit, radius to maximum winds, maximum wind velocity, minimum distance from the eye of the storm to the project site, forward speed of the eye, tidal phase, and amplitude during the event. Typical response vectors that are computed by the program include: maximum surge of flood elevation and shoreline erosion. The maximum surge flood elevation may require a hydrodynamic model coupled with a tropical storm model or database containing extra tropical wind fields (CEDAS, 2006).

METEOROLOGICAL AND OCEANOGRAPHIC PARAMETERS

Table 14 presents a list of measurable meteorological or oceanographic parameters to be used in bridge superstructure design.

Table 14. List of measurable meteorological or oceanographic hurricane design parameters

Meteorological parameter	Symbol	Units	Obtained from (depends on)
Mean sea level	MSL	in.	Records* (Bridge location / bathymetry)
Normal high tide	NHT	in.	Records*
Rain	R	in./day	Records* (Storm forward speed (mph)/100)
Wind speed	WS	Mph	Records* (Design storm – hurricane category)
Wind direction	WD	Deg	(Bridge location and orientation)
Wave height	WH	in.	Records* (WS, Slope of sea bottom)
Period of wave	TW	Sec	Records*
Bathymetry/hydrography	BAT	None	(Bridge location)
Forward speed of storm	FSS	Mph	Records*
Central pressure of storm	CPS	in. Hg	Records*
Atmospheric pressure difference	APD	in. Hg	Records*
Earth's rotation	ER	deg/hr	Records*
Radius of maximum winds	RMW	Miles	Records*
Storm track	ST	None	Records*

* A number of these parameters could also be predicted with a model

Maximum rainfall in a day can be estimated by the following equation (Ruch, 1983):

Maximum rainfall (*in.*) = 100 / forward speed of storm (mph)   Equation 112

Rainfall depends on the storm speed, and the precipitation rate is highest near the center of the storm, however, the maximum rainfall is typically less than 12 inches (Simpson and Riehl, 1981). Heavy rainfalls tend to occur on land, where the hurricane forward speed tends to slow down and may stall, while in water the hurricane typically moves faster.

VI. DATABASE OF BRIDGE DESIGN PARAMETERS

Crucial to any design is the availability of data to be used in the design equations. Due to the fact that meteorological data is difficult to find and sometimes to interpret, this section will provide a compilation of hurricane, wave, and meteorological data obtained from four different data sources. Most of the information has been formatted to condense and facilitate its interpretation. The four main sources of databases are: the Texas Coastal Ocean Observatory Network (TCOON) from the Division of Nearshore Research (DNR), the website weatherunderground.com, the National Oceanic and Atmospheric Administration's (NOOA) data buoy center, and NOAA's National Hurricane Center. A brief description and linked references to a world tsunami database are also provided in this chapter. Information contained in this chapter does not necessarily include information on all the parameters needed for the design of bridge superstructures against wave action.

An electronic copy of this database is provided on a compact disc containing four folders. One folder is named TCOON and contains a condensed database for 32 weather stations retrieved from the Texas Coastal Ocean Observation Network. Each station folder contains an Excel file. The Excel file summarizes all the data available at that station, including an overview sheet that describes in a graphical format the availability of each parameter. The overview sheet also indicates the station name, ID, location, and a summary of data on barometric pressure, primary water level, wind speed, and water temperature for each year of data recorded. Separate sheets within the same Excel file list data recorded every hour for four parameters: barometric pressure, primary water level, wind speed, and water temperature.

The CD contains another folder named UNDERGROUND that includes two Excel files: one labeled "Historical Atlantic Coast Data," and another called "Historical Texas Coast Data." The "Historical Atlantic Coast Data" file contains a summary page

showing a plot of the number of events for each year recorded. This Excel file also includes 120 sheets, one for each year of recorded storms from 1886 to 2005. The data contained in each sheet are described in the weather underground database section of this chapter. The second Excel file under the weather underground folder is labeled "Historical Texas Coast Data." This file presents the same information as the Historical Atlantic Coast Data file, except that this file includes only data about hurricanes and tropical storms that have landed on the Texas coast. The summary page of this file includes a plot of storm frequency for the Texas coast by month. Further description of this folder is given under the weatherunderground database of this chapter.

The third folder is named NOAA and contains one Excel file and a folder. The Excel file is labeled "NOAA Historical" and contains historical data retrieved from NOAA's National Hurricane Center. The contents of this file are described further in the NOAA's National Hurricane Center section of this chapter. The folder located under the NOAA folder is labeled "NOAA National Data Buoy Center" and contains weather data retrieved from 12 buoys. The folder includes reports of data for hurricanes Katrina, Rita, and Wilma in word document format. The data from the buoy stations are provided in separate folders, each identified by the buoy's ID number. Further information about this database is given in the NOAA's National Data Buoy Center database description of this chapter.

The fourth folder termed TSUNAMI contains copies of two pdf files containing two journal articles that relate to tsunami and tsunami-like waves recorded in the eastern United States and the Caribbean Sea.

TEXAS COASTAL OCEAN OBSERVATORY NETWORK

This section includes a description of the type of information available in the Texas Coastal Ocean Observation Network (TCOON). The network is part of the

Division of Nearshore Research, and some of the data collected includes: water level, wave period and height, temperature, wind speed and direction, barometric pressure, cumulative rainfall, water velocity, and tides.

This database collects data at 32 stations along the Texas coast (TCOON-1, 2005). The data are transmitted to Texas A&M University-Corpus Christi at multiples of six-minute intervals via line-of-sight packet radio, cellular phone, or GOES satellite. The data is then processed and stored in real time in a database linked to the world wide web. TCOON has been in operation since 1988. A description of the information provided in the web page is presented below.

Figure 45 shows the location of the 32 active TCOON stations on the Texas coast. The TCOON data query web page shown in Figures 46 and 47 allows the user to retrieve data from the DNR on a variety of formats and combinations (TCOON-2, 2005). The data query page is divided into three sections as shown in Table 15:

Table 15. TCOON main page options

Section	Options
Basic query parameters	Enter desired stations, series, dates, and output format
Graph options	Customize graph layout and construction
ACII options	Customize ASCII data formatting

Figure 45. Location of active TCOON stations, source: (TCOON-1, 2005).

Basic Query Parameters		
Stations:	--------------------- TCOON Stations --------------------- Arroyo Colorado (047, ARROYO) Baffin Bay (068, BAFFIN) Battleship Texas State Park (533, BATTLE)	See note I
Series:	-------------------- Water Level -------------------- Primary Water Level (pw l) Backup Water Level (bw l) Harmonic Predicted Water Level (harmw l) Water Level Std Dev (sig)	See note II
Dates:	Africa/Bujumbura ▼ 02/08/2006-02/15/2006	See note III
Format:	⦿ Graph ▢ Text Rows ▢ Spreadsheet ▢ Text Columns	See note IV
Units:	⦿ Metric ▢ English ▢ DNR	See note V
Elevation:	Station Datum ▼	See note VI
Interval:	Default ▼	See note VII
Date Format:	Entered below (default if blank) ▼	See note VIII
	Click here to retrieve data	

Figure 46. Basic query parameters, source: (TCOON-2, 2005).
(See figure notes on following page.)

119

NOTES:

I ⓘSelect the station(s) of interest from the selection box. Stations are grouped by function and listed alphabetically by name within each group. If you already know the identifiers for the station(s) you want, you can enter them directly into the text box. Click for more information on DNR stations and locations.

II ⓘSelect the data series you'd like to view. Note that not all data series are available for all stations. If you already know the abbreviations for the series you want, you can enter them directly into the text box. Click for more information on data series.

III ⓘEnter the range of dates for which you want data. In general you can enter dates in the form **mm/dd/yyyy-mm/dd/yyyy**, but other specifications such as **yesterday**, **now, -7d**, and **mm/yyyy** also work. Click for more information on date ranges.

IV ⓘSelect your desired output format. Click for more information on output formats.

V ⓘSelect your desired output units. **DNR** units indicate the default unit of measurement as stored in our database (always an integer value). Click for more information on units.

VI ⓘWhat do you want vertical elevations (e.g., water level) referenced to? The default is **station datum**, which is an arbitrary zero established at each station. Other elevations may not be available for the station(s) you've requested. Click for more information on elevations.

VII ⓘFor column-style output, select the time interval to use for each row of output. The value reported on each row is the value recorded at the time indicated on the row.

VIII ⓘHow do you want dates to be displayed? The default gives reasonable output for most requests, but if you need more control you can either select a predefined format from the top selection box or enter your own strftime specification in the bottom box. Click for more information on date formats.

Graphical Output Parameters		
Title:		ⓘSpecify an optional title for the graph.
Width:	600	ⓘSpecify the width of the graph output image.
Height:	400	ⓘSpecify the height of the graph output image.
Legend Position:	⊙ Default ☐ Top ☐ Left ☐ No Legend ☐ Bottom ☐ Right	ⓘSpecify the position of the legend.
	Click here to retrieve data	

Figure 47. Graphical output parameters, source: (TCOON-2, 2005).

List of TCOON stations

Table 16 shows a list of the 32 active stations in the system. Stations are listed by latitude from north to south. In addition to the active stations there are a total of 162 inactive stations.

Table 16. List of TCOON active stations

No.	Station name	No.	Station name
1	Arroyo Colorado	17	Packery Channel
2	Baffin Bay	18	Port Aransas
3	Battleship Texas State Park	19	Port Arthur
4	Bob Hall Pier	20	Port Isabel
5	Clear Lake	21	Port Mansfield
6	Copano Bay	22	Port O'Connor
7	Eagle Point	23	Rainbow Bridge
8	East Matagorda, Old Gulf Cut	24	Rincon del San Jose
9	Freeport	25	Rockport
10	Galveston Entrance Channel, North Jetty	26	Rollover Pass
11	Galveston Entrance Channel, South Jetty	27	S. Bird Island
12	Galveston Pier 21	28	S. Padre Island Coast Guard Station
13	Galveston Pressure Pier	29	Sabine Pass
14	Ingleside	30	Seadrift
15	Manchester Houston	31	Texas State Aquarium
16	Morgans Point	32	White Point

Basic query parameters

The TCOON database is organized in several groups of data. Each data group will be labeled from A through H for convenience in this report. Group A contains information about the water level, group B about weather, group C about waves, group D related to water velocity, group E about tides, group F regarding water quality, group G related to monthly statistics, and group H about other data. The type of information stored in each data group is described below.

Information available by data group

Table 17 indicates the type of data contained in each data group. Group F collects the following data on water quality: water salinity, conductivity, pH, dissolved oxygen, saturation, turbidity, and water depth. Group H stores data on battery voltage and calibration temperatures A and B. The data collected on Group H gives information about the data acquisition system and measurement apparatuses. Since the data contained in groups F and H are irrelevant to this project, they are not listed in Table 17.

Table 17. Data contained in each group

No.	Data	No.	Data
A - Water level			
1	Primary water level	4	Water level standard deviation
2	Backup water level	5	Water level outliers
3	Harmonic predicted water level	6	Stage height
B - Weather			
1	Air temperature	6	Barometric pressure
2	Water temperature	7	Cumulative rainfall
3	Wind speed	8	Wind speed B
4	Wind gust	9	Wind gusts B
5	Wind direction	10	Wind direction B
C - Waves			
1	Significant wave height	6	RDI wave direction
2	Peak wave period	7	RDI maximum wave height
3	RDI significant wave height	8	RDI mean wave period
4	RDI peak wave period	9	Pressure
5	RDI water depth	10	Average water pressure
D - Water velocity			
1	Velocity X	12	Mid-depth velocity Up
2	Velocity Y	13	Bottom velocity East
3	Velocity Z	14	Bottom velocity North
4	Velocity East	15	Bottom velocity Up
5	Velocity North	16	Signal strength X
6	Velocity Up	17	Signal strength Y
7	Surface velocity East	18	Signal strength Z
8	Surface velocity North	19	ADCP compass heading**
9	Surface velocity Up	20	ACDP sensor tilt
10	Mid-depth velocity East	21	ACDP sensor roll
11	Mid-depth velocity North	22	Percent good
E - Tides			
1	Higher high water	4	Low water
2	Lower high water	5	Higher low water
3	High water	6	Lower low water
G - Monthly statistics			
1	Monthly mean higher high water	7	Monthly great diurnal range
2	Monthly mean high water	8	Monthly mean tide range
3	Monthly mean tide level	9	Monthly DHQ***
4	Monthly mean sea level	10	Monthly DLQ****
5	Monthly mean low water	11	Salinity lower bound
6	Monthly mean lower low water	12	Salinity upper bound

* Relational dimensions instrument (RDI)
** Acoustic Doppler current profiler (ADCP)
*** Diurnal high water inequality (DHQ)
**** Diurnal low water inequality (DLQ)

The following data are also stored at each station regarding elevation: station datum, mean higher high water, mean high water, mean tide level, mean sea level, mean low water, mean lower low water, mean water level, national geodetic vertical datum (1929), North American vertical datum 1988, and COE mean low tide.

An Excel file containing a record of the years in which data is available in all the active TCOON stations is attached to this document. The file is labeled "data available at TCOON stations." The Excel spreadsheets include data for all the elements in the TCOON database (all elements in data groups A through H) for each station.

Nomenclature used in the database

Mean higher high water (MHHW)

MHHW is the average height of the higher high waters over a 19-year period. For shorter periods of observation, corrections are applied to eliminate known variations and reduce the result to the equivalent of a mean 19-year value.

Mean high water (MHW)

MHW is the average height of the high waters over a 19-year period. For shorter periods of observations, corrections are applied to eliminate known variations and reduce the results to the equivalent of a mean 19-year value. So determined, mean high water in the latter case is the same as mean higher high water.

Mean tide level (MTL)

MTL represents a plane midway between mean high water and mean low water. Not necessarily equal to mean sea level. Also known as half-tide level.

Mean sea level (MSL)

MSL is the average height of the surface of the sea for all stages of the tide over a 19-year period, usually determined from hourly height readings. Not necessarily equal to Mean Tide Level. It is also the average water level that would exist in the absence of tides.

Mean low water (MLW)

MLW is the average height of the low waters over a 19-year period. For shorter periods of observations, corrections are applied to eliminate known variations and reduce the results to the equivalent of a mean 19-year value. All low water heights are included in the average where the type of tide is either semidiurnal or mixed. Only lower low water heights are included in the average where the type of tide is diurnal. So determined, mean low water in the latter case is the same as mean lower low water.

Mean lower low water (MLLW)

MLLW is the average height of the lower low waters over a 19-year period. For shorter periods of observations, corrections are applied to eliminate known variations and reduce the results to the equivalent of a mean 19-year value. Frequently abbreviated to Lower Low Water.

WEATHERUNDERGROUND DATABASE

This section includes a brief description of a database existing in the website weatherunderground (Weatherunderground, 2005). The subdirectory labeled "UNDERGROUND" contains a database of historical hurricanes developed on the Atlantic Ocean and the Gulf of Mexico between 1886 and 2005. This database includes information such as storm name, storm track, date of occurrence, maximum wind speed, minimum pressure, and number of deaths caused by the storm. This information is

presented in two separate files: "Historical Atlantic Coast Data" and "Historical Texas Coast Data."

The Atlantic coast data file contains records of tropical storms and hurricanes that landed on the U.S. Atlantic Ocean coast between 1886 and 2005. This file includes plots of storm path and maximum wind speed records for each recorded storm. Data on minimum barometric pressure and number of deaths are also given for some storms. This database summary includes a storm frequency chart that depicts the number of tropical storms and hurricanes that occurred each year.

The Texas coast file includes data on tropical storms and hurricanes that landed on the Texas coast between 1886 and 2005. Plots of storm paths and maximum wind speeds are presented for each event. Charts of storm frequency by year and by month are also given in this file.

NOAA'S NATIONAL DATA BUOY CENTER

The National Data Buoy Center was formed in 1967 with the mission to provide reliable marine data for the National Weather Service (NDBC, 2006). The system has buoys placed around the United States. These buoys measure average wave period, dominant wave period, sea level pressure, significant wave height, sea temperature, peak wind gust, and average wind speed. Each buoy indicates the date it was placed in service. The parameters are available every hour for the years stated in the historical portion of the website. Along with the historical data, the active buoys can provide current wave and weather conditions in real-time weather forecasting in the recent data portion of the records.

This document is complemented with a file folder named "NOAA National Data Buoy Center," located under the "NOAA" folder. The NOAA National Data Buoy

Center folder contains a summary of data retrieved from 12 buoys along the Texas coast. Each buoy record was placed in a separate folder labeled with the buoy's ID number. The buoy ID numbers are shown in Figure 48, obtained from NOAA's web page (NDBC, 2006). Each buoy folder contains a word document that describes the information available for that buoy.
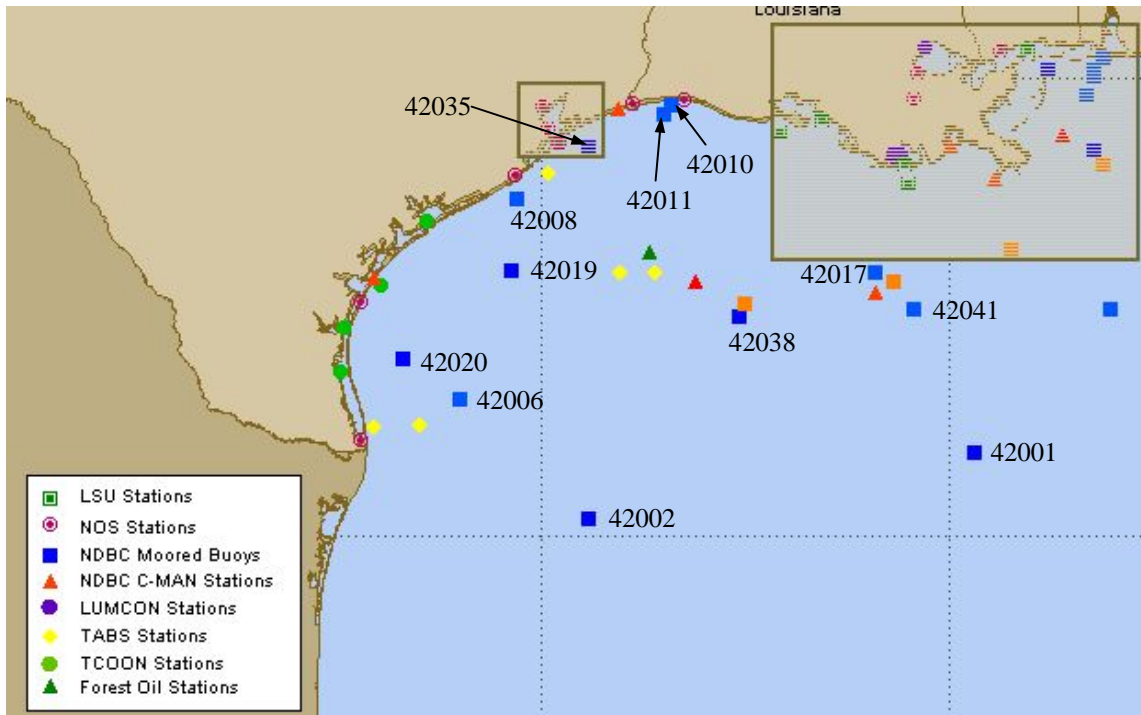
Figure 48. NOAA's buoy location map (only blue squares are buoys) , source: (NDBC, 2006).

This database is also accompanied by three reports about hurricanes Katrina, Rita, and Wilma. The reports were produced by the National Data Buoy Center and include recorded storm track, wind speed, sea level pressure, significant wave height, and dominant wave period. These reports are provided in electronic format on a compact disc.

In addition to this database, NOAA's Environmental Buoy Data has compiled buoy information in CD ROMs, and they are available for sale (NOAA-8, 2006). The

CD-ROMs contain a historical archive of oceanographic and meteorological data obtained by moored buoys and C-MAN stations operated by the NOAA National Data Buoy Center. The set consists of seven discs containing data collected by the buoys from the 1970s through December 1977, with online Internet links to updated data, information, and time series plots. Parameters compiled in the database include air sea temperatures, wind and wave data, and other oceanographic and meteorological data. Disk 1 contains data from the upper North Atlantic buoys, disk 2 has data from the mid and lower North Atlantic buoys, disk 3 compiles data from buoys located in the Gulf of Mexico, disk 4 stores buoy data from the Great Lakes, disk 5 compiles data from buoys in the lower Eastern U.S. coast Pacific, disk 6 has data from buoys in the upper Eastern U.S. coast Pacific, and disk 7 stores data from Alaska, Hawaii, and other Pacific buoys.

NOAA'S NATIONAL HURRICANE CENTER

The National Weather Service and the National Oceanic and Atmospheric Administration made available data from the National Hurricane Center through a web page (NOAA-1, 2006). The following information is provided there:

- an archive of hurricane seasons (NOAA-2, 2006);
- a list of the costliest hurricanes without adjustment for inflation (NOAA-3, 2006);
- a list of the costliest hurricanes adjusted for inflation (NOAA-4, 2006);
- a list of the deadliest hurricanes (NOAA-5, 2006);
- a list of the most intense hurricanes (NOAA-6, 2006); and
- a file containing a list of hurricanes recorded according to the state where they landed (NOAA-7, 2006).

This section is accompanied by a file containing a summary of NOAA's list of hurricanes recorded by state. The file name "NOAA Historical by State," includes a list of hurricane direct hits on the mainland United States between 1851 and 2004. The file

indicates the total number of hurricanes landing on a given state, specifying the category under the Excel sheet labeled "Historical by State." The same file contains another sheet labeled "Historical with Pressure-Speed," presenting a chronological list of all hurricanes which affected the continental United States between 1851 and 2005. This file includes information such as minimum central pressure in millibars and maximum wind speed in knots.

WEATHER INFORMATION STUDIES

The U.S. Army Corps of Engineers through the Coastal and Hydraulics laboratory has developed a set of hindcasts of ocean waves (COE, 2006). The laboratory provides a website labeled Wave Information Studies, that contains a database of wave hindcast data for the entire U.S. Atlantic and Pacific coasts as well as Puerto Rico, Hawaii, and Alaska (COE-2, 2006). The data is produced by numerical simulation of past wind and wave conditions (hindcasting). Data is available for 91 stations located along the Texas coast. The data for the Gulf of Mexico and Atlantic Ocean can provide plots of wave information between 1980 and 1999. The data provided includes: station number, location (latitude and longitude), water depth, significant wave height, peak wave period, overall vector mean wave direction, wind direction, and wind speed. The hindcasting model used is called WISWAVE and is fed using measured wave and wind data from buoys and satellites.

OCEANWEATHER

Oceanweather incorporated is a private company that has applied hindcasting models since 1983 to forecast ocean wind and waves (Oceanweather, 2006). Oceanweather has a forecast center that runs operational global and regional wave models.

WORLD TSUNAMI DATABASE

This section of the document briefly describes two journal articles contained in pdf format under the electronic folder labeled TSUNAMI that accompanies this document. Lander et al. describe a brief history of tsunamis in the Caribbean Sea (Lander et al., 2002). This journal article contains a description of many events and several tables summarizing the events and wave data. An article by Lockridge describes tsunamis and tsunami-like weaves of the eastern United States (Lockridge et al., 2002). This document describes events that occurred since 1668, and describes damage and wave data of the events. The document also summarizes earthquake and tsunami data in tables.

An important world tsunami database is found in the International Tsunami Information Centre (ITIC, 2006). This database contains links to four databases: Mediterranean Sea, Atlantic Ocean, Pacific Ocean, and two world datasets. The databases mentioned in this section typically include the maximum wave height recorded for each tsunami event.

Database for the Mediterranean Sea

The database for the Mediterranean Sea includes Tsunami events between 1628 BC and 1999. This database is hosted at the Novosibirsk Tsunami Laboratory in Russia (NTL-1, 2006).

Database for the Atlantic Ocean

The database for the Atlantic Ocean reports tsunami events in the Atlantic region between 60 BC and today (NTL-2, 2006). The Novosibirsk Tsunami Laboratory maintains the web version of the database. The laboratory is part of the Institute of Computational Mathematics and Mathematical Geophysics of the Siberian Division of

the Russian Academy of Sciences. The database contains two parts; the first one (event data) contains the basic tsunami parameters on 260 historical tsunami events that occurred in the Atlantic. The second part (run-up data) includes available run-up and tide-gage observations for the region.

Database for the Pacific Ocean

This database includes tsunami events that occurred in the Pacific between 47 BC and today. The Novosibirsk Tsunami Laboratory also maintains this database (NTL-3, 2006). This dataset is divided into three parts; the first one (event data) contains information on nearly 1490 historical events. The second part (run-up data) contains almost 8000 coastal run-up and tide-gage observations of wave heights. The third part (earthquake data) contains a worldwide earthquake catalog with close to 6300 events that occurred since pre-historic times.

NOAA/NGDC World Tsunami Database

This database is presented in two formats by the National Oceanic and Atmospheric Administration and by the National Geophysical Data Center of the U.S. The database is presented in GIS graphic format (NOAA/NGDC-1, 2006), as well as in text format (NOAA/NGDC-2, 2006).

FEMA – COASTAL CONSTRUCTION MANUAL

Chapter 7 of the Coastal Construction Manual of the Federal Emergency Management (FEMA) agency contains a table of mean return periods for landfall or nearby passage of tropical cyclones (FEMA, 2000). The return periods are reproduced in Table 18.

Table 18. Mean return period for landfall or nearby passage of tropical cyclones (FEMA, 2000)

Area	Mean return period (years)		
	Passage of all tropical cyclones within 50 miles *	Landfall of all hurricanes (Category 1-5) **	Landfall of all major hurricanes (Category 3-5) **
U.S. (Texas to Maine)	-	0.6	1.5
Texas	1.4	2.7	6.5
South	-	7.5	16
Central	-	16	49
North	-	5.7	14
Louisiana	1.6	3.9	8.1
Mississippi	2.7	12	16
Alabama	2.7	9.7	19
Florida	0.8	1.7	4
Northwest	-	4	14
Southwest	-	5.4	11
Southeast	-	3.7	8.8
Northeast	-	11	#
Georgia	2.0	19	#
South Carolina	2.3	6.9	24
North Carolina	1.7	3.9	8.8
Virginia	4.0	24	97
Maryland	4.2	97	#
Delaware	4.7	#	#
New Jersey	4.7	97	#
New York	3.7	11	19
Connecticut	4.2	19	32
Rhode Island	4.2	19	32
Massachusetts	3.7	16	49
New Hampshire	7.8	49	#
Maine	7.2	19	#
Virgin Islands *	2.0	~	~
Puerto Rico *	2.4	8	~
Hawaii *	7.1	~	~
Guam *	1.0	~	~

*   Based on National Weather Service (NWS) data for period 1899-1992, from FEMA Hurricane Program, 1994

**   for period 1900-1996, from National Oceanic Atmospheric and Administration (NOAA) Technical Memorandum NWS TPC-1, February 1997

\-   No intrastate breakdown by FEMA Hurricane Program

\#   Number not computed (no storms of specified intensity made landfall during 1900-1996)

~   Island; landfall statistics alone may understate hazard

THE HURRICANE AND ITS IMPACT

Simpson and Riehl presented historical data on hurricane impact on the U.S. coast in their book "The Hurricane and Its Impact" (Simpson and Riehl, 1981). Figure 49 obtained from appendix D of the book indicates in box *a* the number of years between occurrences of hurricanes (having maximum wind speeds in excess of 75 mph) and in box *b* the number of years between occurrences of severe hurricanes (having maximum wind speeds in excess of 125 mph) for 58 coastal segments along the Gulf and Atlantic coastlines of the United States.

Table 19 shows data on the number of hurricanes reaching the United States mainland during the period 1886-1970 for each of the 58 coastal segments indicated in Figure 49. Table 20 lists the probability for a hurricane strike in any given year for each of the 58 coastal segments illustrated in Figure 49.
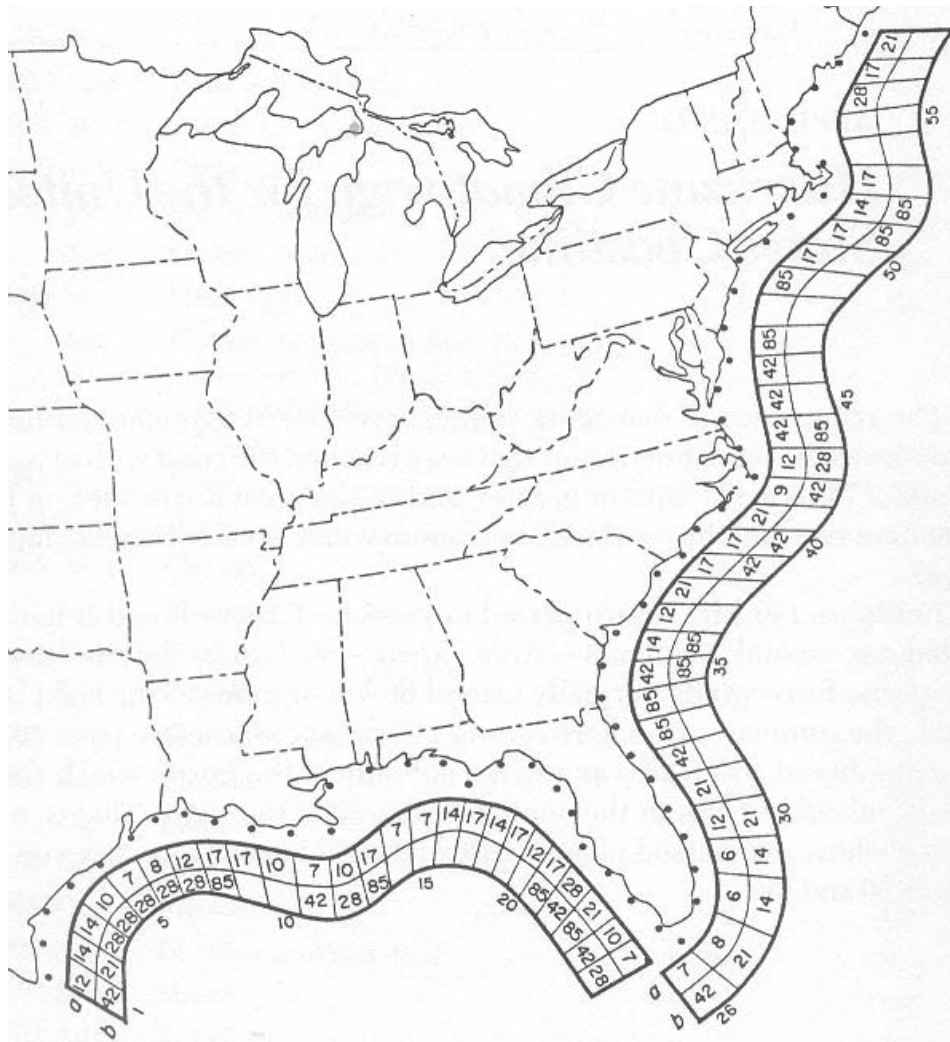
Figure 49. Number of years between occurrences of hurricanes with wind speeds of (*a*) greater than 75 mph and (*b*) greater than 125 mph, source: (Simpson and Riehl, 1981).

Table 19. Number of hurricanes landing on the U.S. coast between 1886 and 1970 for each coastal segment illustrated in Figure 49 (Simpson and Riehl, 1981).

Sector	All hurricanes	Great hurricanes	Sector	All hurricanes	Great hurricanes
1	7	2	30	7	4
2	6	4	31	4	-
3	6	3	32	2	-
4	8	3	33	1	-
5	12	3	34	1	-
6	10	3	35	2	1
7	7	3	36	6	1
8	5	1	37	7	-
9	5	-	38	4	-
10	8	-	39	5	2
11	11	2	40	5	2
12	8	3	41	4	
13	5	1	42	9	2
14	11	-	43	7	3
15	12	-	44	2	1
16	6	-	45	2	-
17	5	-	46	2	-
18	6	-	47	1	-
19	5	-	48	-	-
20	7	-	49	1	-
21	5	1	50	5	-
22	3	2	51	5	1
23	4	1	52	6	1
24	8	2	53	5	-
25	11	3	54	-	-
26	11	2	55	-	-
27	10	4	56	3	-
28	14	6	57	5	-
29	13	6	58	4	-

Note: Hurricane = winds of 75 mph or greater, great hurricane = winds of 125 mph or higher.
Source: Adapted from R.H. Simpson and M.B. Lawrence, Atlantic hurricane Frequencies, Technical memo NWS SR-58 (N. p.: Department of Commerce-NOAA, 1971).

Table 20. Probability for a hurricane strike in any given year for each coastal segment illustrated in Figure 49 (Simpson and Riehl, 1981).

Sector	All hurricanes (%)	Great hurricanes (%)	Sector	All hurricanes (%)	Great hurricanes (%)
1	8	2	30	8	5
2	7	5	31	5	-
3	7	4	32	2	-
4	9	4	33	1	-
5	14	4	34	1	-
6	12	4	35	2	1
7	8	4	36	7	1
8	6	1	37	8	-
9	6	-	38	5	-
10	9	-	39	6	2
11	13	2	40	6	2
12	9	4	41	5	
13	6	1	42	11	2
14	13	-	43	8	4
15	14	-	44	2	1
16	7	-	45	2	-
17	6	-	46	2	-
18	7	-	47	1	-
19	6	-	48	-	-
20	8	-	49	1	-
21	6	1	50	6	-
22	4	2	51	6	1
23	5	1	52	7	1
24	9	2	53	6	-
25	13	4	54	-	-
26	13	2	55	-	-
27	12	5	56	4	-
28	16	7	57	6	-
29	15	7	58	5	-

Note: Hurricane = winds of 75 mph or greater, great hurricane = winds of 125 mph or higher.
Source: Adapted from R.H. Simpson and M.B. Lawrence, Atlantic hurricane Frequencies, Technical memo NWS SR-58 (N. p.: Department of Commerce-NOAA, 1971).

Table 21 shows the expected daily ranges of astronomical tides during hurricane season for the Atlantic and Gulf of Mexico coasts of the United States.

Table 21. Expected daily ranges of astronomical tides during hurricane season (Simpson and Riehl, 1981).

Location	Jun		Jul		Aug		Sep		Oct		Nov	
	M	X	M	X	M	X	M	X	M	X	M	X
Tampico (Mexico)	1.3	2.6	1.0	2.6	1.0	2.3	1.0	2.0	1.0	2.0	1.3	2.6
Galveston (TX)	1.0	2.0	0.7	2.3	1.0	2.3	1.0	2.0	1.0	2.0	1.0	1.6
Mobile (AL)	1.6	2.6	1.3	2.6	1.3	2.3	1.0	2.0	1.0	2.3	1.3	2.6
St. Marks (FL)	2.3	4.9	2.3	4.9	2.3	4.6	2.3	4.3	2.3	4.6	2.3	4.9
St. Petersburg (FL)	1.6	3.3	1.3	3.3	1.3	3.0	1.3	2.6	1.3	3.0	1.3	3.3
Key West (FL)	1.3	3.0	1.3	3.0	1.3	2.6	1.3	2.3	1.3	2.6	1.3	2.6
Miami (FL)	2.6	3.6	2.6	3.6	2.6	3.6	2.6	3.3	2.6	3.6	2.6	3.6
Mayport (FL)	4.9	6.6	4.6	6.2	4.6	6.2	4.6	5.9	4.6	5.9	4.6	6.6
Savannah (GA)	7.9	10.2	7.5	10.2	7.5	9.8	7.5	9.5	7.5	9.2	7.5	9.5
Charleston (SC)	5.2	7.2	4.9	7.2	4.9	6.9	5.2	6.6	4.9	6.6	5.2	7.2
Wilmington (NC)	3.6	4.6	3.6	4.6	3.6	4.6	3.6	4.6	3.6	4.3	3.6	4.3
Hampton Rds (VA)	2.3	3.9	2.3	3.9	2.3	3.6	2.6	3.3	2.6	3.6	2.6	3.6
Reedy Pt (DE)	5.6	7.5	5.6	7.5	5.2	6.9	5.2	6.6	5.2	6.6	5.2	6.6
Sandy Hook (NJ)	4.9	7.2	4.6	6.9	4.6	6.9	4.6	6.6	4.6	6.6	4.9	6.9
New York (Battery)	4.6	6.9	4.6	6.9	4.6	6.6	4.6	6.2	4.6	6.2	4.6	6.6
Bridgeport (CN)	6.6	9.8	6.6	9.5	6.9	8.9	6.9	8.5	6.6	9.2	6.6	9.5
Newport (RI)	3.6	5.6	3.6	5.6	3.6	5.2	3.6	4.9	3.6	5.2	3.6	5.6
Boston (MA)	9.5	14.1	9.8	13.5	12.8	13.1	9.5	12.1	9.5	12.8	9.5	13.8
Eastport (ME)	17.4	24.6	17.7	24.0	17.7	23.3	17.7	22.3	17.7	23.6	17.7	24.6

HURRICANE CLIMATOLOGY FOR THE ATLANTIC AND GULF COASTS OF THE UNITED STATES

This document contains information on the following subjects: sources of data, hurricane central pressure data, hurricane radius of maximum winds, hurricane speed and direction of forward motion, source of speed and direction of forward motion data, meteorological parameters and their interrelations, consideration of data samples for statistical tests, selection of hurricane groups for the Gulf, Florida, and Atlantic coasts, joint probability analysis of central pressure and radius of maximum winds, frequency of hurricane and tropical storm occurrences (Ho et al., 1987).

OTHER DATA

Data on bathymetry of the Texas coast can be found on the National Geophysical Data Center (NGDC, 2006), where posters, slides sets, and digital data are available for purchase. The Bureau on Economic Geology distributes a map of the bathymetry of the Gulf of Mexico made by Elazar Uchupi (Uchupi, 1967).

VII. DATABASE UPDATING PROCESS

This chapter describes the process that can be followed to update the databases presented in the previous chapter. The updating processes are presented in the same order as the databases in the previous chapters, beginning with the TCOON archive, following with the weather underground database. This chapter also includes the updating process for data obtained from NOAA's National Data Buoy Center and the data obtained from NOAA's National Hurricane Center.

TEXAS COASTAL OCEAN OBSERVATORY NETWORK

To update this database first go to the TCOON website (TCOON-1, 2006). Then, under the quick links portion choose data query. This brings the page in Figure 46 onto the screen. At this page choose a station, the parameter needed, the dates desired, the spreadsheet format, metric units, and an hourly interval. Then click the designated icon to retrieve the data. The data will save in an Excel file in one vertical column. Select the data in Excel to copy and paste it into the format set in the database. Then, use Excel's formulas to find the statistical values desired and place on overview sheet within the stations folder.

WEATHERUNDERGROUND DATABASE

Enter the weather underground web page (Weatherunderground, 2005). On the main page select the "Tropical/Hurricane" tab. Scroll down the hurricane archive portion of the page. On the right side of the page under the heading "Historical Hurricane Statistics," select "View the Entire Hurricane Archive." On this page select the year of interest, and this will bring up a map of all the hurricane tracks for that year. Simply copy and paste that picture to an Excel file, and then sort the data, and plot it in tables. To compile the database with hurricanes and tropical storms landing on the Texas coast, each hurricane has to be accessed through its own link shown under the picture

indicating storm paths for any given year. This link depicts each storm's path, as well as an account of every six hours the storm was active. The archive reports changes in category, wind speed, pressure, latitude, and longitude with time.

NOAA'S NATIONAL DATA BUOY CENTER

To update the archive described in the previous chapter, first visit the NOAA National Data Buoy Center website (NDBC, 2006). Then click on the "Historical Data" tab. Choose the western Gulf of Mexico portion of the map by clicking on it. This will bring up only this region. From this new map click on one of the blue squares, labeled with the buoy's ID number. This will open the buoys pages where historical data may be retrieved. There is constant data in text form or graphical data over an extended period of time in box-whisker plots. If more recent information of current weather or wave conditions is needed, simply choose the "Recent Data" tab instead of the "Historical Data" tab on the main page of the National Data Buoy Center. This will bring up the same maps, excluding the inactive buoys. The data retrieval is self-explanatory. Conditions are available in real time for weather forecasting if needed.

NOAA'S NATIONAL HURRICANE CENTER

Updating the database presented in the previous chapter only requires to copy information from the data presented in a table format at the web site referenced in the previous chapter, and paste it in the Excel file indicated previously.

OTHER DATABASES

Since no data was summarized from the Weather Information Studies, Oceanweather, and the World Tsunami Database listed in the previous chapter, no updating information is necessary. Likewise, no updating process is given for the data collected from the FEMA Coastal Construction Manual, the book "The Hurricane and Its

Impact," NOAA's report "Hurricane Climatology for the Atlantic and Gulf Coasts of the United States," and the maps of the bathymetry of the Gulf of Mexico, since no updating is required.

VIII. PLAN OF ACTION TO DEVELOP DESIGN METHODOLOGIES

From the literature search conducted it can be seen that most of the work on the field of wave forces has been developed for offshore structures. The existing methods to estimate wave induced forces on bridge decks show significant discrepancies. It is also evident that current bridge design codes do not provide adequate guidance to account for the action of wave forces on bridge superstructures. Thus, it seems that the development of a design methodology to estimate the action of waves on bridge decks is necessary. The design method needs to provide bridge designers with the necessary tools in a relatively simple format. A designer would need a design process that can take into account the following factors:

1. Design wave conditions:
    a. Significant wave height
    b. Wave direction
    c. Period of design wave
    d. Wave length
2. Water depth at the site (bathymetry)
3. Storm surge
4. Magnitude of design current and direction
5. Allowable damage to structure under design event
6. Allowable environmental conditions that would produce no damage to the structure

The design method shall help the designer arrive at a structure that remains standing after the structure faces the design conditions. The design equations should account for buoyancy of the bridge deck and upward vertical impact forces, as well as lateral hydrostatic pressure and impact pressure. The design method developed should

account for different bridge and railing geometries, location of the bridge, the likelihood of being hit by a hurricane, tides, and foundation stresses.

Numerical and/or experimental investigations may be necessary to develop the new design methodology. If numerical and/or experimental investigations are warranted, all steps should be identified and justified, and the procedure to be followed to arrive at the desired results properly described. The new design methodology should clearly state its limitations. The design method should be presented in a format consistent with the AASHTO Bridge Design Specifications.

IX. BENEFITS OF EXPANDING THIS RESEARCH

The benefits of expanding this research in safety and financial terms are discussed in this chapter. The potential financial benefits of the new methodology will be compared to the expenses incurred in developing it.

SAFETY

No deaths of drivers on bridges are expected to occur due to collapse of a coastal bridge. This statement was made assuming people follow evacuation warnings and directions. This scenario is also assumed because NOAA's hurricane tracking technology can forecast impact from a storm at least three days in advance. However, it is worth mentioning that the death a truck driver was reported after his truck was washed over the side of the Escambia Bay Bridge by hurricane Ivan.

The collapse of a bridge would hinder rescue operations and would affect the safety of stranded residents with possible catastrophic loss of lives. It is hoped that the next research step should provide guidelines to design coastal bridges against the action of wave forces. However, the methodology will have to be defined, e.g., target levels of safety such as those used in the design specification of earthquake resistant structures. For instance, in earthquake engineering, it is common to design a structure to sustain major damage but avoid collapse due to the largest magnitude earthquake estimated to occur within the life span of the structure. It is also common to design the structure to withstand minimal damage due to the most probable earthquake estimated to occur within the life span of the structure. These principles were developed to prevent loss of lives of people working or living in the structure while the earthquake happens. Coastal bridges are somewhat different in the sense that they may not cause a direct loss of lives, however, as indicated earlier, lives may be lost due to inability to carry out timely rescue operations if the structure is rendered impassable after a storm, just as happened with hurricane Katrina in 2005.

FINANCIAL

The most expensive research scenario would be to expand this research to an experimental stage that would involve numerical and physical modeling. The cost of this research would be approximately one million dollars. This assumed cost of research will be used to estimate the financial benefits that could be realized with this approach.

Severe hurricane return period

It seems reasonable to assume that only major hurricanes will cause important damage to a coastal bridge. The main return period of all major hurricanes (categories 3-5) given by FEMA for Texas will be used in this document to estimate the future value of the research investment. FEMA indicates that the mean return period of major hurricanes based on 90 years of data for the Texas coast are as follows: South 16 years, Central 49 years, and North 14 years - see Table 18 of this report - (FEMA, 2000). A chart indicating the number of hurricane impacts on the Gulf and Atlantic coasts of the U.S. is shown in Figure 50. It can be observed that for Texas, the area of Houston and Galveston are the most active.

Assumptions for economic analysis

It is assumed for the economic analysis of this section that the area of Galveston Texas has a severe hurricane (categories 3-5) return period of 49 years. This assumption could fall on the conservative side economically speaking, since the return periods given in the previous paragraph indicate 14 years. Thus, the longer it takes a hurricane to impact a bridge and damage it, the older and less valuable the bridge will be. It will be assumed that the value of the bridge decreases linearly from its initial cost, when the bridge is just open to traffic, to zero, when the bridge reaches the end of its design life. The bridge is assumed to retain full strength during its service life, after which the

structure will be deemed structurally unfit or functionally obsolete. The design life of the bridges analyzed in this section will be assumed to be 75 years. This section will assume that when a major hurricane impacts a bridge that was not designed to withstand wave loads, the bridge will be replaced by a new structure.
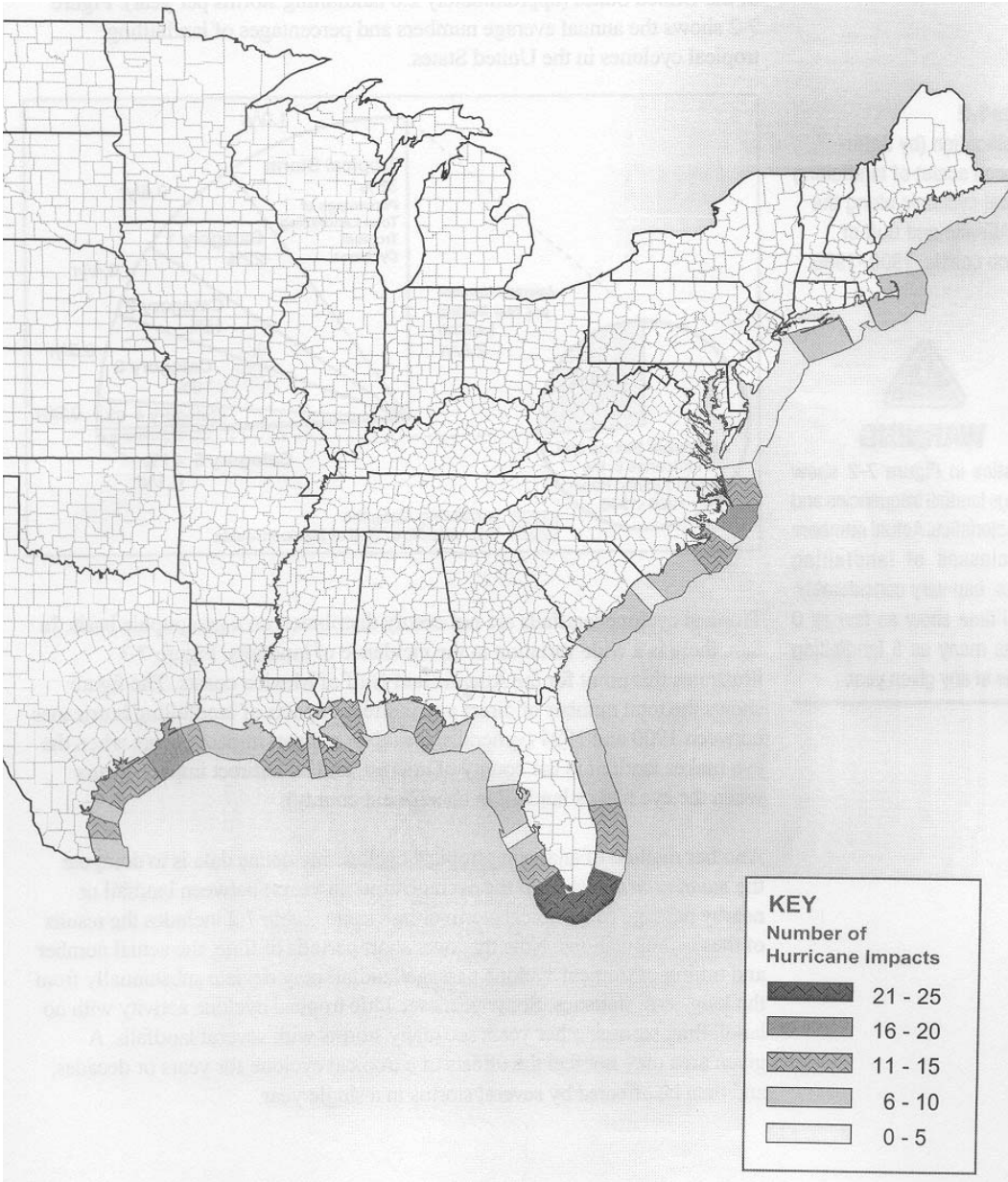

Figure 50. Total number of direct and indirect impacts by landfalling hurricanes for coastal counties from Texas to Maine, 1900-1994, source: (FEMA, 2000).

147

Additionally, it is assumed that when a bridge designed to withstand wave loads is hit by a major hurricane, repairs will be necessary for an amount equivalent to the emergency repairs incurred on the I-10 bridge over Lake Pontchartrain in New Orleans. However, the bridge would not need to be replaced.

Bridge costs incurred by hurricane damage

Since cost data for bridge damage is scarce, data from the I-10 bridge across Lake Pontchartrain in New Orleans will be used to estimate hurricane related bridge damage costs. The level section of the superstructure of I-10 bridge across Lake Pontchartrain consisted of two 48 ft-8 in. wide sections each carrying two lanes, simply supported on 65 ft long spans. The bridge had a total length of 5.4 miles (per original blue prints provided by Louisiana DOT). The superstructure rested on pile caps supported by three 54 in. diameter concrete piles. The deck was supported by six prestressed concrete I-beams, each 3 ft 9 in. tall. The mean water level under the level sections of the bridge was variable, but it was approximately 8 ft. The deck clearance above water was approximately 8 ft. A number of spans of the level section were tossed into the water by hurricane Katrina, and the emergency repair operations consisted in restoring one of the two-lane bodies, by moving structurally sound spans from the most damaged body to the other. Several spans had to be rebuilt with a temporary galvanized steel truss system. The foundations for some of the rebuilt spans had to be constructed anew. The total cost for the emergency reconstruction was approximately $35 million. A bridge with 135 ft long spans having the superstructure placed approximately 30 ft above mean sea level will replace the I-10 bridge. The new bridge will be the most expensive project in the history of the state of Louisiana and will cost approximately $400 million dollars.

Economic analysis

The bridge on I-45 crossing Galveston Bay will be used for this analysis. The bridge has an approximate length of 1.9 miles. It will be assumed the costs of the bridge on I-10 across Lake Pontchartrain could be applied to the bridge on I-45 across Galveston Bay. This implies that the superstructures of the old I-10 bridge and the current bridge on I-45 have approximately the same elevation over mean sea level, they have approximately the same water depth, and the wave forces produced by hurricane Katrina on the bridge on I-10 could also be produced by a major hurricane on the I-45 bridge. Then, it could be estimated that the cost of emergency repair and a new bridge on I-45 are proportional to the costs incurred by the New Orleans I-10 bridge. Thus, the costs of emergency repair and a new bridge on I-45 could be estimated as follows:

Cost of emergency repair on I-45

$$CER_{I-45} = CER_{I-10}\left(\frac{1.9 miles}{5.4 miles}\right) = \$35,000,000 * 0.35 = \$12,250,000 \qquad \text{Equation 113}$$

Cost of new bridge on I-45

$$CNB_{I-45} = CNB_{I-10}\left(\frac{1.9 miles}{5.4 miles}\right) = \$400,000,000 * 0.35 = \$140,000,000 \qquad \text{Equation 114}$$

Assuming an average inflation rate of 3% per year the costs of emergency repair and new bridge construction in actual dollars on I-45 in 49 years would be:

Cost of emergency repair on I-45 in 49 years

$$\left(CER_{I-45}\right)_{49} = \$12,250,000 \cdot (1.03)^{49} = \$52,139,000 \qquad \text{Equation 115}$$

Cost of new bridge on I-45 in 49 years

$$\left(CNB_{I-45}\right)_{49} = \$140,000,000 \cdot (1.03)^{49} = \$595,870,000 \qquad \text{Equation 116}$$

If the one million dollars used for research was invested at 3% per year interest rate, the account would have accumulated the following amount in 49 years:

$$\text{Research funds in 49 years} = \$1,000,000 \cdot (1.03)^{49} = \$4,256,000 \qquad \text{Equation 117}$$

The economic value of a new bridge on I-45 is estimated based on the following assumptions:

a. Cost of new bridge is approximately $140 million.
b. Life span of the bridge will be 75 years.
c. The salvage value of the bridge with a decreasing yearly value is $0.

The value of the bridge per year is then calculated as shown below.

$$A = P\left[\frac{i(1+1)^N}{(1+i)^N - 1}\right] \qquad \text{Equation 118}$$

where,

A = Annual worth

P = Present worth

N = Number of periods

i = interest rate

So

$$A = \$140,000,000\left[\frac{0.03(1.03)^{75}}{(1.03)^{75} - 1}\right] = \$4,714,000 \qquad \text{Equation 119}$$

Thus, in 49 years the future value of the bridge worn out would be:

$$F_{49} = A\left[\frac{(1+i)^N - 1}{i}\right] = \$4,714,000 \cdot \left[\frac{(1.03)^{49} - 1}{0.03}\right] = \$511,661,000 \qquad \text{Equation 120}$$

And the salvage value of the bridge left would be equal to the cost in 49 years minus the value worn out.

$$SV_{49} = \$595{,}870{,}000 - \$511{,}661{,}000 = \$84{,}209{,}000 \qquad \text{Equation 121}$$

The salvage value would be lost if a hurricane destroys the bridge.

The total investment left on a bridge designed for wave loading would include: salvage value, research expenses, and emergency repair costs.

$$TI_{49\,yrs\cdot Wave\text{-}design} = \$84{,}209{,}000 + \$4{,}256{,}000 + \$52{,}139{,}000 = \$140{,}604{,}000 \quad \text{Equation 122}$$

If we consider this value as the initial investment for the remaining 26 years of life of the structure, the annual cost of the structure would be:

$$A_{Wave\text{-}design} = \$140{,}604{,}000 \left[\frac{0.03(1.03)^{26}}{(1.03)^{26} - 1} \right] = \$7{,}865{,}000 \qquad \text{Equation 123}$$

The total investment for a bridge not designed for wave loading would include only new construction in 49 years.

$$TI_{49\,yrs\cdot New\text{-}bridge} = \$595{,}870{,}000 \qquad \text{Equation 124}$$

Considering this value as the initial investment for the remaining 75 years of life of the structure, the cost of the structure per year would be:

$$A_{New\text{-}bridge} = \$595{,}870{,}000 \left[\frac{0.03(1.03)^{75}}{(1.03)^{75} - 1} \right] = \$20{,}062{,}000 \qquad \text{Equation 125}$$

According to this analysis, developing a design methodology for wave loading through research could result in savings of $20,062,000–$7,865,000 = $12,197,000 per year for the remaining 26 years of life of the bridge. It should be mentioned that this result could change if the field conditions differ from the assumptions made. For example, if the bridge on I-45 on Galveston Bay has the superstructure located well above mean sea level, waves may not be able to reach it during a strong hurricane.

According to information supplied by the director of this research project there are approximately 11 potential bridges that could be affected by a hurricane strike along

the coast of Texas. The economical analysis performed in this chapter assumes the only losses incurred are the material losses associated with the bridge structure. However, material losses can also be associated to damage to the local economy caused by the absence of the bridge and the damage to the area hit by a strong hurricane. For example, the area of Biloxi, Mississippi, is experiencing high economic losses due to the fact that two nearby bridges were lost to hurricane Katrina, and tourism has not returned to the area yet, since most casinos were severely damaged in 2005. Another item not accounted for in this analysis is cost increase after a hurricane impact. The Seattle Times reported the costs for a viaduct that was to be constructed in the state of Washington rose from $2.4 billion to $2.8 billion (17%), the cost of building a tunnel rose from $3.6 billion to $4.6 billion (28%), and the cost for a highway bridge jumped from $3.1 billion to $4.4 billion (41%) after hurricane Katrina hit the New Orleans area in August of 2005 (The Seattle Times, 2006).

X. CONCLUSIONS AND RECOMMENDATIONS

This chapter describes the conclusions arrived at after analyzing the information found in the preparation of this document. This section also addresses some of the questions originally asked by the TxDOT bridge design group, which prompted this investigation.

To a bridge designer who is designing a coastal bridge and is not familiar with coastal engineering, the Coastal Engineering Manual can be confusing. One of the questions that prompted this investigation was: Which wave theory should be used for design of a bridge superstructure? This research has shown that an appropriate wave theory should account for the state of the sea during a hurricane event as well as for the site conditions. It seems that one of the most common wave theories used to determine wave forces for coastal structures is stream function wave theory. It has also been found that linear wave theory has limited applicability, since the sea state generated by strong hurricane winds would produce non-linear waves. Thus, a non-linear wave theory is recommended to estimate the wave parameters.

A verifiable method for design of the superstructure of coastal bridges that can withstand the action of wave forces is not currently available in the literature. A vast amount of information is available about waves and wave loading, but only two documents were specifically developed for coastal bridges (Denson, 1978 and Denson, 1980). El Ghamry presented one of the earliest studies, although it was developed for a dock (El Ghamry, 1963).

An important conclusion is that horizontal forces produced by waves acting on a bridge deck are smaller than vertical forces. Apparently horizontal pressures can be twice as high as the hydrostatic horizontal pressures, while vertical pressures can be approximately six times as high as vertical hydrostatic pressures (McConnell et al.,

2004). However, El Ghamry reported that extraordinarily high vertical pressures were rarely recorded (El Ghamry, 1963). El Ghamry also reported that the vertical pressure head reached values as high as 2.5 times the incident wave height but was typically less than that.

By reviewing the vertical and lateral force estimates obtained using the studies performed by Bea et al. 1999, Denson 1978, Denson 1980, El Ghamry 1963, McConnell et al. 2004, and Douglass et al. 2006, we can observe significant discrepancies. Most of the methods predicted uplift forces in excess of the 340 kips weight of the Biloxi Bay Bridge span, except for the study carried out by El Ghamry, which predicted force values slightly under the bridge weight.

A more detailed comparison of estimates of forces obtained from different methods should be done, since different methods made different assumptions, and the experiments used to arrive at the various methods proposed involved structures with different characteristics. Some of the differences are attributed to the fact that some methods predict average force values, while others estimate maximum forces.

Most methods were not developed for bridge structures, which are unique in their design. Thus, new numerical or physical studies on typical bridge configurations are necessary to validate the force prediction methods proposed in the literature.

An investigation of the state of knowledge in design aids and codes showed that some documents account for the effects of wave-induced forces. However, none of the design aids reviewed proposes a method developed specifically to estimate wave forces on bridge decks.

All experimental reports presented great variability in the data obtained. In this regard, due to the uncertainties involved in the prediction of pressure imposed by waves

on structures, the Coastal Engineering Manual proposes the designer to use the equations they provide as a preliminary estimate. The CEM recommends the final design of important structures to include laboratory tests. The CEM also states that no reliable method exists to predict impulsive pressures produced by breaking waves, due to the extremely stochastic nature of wave impacts. This shows the level of uncertainty involved in this type of environmental loading. Thus, the need of coastal engineering knowledge for the design of bridges is evident.

The financial analysis carried out in this study estimated that an investment of one million dollars was necessary to develop a design methodology that would allow bridge decks to withstand wave forces. The design methodology developed through research could result in annual savings of approximately 12 million dollars for 26 years for one bridge.

REFERENCES

Aagaard, P.M. and Dean, R.G., *Wave Forces: Data Analysis and Engineering Calculation Method*, Offshore Technology Conference, Dallas, Texas, Paper No. OTC 1008, pp. I95-I107, 1969.

AASHTO, *LRFD Bridge Design Specifications*, Customary U.S. Units, Third Edition, 2004.

Allaby, M., 1997, *Hurricanes: Facts on File*, Dangerous Weather Series.

Anderson, P., *Substructure Analysis and Design*, Ronald Press, 1995.

ASCE/SEI 7-05, *Minimum Design Loads for Buildings and Other Structures*, ASCE Standard, American Society of Civil Engineers, 2006.

ASCE/SEI 24-05, *Flood Resistant Design and Construction*, ASCE Standard, American Society of Civil Engineers, 2006.

Barltrop, N.D.P., Mitchell, G.M., and Atkins, J.B., *Fluid Loading on Fixed Offshore Structures*, UK Department of Energy, OTH 90 322, 2 Volumes, HMSO Books, London, 1990.

Bea, R.G., Xu, T., and Ramos, R., *Wave Forces on Decks of Offshore Platforms*, Journal of Waterway, Port, Coastal, and Ocean Engineering, May/June 1999, pp. 136-144.

CALTRANS 2005a, *Bridge Design Practice*, California Department of Transportation, 2005, http://www.dot.ca.gov/manuals.htm, Accessed on March 19, 2005.

CALTRANS 2005b, *Bridge Design Aids*, California Department of Transportation, 2005, http://www.dot.ca.gov/manuals.htm, Accessed on March 19, 2005.

CALTRANS 2005c, *Bridge Design Specifications*, California Department of Transportation, 2005, http://www.dot.ca.gov/manuals.htm, Accessed on March 19, 2005.

Campbell, I.M.C. and Weynberg, P.A., *Measurement of Parameters Affecting Slamming*, Final Report, Report No. 440, Technology Reports Centre No. OT-R-8042, Southampton University: Wolfston Unit for Marine Technology, 1980.

CEDAS, *Coastal Engineering Design and Analysis System*, Veri-Tech, Inc., http://www.veritechinc.net/products/cedas/index.htm#Overview, Accessed on May 20, 2006.

CEM, *Coastal Engineering Manual*, U. S. Army Corps of Engineers, EM1110-2-1100, 2002.

CEM, *Coastal Engineering Manual*, U. S. Army Corps of Engineers, EM1110-2-1100, 2003.

CEM, 2006, *Coastal Engineering Manual*, U. S. Army Corps of Engineers, EM1110-2-1100, Accessed on 7-14-06, http://users.coastal.ufl.edu/~sheppard/eoc6430/Coastal_Engineering_Manual.htm.

Çengel and Cimbala, *Fluid Mechanics Fundamentals and Applications*, McGraw Hill, 2006.

Chan, E.S, Cheong H.F., and Gin, K.Y.H., *Breaking-Wave Loads on Vertical Walls Suspended Above Mean Sea Level*, Journal of Waterway, Port, Coastal, and Ocean Engineering, July/August, pp. 195-202, 1995.

Chen, W.F. and Duan, L., *Bridge Engineering Handbook*, Eds., CRC Press, 1999.

COE, U.S. Army Corps of Engineers, Coastal and Hydraulics Laboratory, http://chl.erdc.usace.army.mil/CHL.aspx?p=s&a=ARTICLES;474, 2006.

COE-2, *Wave Information Studies*, U. S. Army Corps of Engineers, Coastal and Hydraulics Laboratory, http://frf.usace.army.mil/cgi-bin/wis/atl/atl_main.html, 2006.

Dean, R.G., *Stream Function Representation of Nonlinear Ocean Waves*, Journal of Geophysical Research, Vol. 70, pp. 4561-4572, 1965.

Dean, R.G., *Evolution and Development of Water Wave Theories for Engineering Applications*, U.S. Army Coastal Engineering Research Center, Fort Belvoir, VA, Vols. I and II, U.S. Army, Coastal Engineering Research Center, Special Report No. 1, 1974.

Dean, R.G. and Darlrymple, R.A., *Water Wave Mechanics for Engineers and Scientists*, World Scientific, Advanced Series on Ocean Engineering – Volume 2, 1991.

Denson, K.H., *Wave Forces on Causeway-Type Coastal Bridges*, Technical Report, Water Resources Research Institute, Mississippi State University, Project No. A-118-MISS, 1978.

Denson, K.H., *Wave Forces on Causeway-Type Coastal Bridges: Effects of Angle of Wave Incidence and Cross-Section Shape*, Water Resources Research Institute, Report No. MSHD-RD-80-070, Department of Civil Engineering, Mississippi State University, 1980.

Douglass, S.L., Chen, Q., Olsen, J.M., Edge, B.L., and Brown, D., *Wave Forces on Bridge Decks*, Draft Report, Prepared for the U.S. Department of Transportation, Federal Highway Administration, Office of Bridge Technology, Washington, D.C., April 2006, http://www.usouthal.edu/usacterec/waveforces.pdf, Accessed on July 20, 2006.

Edge, B., Scheffner, N., Fisher, J., and Vignet, S., *Determination of Velocity in Estuary for Bridge Scour Computations*, Journal of Hydraulic Engineering, Vol. 124, No. 6, pp. 619-628, June 1998.

El Ghamry, O.A., *Wave Forces on a Dock*, Hydraulic Engineering Laboratory, Wave Research Projects, University of California, Berkeley, Institute of Engineering Research Technical Report HEL-9-1, 1963.

Faltinsen, O.M., *Sea Loads on Ships and Offshore Structures*, Cambridge Ocean Technology Series, Cambridge University Press, 1990.

FEMA, *Coastal Construction Manual*, Third Edition, Federal Emergency Management, CD, Vols. I, II, and III, June 2000.

FHWA, *Stream Stability at Highway Structures*, U.S., Federal Highway Administration, Hydraulic Engineering Circular No. 20, February 1991.

FHWA, *Evaluating Scour at Bridges*, U.S. Department of Transportation, Federal Highway Administration, Hydraulic Engineering Circular No. 18, Fourth Edition, May 2001.

FHWA, *Tidal Hydrology, Hydraulics and Scour at Bridges*, U.S. Department of Transportation, Federal Highway Administration, Hydraulic Engineering Circular No. 25, Publication No. FHWA-NHI 04-077, December 2004.

Garrison, *Oceanography: An Invitation to Marine Science*, 5th Edition, Thomson Brooks/Cole, Australia, 2005.

Goda, Y., *A New Method of Wave Pressure Calculation for the Design of Composite Breakwater*, Proceedings 14th International Conference of Coastal Engineering, Copenhagen, pp. 1702-1720, 1974.

Goda, Y., *Random Seas and Design of Maritime Structures*, University of Tokyo Press, Tokyo, 1985.

Goda, Y. *Random Seas and Design of Maritime Structures*, Advanced Series on Ocean Engineering –Volume 15, Second Edition, World Scientific, 2000.

Hagiwara, K. and Yuhara, T., *Fundamental Study of Wave Impact Loads on Ship Bow*, Selected papers from the Journal of the Society of Naval Architecture, Japan, Vol. 14, pp. 73-85, 1976.

Hamill, L., *Bridge Hydraulics*, E and FN Spon (Routhledge), London, 1999.

Harris, D.L., *An Interim Hurricane Storm Surge Forecasting Guide*, National Hurricane Research Project Report No. 32, Weather Bureau, U.S. Department of Commerce, Washington, D.C., 1959.

Hedges, T.S., Proceedings of the Institution of Civil Engineers, Vol. 82, pp. 567-585, 1987.

Hinwood, J., *Design for Tsunamis Coastal Engineering Considerations*, Structural Engineering International, Vol. 3, pp. 189-193, 2005.

Ho, F.P., Su, J.M., Hanevich, K.L., Smith, R.J., and Richards, F.P., *Hurricane Climatology for the Atlantic and Gulf Coasts of the United States*, NOAA Technical Report NWS 38, Silver Spring, MD, April 1987.

Isaacson, M., and Prasad, S., Wave Slamming on a Horizontal Circular Cylinder, Proceedings of Civil Engineering in the Oceans V, R.T. Hudspeth, (Ed.), ASCE, Reston, VA, 1992.

ITIC, International Tsunami Information Centre, http://ioc3.unesco.org/itic/categories.php?category_no=72, Intergovernmental Oceanographic Commission of UNESCO, Accessed on May 15, 2006.

ITTC, *Final Report and Recommendations to the 22nd ITTC*, The Specialist Committee on Environmental Modeling, Proceeding of the 22nd International Towing Tank Conference, Seoul and Shanghai, 1999, http://ittc.sname.org/Environmental%20Modelling.pdf, Accessed July 26, 2006.

Kamphuis, J.W., *Introduction to Coastal Engineering and Management*, Advanced Series on Ocean Engineering, Vol. 16, World Scientific, 2000.

Kaplan, P., *Wave Impact Forces on Offshore Structures: Re-Examination and New Interpretations*, 24th Annual Offshore Technology Conference, Houston, Texas, OTC 6814, May 4-7, pp. 79-86, 1992.

Lander, J.F., Whiteside, L.S., and Lockridge, P.A., *A Brief History of Tsunamis in the Caribbean Sea*, Science of Tsunami Hazards, The International Journal of The Tsunami Society, Vol. 20, No. 2, pp. 57-94, 2002.

Leenknecht, A.S., Szuwalski, A., and Sherock, A.R., *Automated Coastal Engineering System*, U.S. Army Corps of Engineers, Coastal Engineering Research Center, Vicksburg, MS, 1992.

Leira, B. and Langen, I., *On Probabilistic Design of a Concrete Floating Bridge*, Nordic Concrete Research, Vol. 3, pp. 140-166, December 1984.

Lockridge, P.A., Whiteside, L.S., and, Lander, J.F., *Tsunami and Tsunami-Like Waves of the Eastern United States*, Science of Tsunami Hazards, The International Journal of The Tsunami Society, Vol. 20, No. 3, pp. 120-157, 2002.

Lwin, M., *Floating Bridges*, in Bridge Engineering Handbook, Chen, W.F. and Duan, L. (Eds.), CRC Press, 1999.

McConnell, K., Allsop, W., and Cruikshank, I., *Piers, Jetties and Related Structures, Exposed to Waves*, Guidelines for Hydraulic Loadings, HR Wallingford, Thomas Telford, 2004.

Minikin, R.R., *Winds, Waves and Maritime Structures*, Griffin, London, 1950.

Met Office, National Meteorological Library and Archive, Fact Sheet No. 6, The Beaufort Scale, U.K., 2006, http://www.metoffice.gov.uk/corporate/library/factsheets/factsheet06.pdf.

Mitchell, J.H., *On the Highest Waves in Water*, Philosophical Magazine, XXXVI, No. 222, pp. 430-437, 1893.

Mitsuyasu, H., *Experimental Study on Wave Force Against a Wall*, Report Transportation Technical Research Institute, Ministry of Transport, Japan, Vol. 47, 1962.

Munk, W.H., *The Solitary Wave Theory and Its Application to Surf Problems*, Annals of the New York Academy of Sciences, LI, pp. 376-462, 1949.

National Academy of Sciences, *Methodology for Calculating Wave Action Effects Associated with Storm Surges*, 1977.

NDBC, http://www.ndbc.noaa.gov/, National Data Buoy Center, National Oceanic and Atmospheric Administration, Accessed on May 15, 2006.

NGDC, http://www.ngdc.noaa.gov/mgg/fliers/00mgg02.html, Poster: Bathymetry of the Northern Gulf of Mexico and Atlantic Coast East of Florida, World Data Center for Marine Geology and Geophysics, Boulder, National Geophysical Data Center, Accessed on July 20, 2006.

NOAA/NGDC-1, http://tsun.sscc.ru/htdbmed/, World Tsunami Database in GIS graphic format, National Oceanic and Atmospheric Administration, U.S., Accessed on May 15, 2006.

NOAA-1, http://www.nhc.noaa.gov/, National Hurricane Center, National Oceanic and Atmospheric Administration, Accessed on May 15, 2006.

NOAA-2, http://www.nhc.noaa.gov/pastall.shtml, Archive of Hurricane Seasons, National Oceanic and Atmospheric Administration, Accessed on May 15, 2006.

NOAA-3, http://www.nhc.noaa.gov/pastcost.shtml?, Costliest Hurricanes Unadjusted for Inflation, National Oceanic and Atmospheric Administration, Accessed on May 15, 2006.

NOAA-4, http://www.nhc.noaa.gov/pastcost2.shtml?, Costliest Hurricanes Adjusted for Inflation, National Oceanic and Atmospheric Administration, Accessed on May 15, 2006.

NOAA-5, http://www.nhc.noaa.gov/gifs/table2.gif, Deadliest Hurricanes, National Oceanic and Atmospheric Administration, Accessed on May 15, 2006.

NOAA-6, http://www.nhc.noaa.gov/pastint.shtml?, Most Intense Hurricanes, National Oceanic and Atmospheric Administration, Accessed on May 15, 2006.

NOAA-7, http://www.nhc.noaa.gov/paststate.shtml?, Hurricanes by State Where they Landed, National Oceanic and Atmospheric Administration, Accessed on May 15, 2006.

NOAA-8, http://ols.nndc.noaa.gov/plolstore/plsql/olstore.prodspecific?prodnum=W00010-CDR-S0002, National Data Centers, U.S. Department of Commerce, Accessed on July 27, 2006.

NOAA/NGDC-1, http://tsun.sscc.ru/htdbmed/, World Tsunami Database in GIS graphic format, National Oceanic and Atmospheric Administration, U.S., Accessed on May 15, 2006.

NOAA/NGDC-2, http://www.ngdc.noaa.gov/seg/hazard/tsevsrch_idb.shtml, World Tsunami Database in text format, National Geophysical Data Center, U.S., Accessed on May 15, 2006.

NTL-1, http://tsun.sscc.ru/htdbmed/, Tsunami Database for the Mediterranean Sea, Novosibirsk Tsunami Laboratory, Russia, Accessed on May 15, 2006.

NTL-2, http://tsun.sscc.ru/htdbatl/, Tsunami Database for the Atlantic Ocean, Novosibirsk Tsunami Laboratory, Russia, Accessed on May 15, 2006.

NTL-3, http://tsun.sscc.ru/htdbpac/, Tsunami Database for the Pacific Ocean, Novosibirsk Tsunami Laboratory, Russia, Accessed on May 15, 2006.

Oceanweather, Inc., http://www.oceanweather.com/forecast/, 2006.

Overbeek, J. and Klabbers, I.M., *Design of Jetty Decks for Extreme Vertical Wave Loads*, Proceedings of the Ports 2001 Conference, American Society of Civil Engineers, 10 pp., 2001.

Ruch, C., *Hurricane Vulnerability Analysis for Bazoria, Galveston, and Chambers Counties*, Study Prepared by the Research Division, College of Architecture and Environmental Design, Texas A&M University, College Station, TX, August 1983.

Sarpkaya, T and Isaacson, M., *Mechanics of Wave Forces on Offshore Structures*, Van Nostrand Reinhold, 1981.

Scheffner, N.W., Mark, D.J., Blain, C.A., Westerlink, J.J., and Luettich Jr., R.A., *A Tropical Storm Database for the East and Gulf of Mexico Coasts of the United States*, U.S. Army Corps of Engineers Coastal Engineering Research Center, Vicksburg, MS., 1994.

Sheppard, D.M., and Miller, W., *Design Storm Surge Hydrographs for the Florida Coast*, Florida Department of Transportation, Final Report, FDOT Contract Number BC-354 RWPO 70, Tallahassee, Florida, 126 pages, 2003.

Shih, R.W. and Anastasiou, K., *Wave Induced Uplift Pressures Acting on a Horizontal Platform,* Presented at the Eighth International Conference on Offshore Mechanics and Arctic Engineering, March 19-23, The Hague, 1989.

Simpson, R.H. and Riehl, H., *The Hurricane and Its Impact*, Louisiana State University Press, Baton Rouge, LA, 1981.

SLOSH, *Slosh Model*, National Oceanic and Atmospheric Administration, http://www.nhc.noaa.gov/HAW2/english/surge/slosh.shtml, Accessed on May 16, 2006.

SPM, Shore Protection Manual, Department of the Navy Waterways Experiment Station, Corps of Engineers, 1984.

Suchithra, N. and Koola, P.M., *A Study of Wave Impact on Horizontal Slabs*, Ocean Engineering, Vol. 22, No. 7, pp. 687-697, 1995.

Taly, N., Design of Modern Highway Bridges, McGraw Hill, 1998.

Tanimoto, K., *Wave Forces on a Composite-Type Breakwater*, Proceedings of the 1976 Annual Research Presentation of Port and Harbour Research Institute, pp. 1-26, 1976 (in Japanese).

TCOON-1, *Texas Coastal Ocean Observation Network*, TCOON Page, http://lighthouse.tamucc.edu/TCOON/HomePage, Accessed on December 10, 2005.

TCOON-2, *Texas Coastal Ocean Observation Network*, Data Query Page http://lighthouse.tamucc.edu/pq , Accessed on December 10, 2005.

Tedesco, J.W., McDougal, W.G., and Ross, C.A., *Structural Dynamics, Theory and Applications*, Addison Wesley, 1999.

The Seattle Times, *Rising Costs of Replacing Viaduct, 520 Bridge Complicate Decisions*, http://seattletimes.nwsource.com/html/localnews/2003268579_highwaycosts21m.html, accessed on September 21, 2006.

Tickell, R.G., *Wave Forces on Structures*, Chapter 28, *Coastal, Estuarial and Harbour Engineer's Reference Book*, Abbott, M.B., and Price, W.A., (Eds.), Chapman and Hall, pp. 369-380, 1993.

TxDOT, *Bridge Design Manual*, http://manuals.dot.state.tx.us/docs/colbridg/forms/des.pdf, Accessed on March 18, 2005, Edition 2001.

TxDOT, *Hydraulic Design Manual*, Chapter 8 - Bridges, Texas Department of Transportation, January, 1997.

Uchupi, E., *Bathymetry of the Gulf of Mexico*, Publication GCAGS 403M, Geological Society, Bureau of Economic Geology, 1967.

Wang, H., *Water Wave Pressure on Horizontal Plate*, Journal of the Hydraulics Division, Proceedings of the American Society of Civil Engineers, Vol. 96, No. HY10, pp. 1997-2017, 1970.

Weatherunderground, http://www.weatherunderground.com, Accessed on December 1, 2005.

Weggel, J.R., *Maximum Breaker Height for Design*, Proceedings 13th Coastal Engineering Conference, Vancouver, Vol. 1, pp. 419-432, 1972.

Weggel, J.R., *Discussion of Article: Breaking-Wave Loads on Vertical Walls Suspended Above Mean Sea Level*, Journal of Waterway, Port, Coastal, and Ocean Engineering, ASCE, May/June, pp. 143-147, 1997.

Wilson, J.F., *Dynamics of Offshore Structures*, Second Edition, John Wiley and Sons, 2003.

Xanthakos, P., *Bridge Substructure and Foundation Design*, Prentice Hall, 1995.